MODIFICATION OF PEBAX AND ZIF-8/PEBAX MEMBRANES BY ADDITIONAL SOLVENT TREATMENT TO IMPROVE CO_2/N_2 SEPARATION PERFORMANCE

A THESIS SUBMITTED TO
THE GRADUATE SCHOOL OF NATURAL AND APPLIED SCIENCES
OF
MIDDLE EAST TECHNICAL UNIVERSITY

BY

ALA ABDULALEM ABDO MOQBEL ALSUHILE

IN PARTIAL FULFILLMENT OF THE REQUIREMENTS
FOR
THE DEGREE OF MASTER OF SCIENCE
IN
CHEMICAL ENGINEERING

SEPTEMBER 2020

Approval of the Thesis:

MODIFICATION OF PEBAX AND ZIF-8/PEBAX MEMBRANES BY ADDITIONAL SOLVENT TREATMENT TO IMPROVE CO₂/N₂ SEPARATION PERFORMANCE

submitted by **ALA ABDULALEM ABDO MOQBEL ALSUHILE** in partial fulfillment of the requirements for the degree of **Master of Science in Chemical Engineering Department, Middle East Technical University** by,

Prof. Dr. Halil Kalıpçılar
Dean, Graduate School of **Natural and Applied Sciences**   ——————————

Prof. Dr. Pınar Çalık
Head of Department, **Chemical Engineering**   ——————————

Prof. Dr. Halil Kalıpçılar
Supervisor, **Chemical Eng. Dept., METU**   ——————————

Asst. Prof. Dr. Emre Büküşoğlu
Co-Supervisor, **Chemical Eng. Dept., METU**   ——————————

Examining Committee Members:

Prof. Dr. Yusuf Uludağ
Chemical Engineering Dept., METU   ——————————

Prof. Dr. Halil Kalıpçılar
Chemical Engineering Dept., METU   ——————————

Asst. Prof. Dr. Emre Büküşoğlu
Chemical Engineering Dept., METU   ——————————

Prof. Dr. Birgül Tantekin Ersolmaz
Chemical Engineering Dept., İTÜ   ——————————

Assoc. Prof. Dr. Zeynep Çulfaz Emecen
Chemical Engineering Dept., METU   ——————————

Date: 09.09.2020

I hereby declare that all information in this document has been obtained and presented in accordance with academic rules and ethical conduct. I also declare that, as required by these rules and conduct, I have fully cited and referenced all material and results that are not original to this work.

Name Last name: Ala Abdulalem Abdo Moqbel Alsuhile

Signature:

ABSTRACT

Alsuhile, Ala Abdulalem Abdo Moqbel
M.Sc., Department of Chemical Engineering
Supervisor: Prof. Dr. Halil Kalıpçılar
Co-supervisor: Asst. Prof. Dr. Emre Büküşoğlu

September 2020, 148 pages

Capturing carbon dioxide is currently one of the most attractive research areas due to the serious problems that CO_2 emission creates for the environment. The main aim of this work is to utilize cheap and environmentally friendly methods with simple synthesizing systems to enhance the separation performance of CO_2 from N_2 using PEBAX 1657 membranes. Thus, in this study, solvent modification and double-layer methods were used to improve the permeability of carbon dioxide in pure PEBAX 1657 and ZIF-8/PEBAX with an insignificant drop in the selectivity. The membrane modified by the solvent modification method improved the CO_2 permeability by 1.21 compared to the single-layer 4 wt % PEBAX 1657 membrane which has a CO_2 permeability of 155.2 Barrer. The modified membranes achieved a permeability of 188 Barrer. Furthermore, the CO_2 permeability of double-layer membranes with different PEBAX 1657 in the top layer (4, 2, and 1 wt%) was higher by 1.13, 1.23, and 1.33; respectively, compared to single-layer 4 wt % PEBAX 1657 membrane. In MMMs, the double-layers membranes had permeabilities of 209.0 and 254.0 Barrer. These values are higher than single-layer membranes of MMMs by 1.14 and 1.3, respectively. The selectivity for separating CO_2/N_2 of all membranes ranged between 34.0-41.0. Thus, this study proposed two cheap synthesizing processes that enhanced the permeability of PEBAX 1657 membranes.

Keywords: Capturing CO_2, PEBAX 1657, Double-layer membranes, Solvent modification, and ZIF-8/PEBAX 1657 MMMs

ÖZ

Alsuhile, Ala Abdulalem Abdo Moqbel
Yüksek Lisans, Kimya Mühendisliği Bölümü
Tez Danışmanı: Prof. Dr. Halil Kalıpçılar
Ortak Tez Danışmanı: Dr. Öğr. Üyesi Emre Büküşoğlu

Eylul 2020, 148 sayfa

Capturing Karbondioksitin yakalanması, CO_2 emisyonunun çevre için yarattığı ciddi sorunlar nedeniyle şu anda en popüler araştırma alanlarından biridir. Bu çalışmanın temel amacı, PEBAX 1657 membranları kullanarak CO_2'nin N_2'den ayrılma performansını artırmak için basit sentezleme sistemleriyle ucuz ve çevre dostu yöntemler kullanmaktır. Bu nedenle, bu çalışmada, seçicilikte önemsiz bir düşüş ile saf PEBAX 1657 ve ZIF-8 / PEBAX'da karbondioksitin geçirgenliğini artırmak için solvent modifikasyonu ve çift katman yöntemleri kullanılmıştır. Solvent modifikasyon yöntemiyle modifiye edilen membran, 155.2 Barrer CO_2 geçirgenliğine sahip tek katmanlı ağırlıkça % 4 PEBAX 1657 membrana kıyasla CO_2 geçirgenliğini 1.21 oranında artırdı. Modifiye membranlar, 188 Barrer'lık bir geçirgenliğe ulaştı. Ayrıca, üst katmanda (ağırlıkça % 4, 2 ve 1) farklı PEBAX 1657'ye sahip çift katmanlı membranların CO_2 geçirgenliği tek katmanlı ağırlıkça % 4 PEBAX 1657 membran ile karşılaştırıldığında sırasıyla 1.13, 1.23 ve 1.33 oranında daha yüksektir. MMM'lerde, çift katmanlı membranlar 209.0 ve 254.0 Barrer geçirgenliklere sahipti. Bu değerler, MMM'lerin tek katmanlı membranlarından sırasıyla 1.14 ve 1.3 kat daha yüksektir. Tüm membranların CO_2 / N_2 ayırma seçiciliği 34.0-41.0 arasında değişmiştir. Bu nedenle, bu çalışma, PEBAX 1657 membranlarının geçirgenliğini artıran iki ucuz sentezleme işlemi önermiştir.

Anahtar Kelimeler: CO_2 yakalanması, PEBAX 1657, Çift katmanlı membranlar, Solvent modifikasyonu ve ZIF-8 / PEBAX 1657 MMM'ler

To My Grandfather & My Family

ACKNOWLEDGEMENTS

TABLE OF CONTENTS

LIST OF TABLES

TABLES

FIGURES

CHAPTER 1

INTRODUCTION

The membrane process is a separation technique where a membrane is considered to be a perm-selective barrier between two phases. It mainly depends on the mass rate of a component and it is not considered as an equilibrium stage (Mccabe, Smith, and Harriott 2012). As it is shown in Figure 1, the feed stream is separated into retentate and permeate. As apparent from the names, the permeate stream contains the components that could permeate through the membrane whereas the retentate contains mostly the rejected/retained ones.
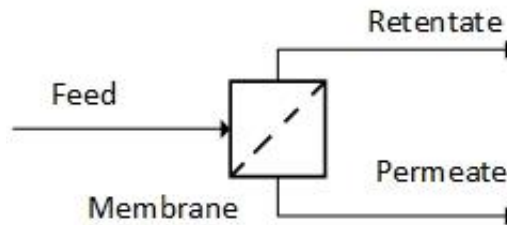
Figure 1. Simple schematic for the membrane process

The driving forces in the membrane technology can be categorized as the difference in pressure (ΔP), the difference in concentration (ΔC), the difference in temperature (ΔT), and the difference in electrical potential force. The efficiency of the membrane can be measured by calculating the flux which is the flow rate per unit of area and selectivity that

depends on the concentration of desired product in permeate and feed streams (Mulder 1991).

The advantages of membrane processes can be listed as (Mulder 1991):

- Separation is a continuous process

- Consume less energy compared to the traditional methods

- Capability to be used with other separation methods to form hybrid processes

- Easy to be scaled up

- It can separate azeotrope mixtures without introducing any additive component.

On the other hand, membranes have some disadvantages such as (Mulder 1991):

- Concentration polarization

- Membrane fouling

- Generally low lifetime

- Low selectivity for some membranes

The membrane is an attractive technology in reducing carbon dioxide emission which can be considered as one of its major applications (Basile et al. 2011). Although, the industrial revolution has caused a dramatic increase in economic growth it has some drawbacks such as global warming and climate change. Kasman and Duman believe that this revolution made the industry rely on inorganic economics instead of organic economics which had been based mostly on human and animal power (Kasman and Duman 2015). This conversion led the industry to consume fossil fuels continuously which affected the carbon dioxide level in the atmosphere. Figure 2 shows that carbon dioxide has been rising to two parts per million each year from 2013 until 2018 (Baena-Moreno et al. 2019).
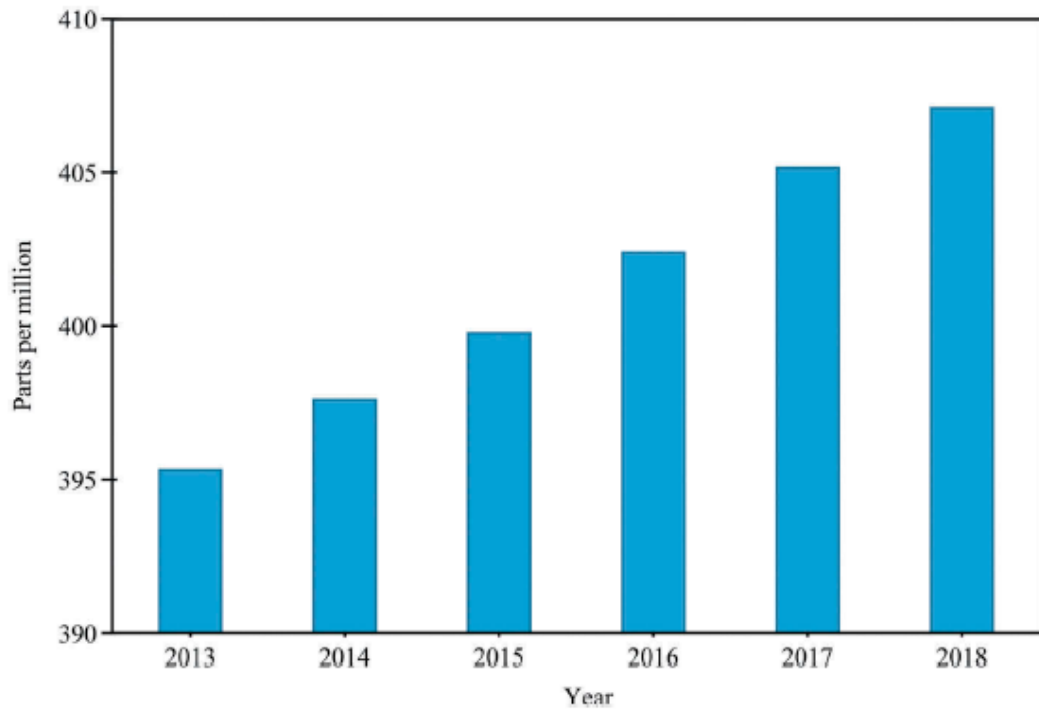
Figure 2. CO_2 concentration in the atmosphere, Adapted from Scripps Institution of Oceanography (Baena-Moreno et al. 2019)

Moreover, the Intergovernmental Panel on Climate Change (IPCC) reported in 2007 that there is a direct relationship between the global average temperature and emissions of greenhouse gases. For instance, carbon dioxide emission has risen by 1.9% over the last three years due to the use of fossil fuels. Besides, IPPC stated in the same report that average global temperature is predicted to go up within the range of 1.1 – 6.4 °C in the next 100 years (Kasman and Duman 2015).
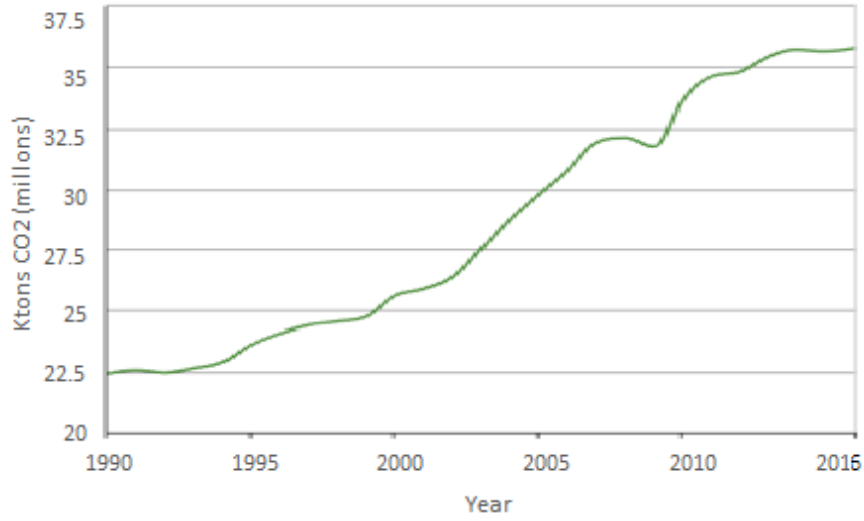
a
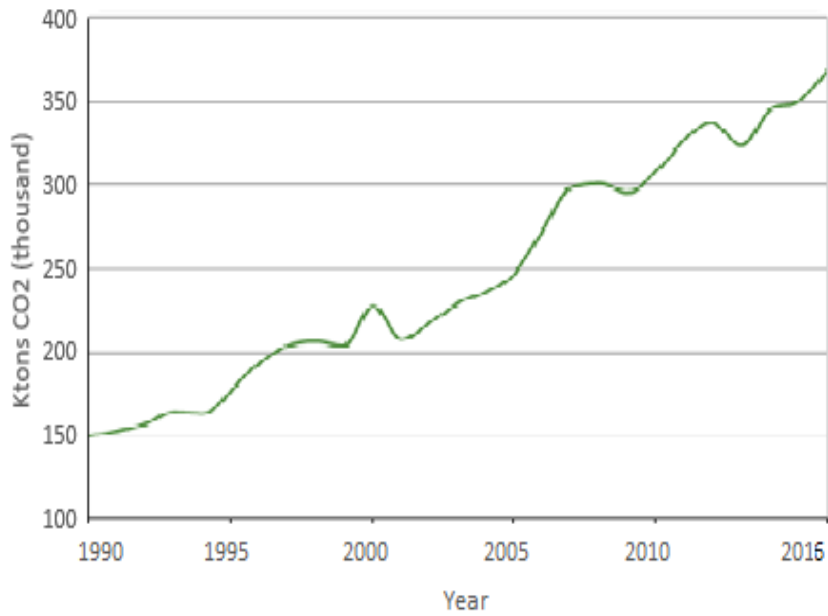
b

Figure 3. Total carbon dioxide emission (a) globally and (b) locally (Anon 2019)

Figure 3 indicates that carbon dioxide has an upward trend globally and in Turkey (Anon 2019). Besides, International Energy Agency (IEA) claimed that global average

4

temperature is going to be increased by 2 °C by 2040 which is supposed to be reached at the end of this century to meet the safety requirements. Consequently, economic activity in the world should be dropped by a total of 20 gigatons-equivalent which means below the baseline projections by 2040 (Anon 2009). To further clarify the seriousness of this problem, Paris Agreement's ''Well below 2 °C'' will not satisfy the earlier requirements. Under this estimation by IEA, if all nations meet Paris Agreement limits global average temperature will increase 2 °C after 8 months from the normal business scenario (Yeldan 2017). Locally, Erinc (Yeldan 2017) reported that the current rate of greenhouse gas emission will lead Turkey to approximately 650 million tons-equivalent of carbon dioxide by 2030. Accordingly, international sources insisted that Turkey should cut down its carbon dioxide emission to be 400 million tons-equivalent of CO_2 by 2030 to fulfill its global share responsibility for a better climate (Yeldan 2017).

For these reasons, different methods have been utilized to contribute to minimizing the amount of carbon dioxide. All these methods are listed under three main carbon-capturing methods (Deolalkar 2016):

- Pre combustion

- Oxyfuel combustion

- Post-combustion

A brief description of each method is given as follows:

1. Pre combustion (Deolalkar 2016)

The main idea in this type is to remove CO_2 from fossil fuels before complete combustion occurs. For example, the coal is partially oxidized using air with high temperature and pressure to form synthesis gas that contains hydrogen, carbon monoxide, carbon dioxide, and a small amount of other gaseous components like methane. Then this gaseous mixture undergoes a water-gas shift reaction to produce CO_2 and H_2 from H_2O and CO. After that, CO_2 is captured and H_2 is used as fuel. However, pure Hydrogen is very explosive thus mostly it is diluted with nitrogen or steam.

2. Oxyfuel combustion (Stanger et al. 2015)

In this process, pure oxygen from the air is combusted and flue gas is recycled into a furnace to control the flame temperature. The main target is to have a flue gas enriched with CO_2 and water vapor. Later on, this flue gas can be dehydrated to capture CO_2. The main components of this process are the boiler or gas turbine, flue gas processing unit, and CO_2 processing unit.

3. Post-combustion:

3.1. Amine Scrubbing

Carbon dioxide is sent to monoethalomine to be absorbed. Then the CO_2 in the amine solution is separated, dried, and compressed to a storage site. Figure 4 describes the whole process (Hoenig, Hoppe, and Emberger 2007)
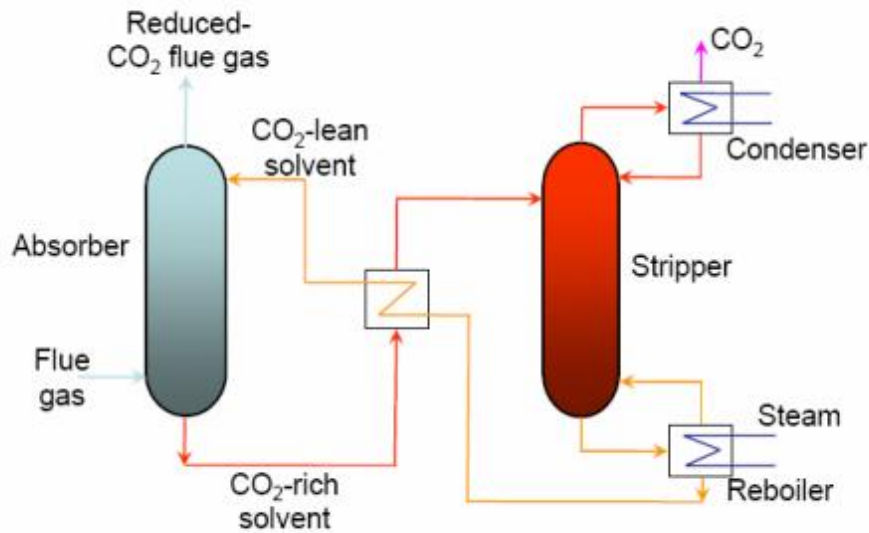
Figure 4. Schematic diagram of amine scrubbing (Hoenig et al. 2007)

3.2. Carbonate looping (Hawthorne et al. 2009)

$$CaO(s) + CO_2(g) \xrightarrow{yields} CaCO_3(s)$$

$$CaCO_3(s) \xrightarrow{\Delta} CO_2(g) + CaO(s)$$
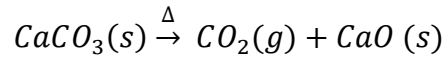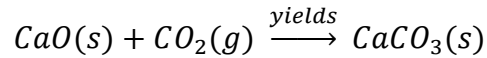
The above two reactions explain the main concept behind this method. In the first reaction, CaO is used to react with CO_2 in a fluidized bed at 650-850 °C. Later on, the produced particles are sent to calciner at almost 950 °C to separate CO_2 and pumped to storage.

The above methods require more than one step process to achieve complete separation. Moreover, some of them are limited by thermodynamic equilibrium such as amine scrubbing (Gary T. Rochelle 2012). For these reasons, researchers are trying to improve other methods that can surpass these conventional methods to meet the environmental regulations and to be economically feasible. Membrane separation is considered one of these processes that grabbed the attention (Tong and Ho 2017). Compared to the traditional methods, membrane separation is a kinetic process that is unaffected by a thermodynamic equilibrium which reduces energy consumption. In addition, membranes have a simple operation process and low carbon footprint in which flat sheet and hollow-fibers can be produced in compact membrane modules (Tong and Ho 2017). Table 1 summarizes the advantages and disadvantages of using membrane technology for capturing CO_2 (Kenarsari et al. 2013).

Table 1. *Pros and cons of membrane technology for CO_2 separation* (Kenarsari et al. 2013)

Advantages	Disadvantages
• Higher separation energy efficiency compared to equilibrium-based processes like absorption and desorption • Good weight and space efficiency • No need for a regeneration process • Environmentally friendly • Low operating and maintaining cost	• Gas should be compressed to drive a permeation between two sides of the membrane • Low permeability • Limitation on the operating temperature

Many membrane types have been used for gas separation. They can be classified depending on the material of the membrane, as polymeric or inorganic. Examples of inorganic membranes are zeolitic membranes, metallic oxide, silicate, and metals. Their chemical, thermal and mechanical stabilities are high. Moreover, controlling the pore sizes, and distribution are much better thus selectivity and permeability can be regulated. Nevertheless, they are brittle, difficult to produce reproducibly and need very high production cost (Ismail, Khulbe, and Matsuura 2015). In contrast, polymeric membranes are more flexible so they may withstand longer without being ruptured. This plays a vital role in industrial applications such as purification of combustion gas. Since this gas (CO_2) is considered to be waste in power plants, they are looking for inexpensive methods with reasonable efficiency to remove CO_2. As a result, polymeric membranes are more

desirable to be used since their production cost is much less than inorganic ones. However, they suffer from the trade-off between selectivity and permeability (Ismail et al. 2015). For these reasons, the field of polymeric membranes is attractive and needs more investigation to surpass its drawbacks. The efficiency of the polymeric membranes to be used in gas separation can be evaluated by Robeson Upper Bound relation as shown in Figure 5 (Panapitiya et al. 2016).
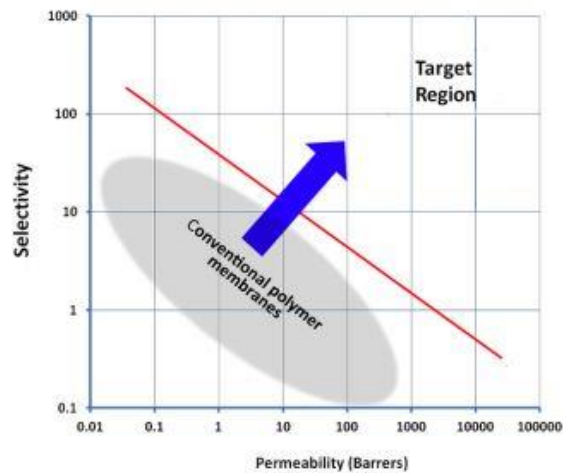
Figure 5. Robeson Upper Bound for polymeric membranes (Panapitiya et al. 2016)

Different methods were used to surpass this limitation such as using new polymers, blending techniques, and additives (Scholes, Ho, and Wiley 2016). However, synthesizing a membrane above this line using these methods may require complex systems or expensive materials that makes it economically infeasible. For example, capturing carbon dioxide requires a large area of membranes for different processes. To illustrate, Table 2 shows the compositions and flow rate of a Natural Gas Combined Cycle (NGCC) process.

9

Table 2. *Flue gas conditions for NGCC (Scholes et al. 2016)*

Flue gas conditions	NGCC
Flow rate (tonne/hr)	2268
Compositions (mol %)	-
CO_2	4.97
N_2	74.28
O_2	9.73
H_2O	11.02

As shown in the table, the flow rate is high and CO_2 mole fraction is low compared to other species thus large area of the synthesized membranes is required. Furthermore, CO_2 is not valuable material that has the potential to be used in different industries, in fact, it is considered as waste for many processes. Consequently, capturing CO_2 from these gases should be cheap to be economically feasible.

The drawbacks of both types of membranes, polymeric and inorganic, opened a new field for research to find novel ways to enhance the performance of the membrane. A mixed matrix membrane is a new type of membrane where two materials emerge. MMM is composed of the polymeric matrix and inorganic particles embedded within the matrix as shown in Figure 6 (Lin et al. 2018).
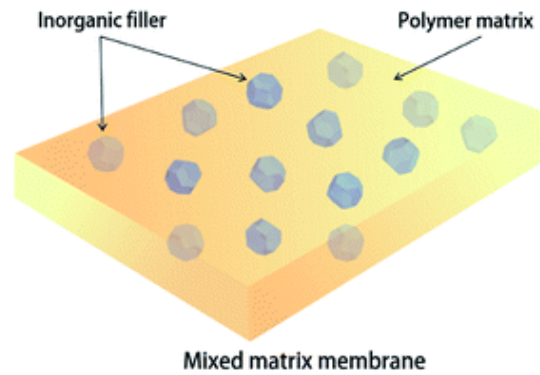
Figure 6. Schematic diagram of a mixed matrix membrane (Lin et al. 2018)

The first work that is related to MMM was in 1973, done by Pual and Kemp. They found that diffusion time lag is enhanced with zeolite-5A fillers in a silicon rubber matrix (Paul and Kemp 1973). Since then, MMM gained considerable interest to improve the efficiency of the membranes. However, MMMs still need to be improved due to the challenges that resulted from the combination of the polymer matrix and inorganic fillers (Hamid and Jeong 2018). For example, agglomeration and sedimentation can exist due to improper dispersion of fillers (Dong, Li, and Chen 2013). Furthermore, the physical properties differences between the fillers and the matrix such as density form a heterogeneous phase. This phase may cause non-selective defects or pinholes that negatively affect the membrane mechanical stability specifically when a high filler amount is loaded to the matrix (Shahid 2015). Besides, an interfacial morphology issue may occur due to the residual stresses that are developed as a result of solvent evaporation (Moore and Koros 2005). Different methods were used to overcome this problem such as filler surface modification (Hillock, Miller, and Koros 2008), use of coupling agents (Li et al. 2006), post-treatment of MMMs (e.g. annealing) (Song et al. 2012a), the preparation of highly concentrated (15-18 %) solutions (Mahajan and Koros 2000), priming procedures (Mahajan and Koros 2002), and high membrane formation temperature (Mahajan and Koros 2000). Table 3 (Dong et al. 2013) summarizes the current fillers that have been used for synthesizing MMM.

Table 3. *Pore size of the particles commonly used for the mixed-matrix membranes (Dong et al. 2013)*

Filler type	Filler name	Pore Diameter ($°A$)
Zeolites	Zeolite-A	3.2–4.3
	ZSM-5	5.1–5.6
	Zeolite-13X	7.3
	Zeolite-KY	7.3
	Silicalite-1	5.2–5.8
	SAPO-34	3.8
Meso-porous materials	MCM-41, 48	>25
	SBA-11, 12, 15	>20
	Meso-porous ZSM-5	27
	Activated carbon	20–30
	TiO$_2$	37.1
	MgO	30
Metal-organic frameworks	MIL-96	2.5–3.5
	MIL-100	5.5×8.6
	MOF-5	8.3
	MOF-177	7.1–7.6
	ZIF-7	3
	ZIF-8	3.4

Table 3. *(cont'd) Pore size of the particles commonly used for the mixed-matrix membranes (Dong et al. 2013)*

Filler type	Filler name	Pore Diameter (°A)
Metal-organic frameworks	Cu-TPA	5.2
	$Cu_3(BTC)_2$	5×9
	Cu-BPY-HFS	8
Lamellar materials	JDF-L1	3
	AlPO	$4.44 \times 3.29 \times 3.17$
	SAMH-3	$4.24 \times 4.10 \times 3.40$

The critical aspect of the fabrication of MMMs is to select the proper filler for the most suitable polymer matrix. An example of perfect matching is Polyether Block Amide (PEBA) which is a copolymer and thermoplastic elastomer with ZIF-8. This combination enhances the carbon dioxide permeability and selectivity where research is still ongoing to improve the separation performance of this collaboration.

This study is motivated to improve the permeability of carbon dioxide in polymeric and mixed matrix membranes with an insignificant drop in the selectivity. Thus, the main aim of this work is to utilize cheap and environmentally friendly methods with simple synthesizing systems to enhance separation performance. As mentioned earlier, the economy plays a crucial role in membrane technology that is intended to be used in industrial applications. If pure PEBAX and ZIF8/PEBAX membranes were treated with ethanol-water mixture a change in their morphologies may result due to solvent penetration through the membrane matrix. This modification may impact factors such as the chain packing and the free volumes of the membranes that may cause an enhancement in their separation performance.

Two methods were investigated to test this hypothesis. First, adding pure solvent of the ethanol-water mixture after one day of casting the membranes. Second, synthesizing double-layer membranes where both layers have the same components and no additional materials were added to the second layer. Moreover, mixed matrix membranes with two different sizes of filler were used. The selected membrane to be improved in this work is PEBAX1657 where ZIF-8 is used as filler for MMM. The reason for this selection is explained in detail in the literature review section. In the same section, the previous work related to separation performance and fabrication methods that were done on these membranes were extensively reviewed. After that, an experimental procedure that was used to prepare, test, and characterize these membranes is mentioned. Finally, the obtained results that prove the significant enhancement of these membranes' performance is given with comprehensive discussion.

CHAPTER 2

LITERATURE REVIEW

2.1 Gas Separation Mechanism Through Membranes

Diffusion controls the gas permeation mechanism in dense membranes. The whole mechanism can be divided into three steps. It begins when the gas molecules are adsorbed by the membrane, then these molecules diffuse within the polymer matrix. Finally, they are desorbed and evaporated from the downside of the membrane. The driving force, in this case, is the partial pressure difference of each species. Permeability and selectivity of any polymeric membrane are two terms that determine the membrane separation performance. The former term depends mainly on the diffusion (D_A) and solubility (S_A) coefficients as it is illustrated in Equation [1] (Kita, Tanaka, and Koga 2008)

$$P_A = D_A * S_A \qquad (1)$$

Another way to calculate the permeability is to use flux (J_A), partial pressure difference (Δp_A) and membrane thickness (L) (Kita et al. 2008)

$$P_A = \frac{J_A * L}{\Delta p_A} \qquad (2)$$

On the other side, ideal selectivity($\alpha_{A/B}$) is the ratio of the permeability of permeated to the rejected species (Kita et al. 2008)

$$\alpha_{A/B} = \frac{P_A}{P_B} \quad (3)$$

George and Thomas generalized the mechanism and claimed that the reason for molecules' transportation through a membrane is their random motion. They believe that the driving force for this process that contains sorption, diffusion, and permeation is the concentration difference between the two separated phases by the membrane. This process can be described by Fick's first law [4] (George and Thomas 2001).

$$J = -D\left(\frac{\partial C}{\partial x}\right) \quad (4)$$

If a steady-state is assumed and diffusion is considered to not be a function of concentration at a fixed temperature equation [4] can be written as follow:

$$J = \frac{D * (c_1 - c_2)}{L} \quad (5)$$

In the case of gaseous media, the concentration can be expressed as a function of pressure (p) and solubility(S) (Kita et al. 2008)

$$c = S * p \quad (6)$$

Substitution of Equation (6) into equation [5] gives Equation [7]

$$J = \frac{D * S(p_1 - p_2)}{L} \quad (7)$$

Where Permeability (P) is the product of diffusion and solubility, thus flux can be calculated as follows

$$J = \frac{P(p_1 - p_2)}{L} \quad (8)$$

Which can be obtained for a specific species by rearranging equation [2].

This transportation process is varied from one polymer to another due to free volume within the polymer matrix and the segmental mobility of its chains. The latter is affected

16

by many factors such as the degree of crystallinity and cross-linking, the extent of unsaturation, and the nature of substituents (Kita et al. 2008). Going back to equation [3], it can be inferred that the ideal selectivity of the membrane depends on the ratio of diffusion and solubility coefficients of two species in the mixture, or in other words, it can be divided to mobility and solubility selectivity as shown in equation [9].

$$\alpha_{A/B} = \left(\frac{D_A}{D_B}\right)\left(\frac{S_A}{S_B}\right) \quad (9)$$
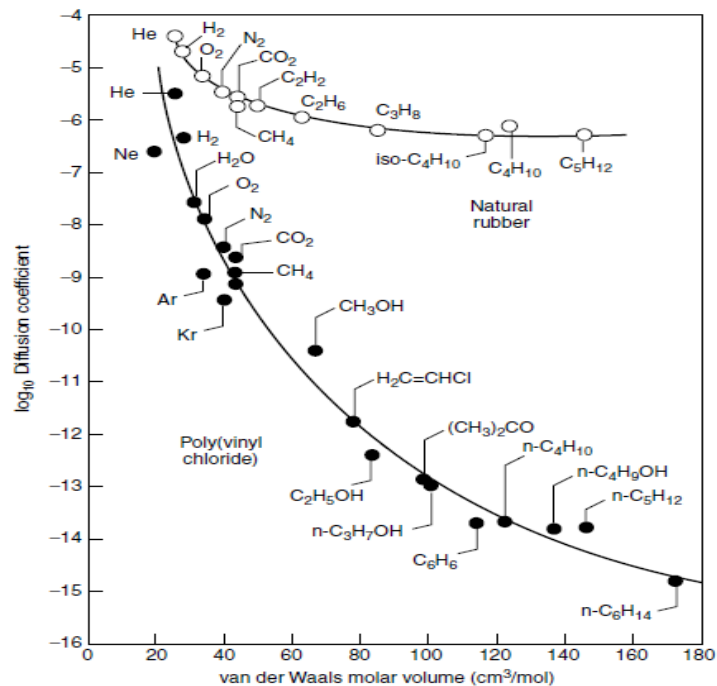
Figure 7. The variation of Diffusion coefficient as a function of molar volume for different permeants in natural rubber and in poly(vinyl chloride) (Grün 1947)

Diffusion has an inverse relation with molecular size since the interaction between molecules and polymer chains is much more in case of large rather than small molecules. Therefore, mobility selectivity prefers small molecules to transport. Nevertheless, its magnitude depends on the glass transition temperature (T_g). For polymers below the T_g, their chains are fixed and do not rotate and they are called glassy polymers. On the other hand, polymers above T_g allow limited rotation around the chain backbone since their

17

chains have sufficient thermal energy thus their mechanical properties change significantly and they become rubbery (Baker 2012). The diffusion coefficient is affected rapidly with the permeate particles' size with the former polymer type and slightly with later one as can be shown in Figure 8 (Grün 1947).

On the other hand, in the solubility or sorption selectivity there is an increasing trend with the condensability of the permeate species thus it has a direct relation with the diameter of molecules. There is a difference between the sorption coefficient in both types of polymeric membranes but it is less marked than the diffusion coefficient (Baker 2012).

To select a membrane, a dominant selectivity factor should be considered depending on the polymer and permeate nature. Mobility term controls the selectivity performance in the glassy membranes; thus, it prefers to permeate small rather than large particles. However, in the rubbery type, sorption selectivity dominates so large particle sizes permeate faster than the small ones (Baker 2012). For example, for nitrogen-organic vapors mixture, glassy membranes are used for separating nitrogen and rubbery types are used to permeate organic vapors (Baker 2012). Figure 8 briefs the performance of each type with different gas molecules (R.D. Behling, K. Ohlrogge 1989)
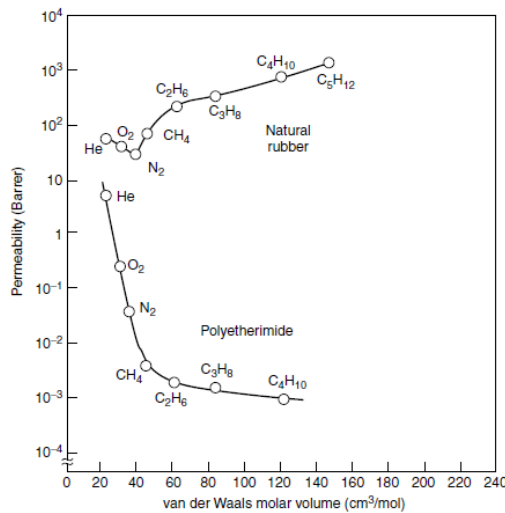
Figure 8. Variation of permeability as a function of molar volume for rubbery and glassy polymers (R.D. Behling, K. Ohlrogge 1989)

18

2.2   Polymeric Membrane Synthesizing Methods and Challenges

There is more than one method of membrane preparation. Each method depends on the membrane material and the application where the membrane is going to be used in. Phase inversion is the most used method to synthesize polymeric membranes. This method has advantages such as being economical and reproducible (Bungay 1987). This technique mainly starts by preparing a homogenous polymeric solution that is later exposed to a certain induced atmosphere to ensure complete transformation from the liquid- to solid-state. This conversion can be achieved in four main ways (Yuan n.d.).

- Immersion induced phase inversion: the dope solution is immersed in a coagulant which is miscible with solvent but immiscible with the polymer. Thus, an exchange of solvent occurs between the solvent in the polymeric solution and non-solvent in the coagulation bath (Yuan n.d.). The flux of the non-solvent diffusion (J1) into the cast film and the other flux of the solvent diffusion (J2) into the coagulation bath determine the pore size of the membrane (Radovanovic, Thiel, and Hwang 1992). Due to this exchange, a solid polymeric membrane is precipitated and obtained. If J2 is much larger than J1 then an ultrafiltration membrane is obtained. Nonetheless, if both fluxes are equal a microfiltration membrane is fabricated (Radovanovic et al. 1992).

- Thermally-induced phase separation: a homogenous polymeric solution is formed when polymer particles are dissolved in high-boiling point solvent. Later, the desired shape is selected to cast the polymeric solution. Finally, this solution is cooled down at certain conditions to extract the solvent (Lloyd 1990).

- Solvent evaporation induced phase separation: a polymer is dissolved in a mixture of solvent and volatile non-solvent or solvent medium alone. After a polymeric homogenous solution is formed, it is cast in specific conditions to evaporate the solvent from the polymer. This slow evaporation process leads to form a membrane with two phases, a polymer-rich and polymer-lean phase. In the end, the later phase is removed to obtain a polymeric membrane (Zhao et al. 2013).

- Vapor-induced phase inversion: a polymeric membrane is produced when a nonsolvent vapor (normally water) is utilized to precipitate polymer from a homogenous solution (Li et al. 2010).

The main challenge for the phase inversion method is the formation of pinholes in the dense layer of the membrane. It was reported that this problem can be fixed by coating the membrane by a highly permeable and very thin layer. This method is called the "caulking" step which helps significantly eliminate the pinholes from the polymeric membranes (Sanders et al. 2013).

The final shape of synthesized membranes mostly is flat sheet or hollow fibers. In industry, flat sheet membranes are prepared as spiral wound modules and the latter type is designed to be a hollow fiber module as it is shown in Figure 9 (Robeson 2012). The main objective of these configurations is to optimize the surface area of the membrane to be located in a given volume. As a result, increasing the ratio of membrane surface area to its volume reduces the cost of the membrane process. For example, this ratio significantly helps in reducing the cost of pressure vessels (Sanders et al. 2013).

a	b
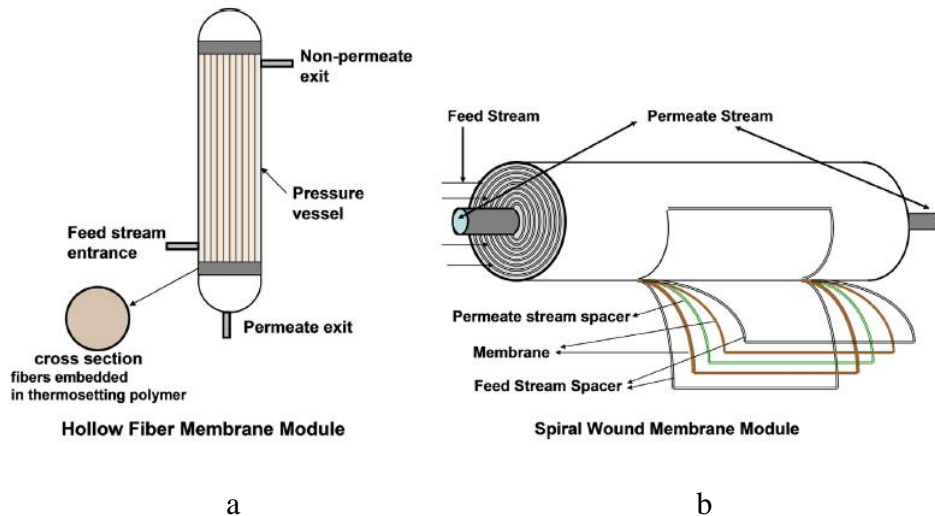
Figure 9. Illustration of (a) hollow fiber and (b) spiral wound modules (Robeson 2012)

2.3 Challenges of Polymeric Membranes in Gas Separation

2.3.1 Permeability/Selectivity Tradeoff

The This can be considered as the main limitation that polymeric membranes have for gas separation. Flux is a function of polymeric material (permeability) and its thickness. Similarly, the selectivity depends on the polymer material and the quality of fabrication which is mainly measured by the presence of pinholes. However, the thickness is a process parameter thus permeability and selectivity are the main factors that determine the separation performance of membrane material. The upper bound relationship is formed to check the validity of a membrane to separate a pair of two gas molecules. An example of an upper bound relation between carbon dioxide and nitrogen is given in Figure 10 (Robeson 2008)
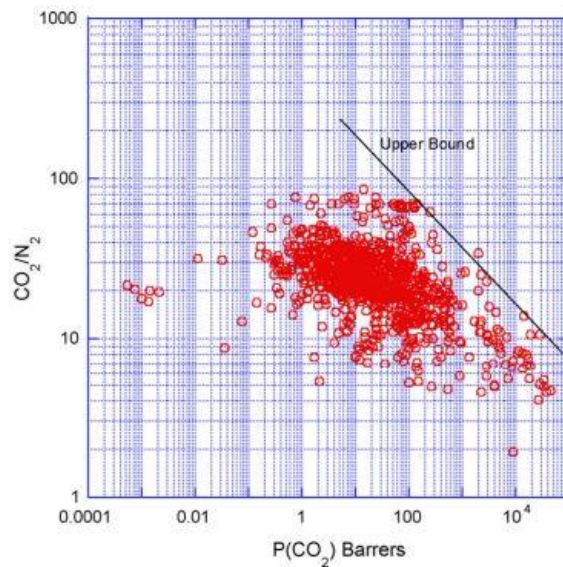
Figure 10. Upper bound correlation for CO_2/N_2 separation (Robeson 2008)

The upper bound resulted from testing a vast number of membranes in the same measurement conditions (Sanders et al. 2013). It was found that, due to the relation between the diffusion and the free volume of the polymer, as the permeability of one gas increases the other one in the pair is also increasing (Robeson et al. 2009). Moreover, for

a wide range of available polymers, solubility is predicted to be within a tight range (Robeson 1991). This explains the challenge of polymeric membranes for gas separation and the reason why researchers have been working on their modification to surpass this limitation.

2.3.2 Physical Aging

Most of the polymeric membranes used for gas separation are glassy type (Rowe, Freeman, and Paul 2011). As these membranes are below their glassy temperature, completely achieving equilibrium properties is prevented due to the kinetic constraints on the polymeric segmental motion. However, local scale segmental motions occur which result in a gradual increase of the density of the polymeric membrane that reduces the free volume to achieve a thermodynamic equilibrium (Dollimore 1982). As a result, it reduces the gas permeability of the membrane and alters other physical properties such as entropy, enthalpy, and specific volume (Anon n.d.). Nonetheless, this reduction of permeability is mostly accompanied by an enhancement in the selectivity (Sanders et al. 2013). Recent studies have been working on the relation of physical aging and membrane thickness, believing that manipulating the thickness of a membrane can reduce the effect of its physical aging. Besides, it was found that physical aging is reduced for two reasons. Firstly, the driving force for physical aging vanishes as excess free volume declines gradually. Secondly, due to a reduction of free volume, mobility of polymers chains decreases that causes a drop in segmental motions that reforms the polymer chains (Rowe, Freeman, and Paul 2009).

2.3.3 Plasticization

The increase of gas concentration in the polymeric membrane matrix may cause a membrane to swell. Consequently, both free volume and polymer chain motion are heightened which enhances the gas diffusion coefficients and reduces diffusion selectivity (Sanders et al. 2013). Plasticization mostly enhances the overall flux of mixture but has a negative impact on the selectivity, particularly at high pressures (Goyena and Fallis 2019). For glassy polymers, before plasticization, gas permeability decreases with increasing the

feed. However, when plasticization occurs the relation is inversed and permeability increases with pressure (Bos et al. 1999). The relative increase of permeability due to plasticization pressure varies from a polymer to another as can be shown in Figure 11 (Bos et al. 1999).
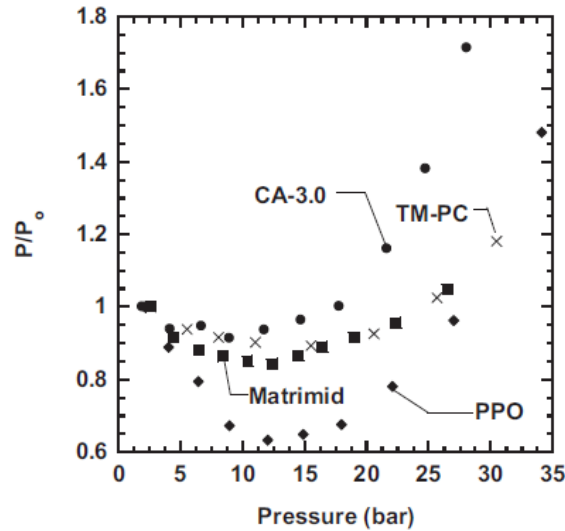
Figure 11. Relative permeability (where P_0 is permeability at a feed pressure of roughly 1 bar) as a function of feed pressure for four different glassy polymeric membranes films Cellulose triacetate (CA-3.0) at 24 °C, Matrimid at 22 °C, tetramethyl bisphenol polycarbonate (TM-PC) at 25 °C, and poly (2,6-dimethyl-1,4-phenylene oxide) (PPO) at 25 °C (Bos et al. 1999)

2.3.4   Relation between Membrane Separation Performance and Economics

The different types of technologies have been used to capture CO_2 such as cryogenic distillation, absorption, adsorption, and membrane gas separation (Cebrucean, Cebrucean, and Ionel 2014). Membrane technology has several advantages over the other methods such as the simplicity of the process. In the case of membranes, the process has no additional chemical nor an additional process of regeneration which is a required step in adsorption and absorption. Moreover, membranes can be fitted into any process easily without any need for a complicated integration. Nevertheless, membrane technology faces

23

challenges of fulfilling the economic feasibility requirements. One of these problems is the low permeability that increases the operating cost of the separation process (Ho, Allinson, and Wiley 2008). A study conducted in 2008 showed the relationship between the CO_2 capturing cost with membrane selectivity and permeability (Ho et al. 2008) as can be seen in Figure 12 and Figure 13.
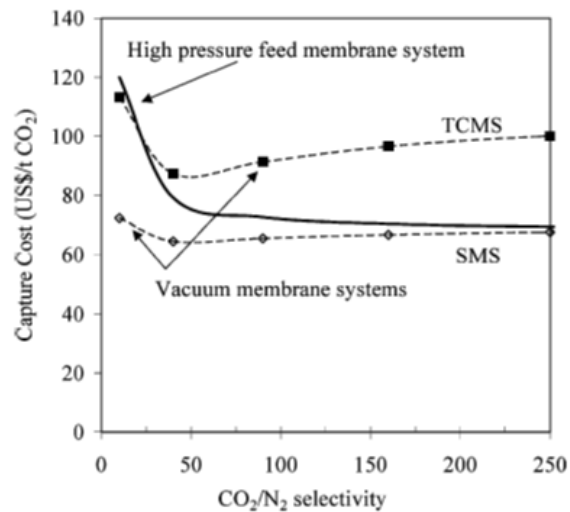
Figure 12. Effect of CO_2 selectivity on the CO_2 capture cost for different membrane vacuum systems SMS (single-stage system) O and TCMS (Two-stage cascade membrane system) ■ (Ho et al. 2008)

24
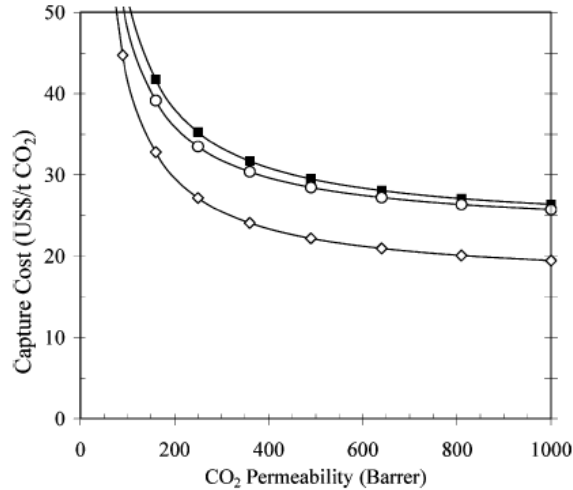
Figure 13. Effect of CO_2 permeability on the CO_2 capture cost for different membrane vacuum systems SMS (single-stage system) ○, TCMS (Two-stage cascade membrane system) ■, and TCMS-RR (Two-stage cascade membrane system with retentate recycle) ◇ (Ho et al. 2008)

The same study claimed that for vacuum membrane systems high permeability (300-550 barrer) with selectivity of (40-60) is required for membranes prices varying from $40/m^2$ to $50/m^2$. Nonetheless, if the price is less (U.S. $10-30/m^2$) the permeability required should be on the order of 200 barrer with keeping a selectivity of 40-60 (Ho et al. 2008).

2.4   Methods to Enhance the Permeability of Polymeric Membranes

Current research on gas separation membranes has been working on surpassing their limitation to make this technology economically and environmentally feasible. The following modifications have been used to improve the membrane separation performance

2.4.1   Physical Modification

Current Blending and coating are the main methods of physical modifications based on complementary principle. They are considered to be simple processes compared to other modification methods (Yuan et al. 2016).

25

2.4.1.1 Blending Modification

In this type of modification, polymers are blended with other types of polymers or nanoparticles of inorganic materials/metals in the same solvent. In this process, the polymer molecules are combined when they are penetrated and diffused with each other via polar and non-polar forces. Homogeneity of the resulted solvent depends on external factors such as mixing power and temperature (Krishna and Pugazhenthi 2011). The main advantage of this method is the simplicity of operation that has a significant positive impact on the property and materials of the membrane (Yang et al. 2010). As an example, Park found that adding of poly(dimethylsiloxane) (PDMS) into polyester membrane enhanced separation performance of the membrane by increasing both the permeability and the selectivity (Ho, Choon, and Young 2002). Moreover, adding Metal-Organic Framework Materials (MOFs) to different types of membranes improved both their selectivity and permeability compared to pure polymeric membranes (Car, Stropnik, and Peinemann 2006). For example, Adams found an improvement in the permeability and selectivity of polyvinyl acetate (PVAc) when CuTPA was blended in the membrane solution (Adams et al. 2010).

2.4.1.2 Heating Treatment

Many studies investigated the effect of heat treatment on membrane performance. They claimed that molecules of the polymer can be rearranged thus both of the membrane's density and flexibility degree can be enhanced (Yuan et al. 2016). PVDF was experimented on where heat treatment was used on the membrane at 393.2 K for 12 min. It was observed that the membrane surface had a higher number of both carbonyl (C=O) and hydroxyl (C-OH) which strengthened the polarity of the membrane surface. This makes the separation performance of the membrane much better (Chun-hong, Jia-qi, and Jian-ping 2006).

2.4.2 Chemical Modification

2.4.2.1 Group substitution

This method includes bromination (Hamad, Khulbe, and Matsuura 2002), sulfonation (Hamad and Matsuura 2005), benzoylation (Bhole et al. 2005), and so on (Li et al. 2011) as it is shown in Figure 14 where polyphenylene oxide (PPO) is chemically modified (Yuan et al. 2016). For illustration, the bromination of PPO increased the permeability of CO_2 to be 78 barrer as well as the selectivity (Cong et al. 2007).
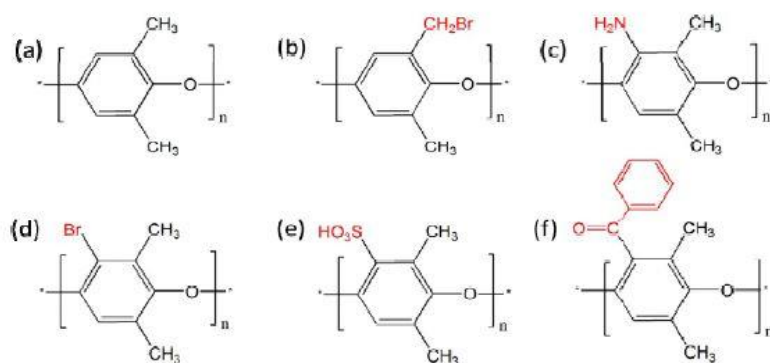
Figure 14. Structure of chemically modified PPO: (a) PPO; (b) BPPO; (c) PPO-NH2; (d) PPOBr; (e) sulfonated PPO; (f) benzoylated PPO (Yuan et al. 2016).

2.4.2.2 Cross-linking

This has been considered as one of the methods that balance both permeability and selectivity (Shao et al. 2004). Cross-linking of the polymer can be achieved using UV irradiation (Marek et al. 1996), chemical reaction (Cao et al. 2003) (Zhao et al. 2008), grafting (Freger, Gilron, and Belfer 2002), or blocking (Husken et al. 2010). A research proved that cross-linking improved the selectivity and reduced the rate of physical aging of the polymeric membrane. Nevertheless, it has a disadvantage of reducing the polymeric membrane permeability (McCaig and Paul 1999).

2.4.2.3 Co-polymerization

In this process, different types of molecules are joined together in random or alternating sequences. This method including alongside grafting have been used to modify many polymers such as PET (Yuan et al. 2016). In these methods, the chain strength and length of the polymer are manipulated to improve the membrane separation performance. Nonetheless, the grafting density is not easy to be controlled thus it may cause blocking of the pores of the membrane specifically if the density of grafting is extensively high. For this reason, the membrane significantly loses the quality of separation (Yuan et al. 2016).

2.4.2.4 Ionic Liquid Modification

Molten salts are used as an ionic liquid that contains cations and anions (Liang, Gan, and Nancarrow 2014) (Cserjési, Nemestóthy, and Bélafi-Bakó 2010) (Berthod, Ruiz-Ángel, and Carda-Broch 2008). A reaction between both the polymer and the ionic liquid occurs to produce a modified polymer that has an ionic charge to enhance the separation performance of the unmodified membrane. For example, PPO was modified with a different ionic solution and the carbon dioxide solubility had a remarkable increase (Cong et al. 2012).

Research on gas separation membranes has been working on surpassing their limitation to make this technology economically and environmentally feasible. The following modifications have been used to improve the membrane separation performance

2.5   Solvent Effect on Membrane Performance

2.5.1   Solvent Type

Several studies investigated the effect of the solvent on the membrane performance. From the point of the phase inversion, the whole solvent should be evaporated thus the remaining material is only the polymer. Thus, it was expected that the solvent type does not affect membrane performance. Shinbol studied the relation between the solvent type and membrane transport efficiency and stability. For a supported liquid membrane (SLM)

where a micro-pores polymer film was used as support, non-volatile organic liquids were investigated. It was reported that for SLMs to be permeable and highly stable, the solvent should have a high dielectric constant and low solubility in water (Shinbo et al. 1993). Moreover, it was found that the casting solvent has a serious impact on the polymer conformation and free volume. For example, although PTMSP can be prepared with a various number of solvents like benzene, toluene, chloroform, cyclohexane, and tetrahydrofuran, it was found that membranes cast with cyclohexane and toluene solvent had larger over-all free volume and higher permeability compared to others (Bi et al. 2000). In addition, composite membranes (PAN +Zeolites) were prepared with different solvents to separate ethanol from water in the pervaporation process. The results showed that both permeability and selectivity were affected by the solvent type as Figure shows (Şener et al. 2010).
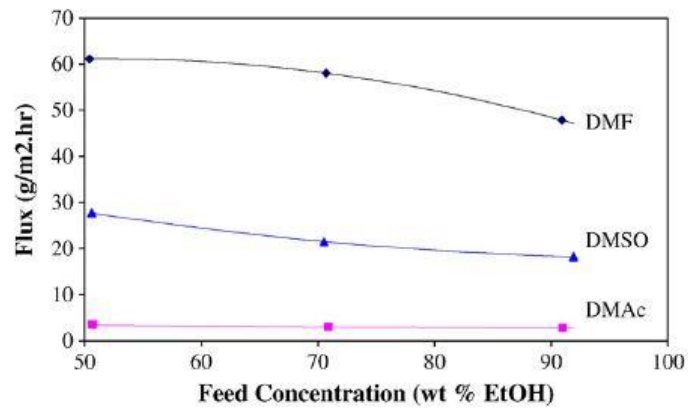
a

Figure 15. The variation of (a) flux and (b) selectivity with three selected solvents (Şener et al. 2010)
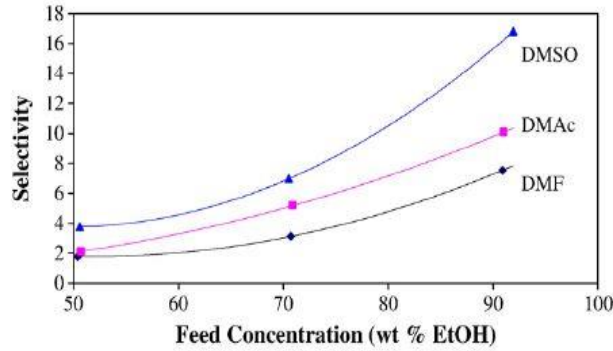
b

Figure 15. (cont'd) The variation of (a) flux and (b) selectivity with three selected solvents (Şener et al. 2010)

2.5.2 Solvent-Evaporation Process and Membrane Morphology

It was proved that membrane performance and morphology are not affected only by the solvent type but also the evaporation process. As an example, a study on poly (ethylene-co-vinyl alcohol) (EVAL)/DMSO/water system showed that evaporation duration played a main role in the membrane structure. After dissolving EVAL (15%) in DMSO, the solvent was evaporated for a certain time then immersed into a water bath to form the polymeric membrane. Figure 16 shows how the solvent evaporation time could affect th morphology of this membrane (Young, Huang, and Chen 2000). It can be observed that the membrane structure differs in the two cases.
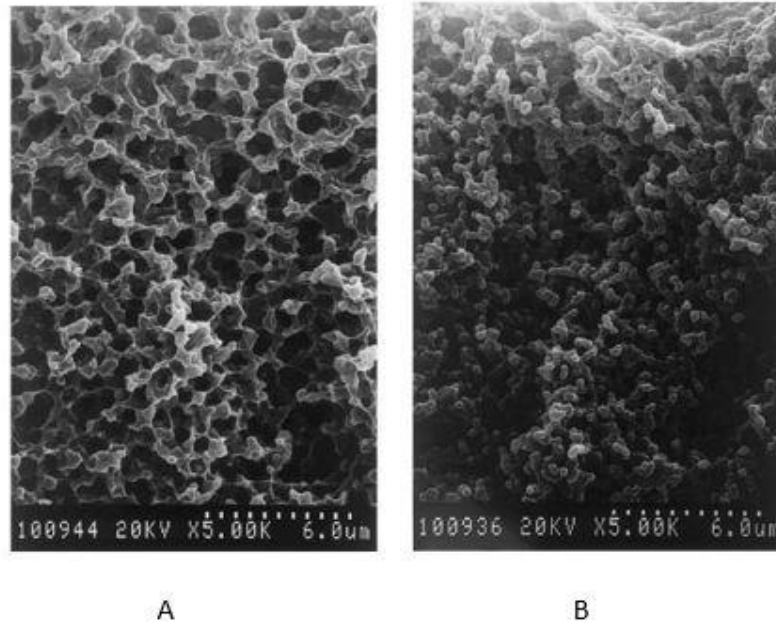
Figure 16. Cross-sectional SEM photomicrographs of membrane from a 15 wt.% of
EVAL solution immersed in water after (A) 30 min and (B) 45 min of evaporation
(Young et al. 2000)

2.6 PEBAX 1657

Among gas separation polymeric membranes, extensive research about rigid polyamides
was done due to their glassy and selective nature. On the other hand, rubbery polymers
such as poly-ethers have large free volume due to their chain flexibility (Surya Murali et
al. 2010a). Poly- (ether block-amide), which is known as PEBAX, is a thermoplastic
elastomer that combines the properties of the two former polymers types. It has linear
chains because of the hard polyamide segments that enhance the mechanical strength.
Moreover, it has flexible polyether segments that improve the gas permeability due to the
chain mobility of ether linkages (Flesher 1986). By varying ether and amide composition,
more than 15 types of PEBAX were synthesized (Tocci et al. 2008) (Potreck et al. 2009)
(Liu, Chakma, and Feng 2006). PEBAX 1657, which is the type that was used in this

31

study, contains 40% of amide groups and 60% ether linkages. PEBAX 1657 structure is shown in Figure 17 (x=0.6 and y=0.4) (Surya Murali et al. 2010a) where the constituting chemical groups with their Van der Waals' volume and molecular weight are given in Table 4 (Surya Murali et al. 2010a). The physical properties of PEBAX 1657 can be summarized in Table 5 (Azizi et al. 2017)
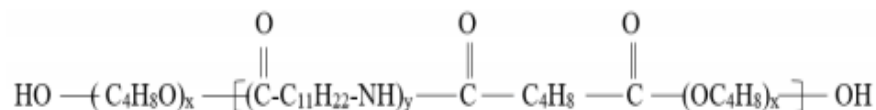
Figure 17. PEBAX 1657 chemical structure (Surya Murali et al. 2010a)

Table 4. *The molecular weights and van der Waals' volume for each chemical group in PEBAX 1657 (Surya Murali et al. 2010a)*
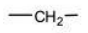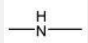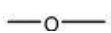
Chemical Group	Molecular weight (g/mol)	Van der Waals' Volume (cm³/mol)
$\overset{O}{\underset{\parallel}{C}}$	28.01	10.7
$-CH_2-$	14.03	11.23
$-\overset{H}{N}-$	15.02	4.0
$-O-$	16.0	5.5

Table 5. *Certain mechanical and thermal properties of PEBAX 1657 (Azizi et al. 2017)*

Mechanical feature	Typical value	unit
Density	1.14	$g.cm^{-3}$
Water absorbency at 23°C and 24 h	120	wt. %
Melting point	204	°C
Glass transition temperature	−56	°C
Stress at break	32	MPa

The typical method to prepare pure PEBAX 1657 membrane is solvent evaporation phase inversion. PEBAX granules dissolve at a certain temperature in ethanol/water mixture (typically 70/30 wt%). Later on, the homogenous solution is cast and the solvent evaporates under specific conditions to form the solid-state of the membrane (Surya Murali et al. 2010a) (Hosseinzadeh Beiragh et al. 2016) (Isanejad, Azizi, and Mohammadi 2017). SEM image for pure PEBAX 1657 membrane is given in Figure 18 (Hosseinzadeh Beiragh et al. 2016)
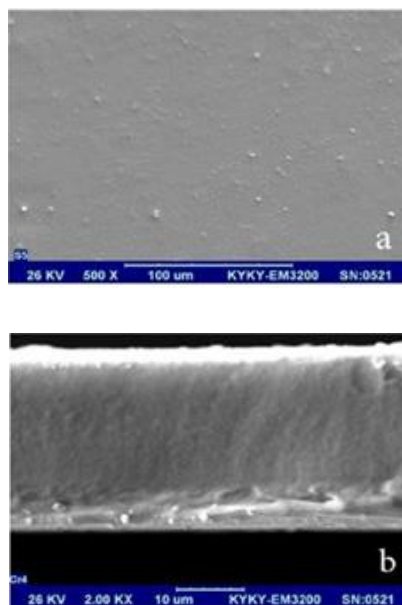
Figure 18. a) top and b) cross-section SEM images for PEBAX 1657 (Hosseinzadeh Beiragh et al. 2016)

Nevertheless, PEBAX 1657 can be dissolved in different types of solvents. Table 6 shows the available candidates with the synthesizing process conditions and the color of the homogenous solution (Isanejad et al. 2017).

Table 6. *Synthesizing process conditions of PEBAX 1657 by different solvents with the final optical properties (Isanejad et al. 2017)*

| Sample | Solvent | Operating conditions | | Drying conditions (°C) | Physical properties: Color |
		Temperature (°C)	Stirring time (h)		
Pebax-NMP	NMP	125	3	70	Opaque-white smoke
Pebax-DMAc	DMAc	125	3	70	Opaque-white smoke
Pebax-DMF	DMF	125	3	70	Opaque-white smoke
Pebax-H_2O/EtOH	H_2O/EtOH (70/30 wt %) mixture	70	3	70	Opaque-colorless
Pebax-formic acid	Formic acid	25	0.5	25	Opaque-colorless

Ethanol-water mixture is not the favorite one among the above solvents for preparation mixed matrix membranes due to its low viscosity that make the fillers to be mobile in the membrane matrix (Isanejad et al. 2017). However, ethanol-water mixture prevents the polymer gelation and solidification at room temperature. Consequently, this solvent makes the polymer solution stable at room temperature which simplifies the manufacturing process thus it is environmentally and economically more feasible (Car et al. 2008).

According to a study in 2014, PEBAX 1657/solvent mass ratio plays a crucial role in the final separation performance. For certain ethanol/water mixture (90/10 wt %) the following results in Table 7 were obtained for different PEBAX 1657 mass ratios (Wang et al. 2014).

Table 7. *The effect of PEBAX 1657 (wt %) on permeability and selectivity (Wang et al.*
2014)

Concentration of Pebax (wt%)	$\alpha_{(CO_2/N_2)}$	CO_2 permeance (GPU)
1	32.6±7.0	111.7±6.3
2	47.9±8.8	30.0±3.0
3	71.0±3.6	22.6±2.8

As it can be seen easily, the selectivity has a direct relation with PEBAX 1657 concentration. On the other hand, carbon dioxide permeance increases as the concentration of PEBAX 1657 declines. It should be mentioned that to achieve desired mechanical stability with defect-free membranes is painstakingly difficult with low PEBAX 1657 concentrations (Wang et al. 2014).

A pure PEBAX 1657 membrane with (4 wt%) that was prepared by dissolving the granules in 70/30 wt% ethanol/water mixture at 90 °C for 6 hours and tested at 30 °C has the following permeability for different gases (Surya Murali et al. 2010a). This makes it a suitable candidate for usage in gas separation, deserving further study.

Table 8. *The separation performance of pure PEBAX (4% wt) (Surya Murali et al.*
2010a)

Gases	Permeability (Barrer)	CO_2 Selectivity
H_2	32.11	1.74
CO_2	55.85	1
N_2	1.39	40.2
O_2	4.69	11.9

2.7 Mixed Matrix membrane (MMM)

As was mentioned previously, MMMs were produced to compensate for the disadvantages of both the organic and inorganic membranes. In MMMs case, inorganic fillers are embedded within a polymeric matrix. The separation mechanism in MMMs can be shown in Figure 19. CO_2 path is shorter than other gas molecules due to the natural properties of the fillers that select CO_2 (Wu et al. 2014a). For this reason, MMMs improve both the selectivity and the permeability of the polymeric membrane. In this study, ZIF-8 was selected to be the inorganic filler for PEBAX 1657 membrane.
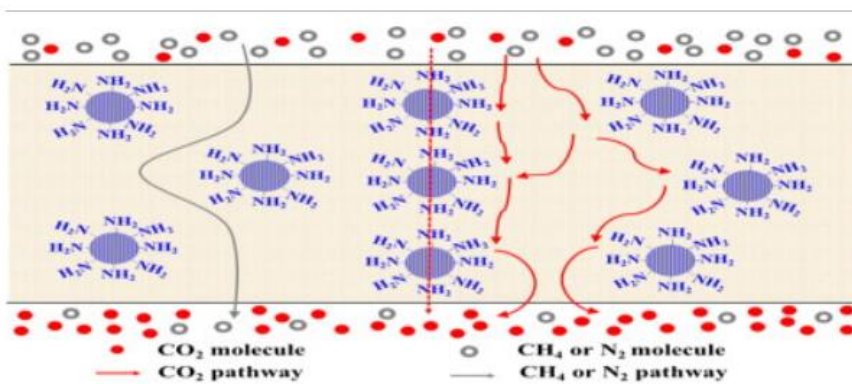
Figure 19. The gas transfer mechanism in through MMMs (Wu et al. 2014a)

2.7.1 Zeolitic imidazolate framework-8 (ZIF-8)

ZIFs in general, are considered as crystalline porous materials that are a subclass of MOFs (Keser 2012). ZIFs have properties such as modifiable organic, bridging ligand, diversity of pore system and framework structure, high surface area, high chemical and thermal stability. These are valuable properties of both zeolites and MOFs (Cravillon et al. 2009). For this reason, ZIFs have the potential to be used in a wide range of applications like separation, catalysis, gas storage, and construction of advanced nanotechnology devices (Venna and Carreon 2010). Zn, Co, or Ni are the divalent metal cations that are generally used in ZIFs production (Hamid and Jeong 2018). Compared to aluminosilicate zeolites, the interfacial property between the polymer matrix and sieve due to the presence of

imidazolate linkers in the ZIF framework. Moreover, it enhances the hydrophobicity of the material (Zhang et al. 2012).

ZIF-8 is a sodalite topology that has large pores of 11.6 A° which are two times larger than sodalite zeolites. These pores can be accessed through channels 3.4 A° in size (Jiang et al. 2009). Materials Studio software calculated the ZIF-8 structure as it can be seen in Figure 20 (Ordoñez et al. 2010). The surface area of ZIF-8 is 1300-1600 m^2/g where it has thermal stability up to approximately 400 °C. The high surface area of ZIF-8 yields perfect contact with the polymer matrix which makes a competitive candidate to be used in mixed matrix membranes (Song et al. 2012b).
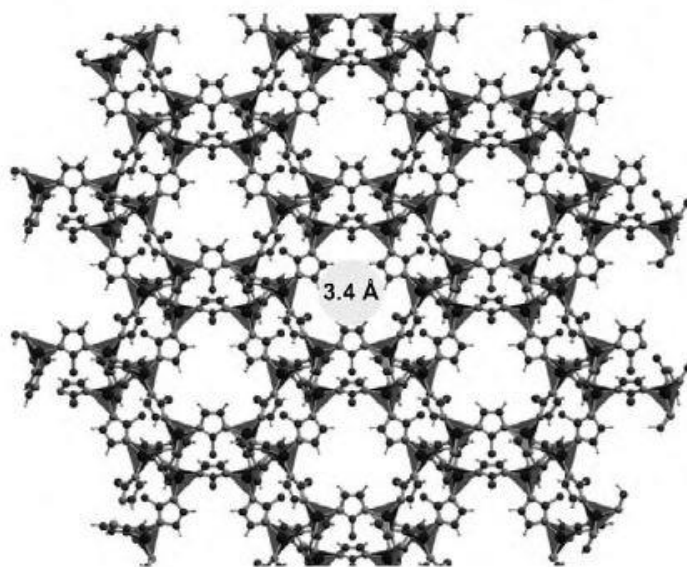
Figure 20. The calculated ZIF-8 particle structure (Ordoñez et al. 2010)

Different solvents were used to synthesize ZIF-8 such as dimethylformamide (DMF) (Ordoñez et al. 2010), methanol, diethylformamide (Pan et al. 2011), and water (Pan et al. 2011) (Huang et al. 2006). The mixing temperature in literature was varied from room temperature to 140 °C (Keser 2012). Moreover, the required synthesis time that was reported had a wide range, from 5 minutes (Pan et al. 2011) to one-month (Huang et al. 2006). For controlling the size of ZIF-8 particles, the concentration can be manipulated

(Di Renzo 1998) (Lethbridge et al. 2005) (Drews and Tsapatsis 2005) (Khan et al. 2011). Two factors that control this process are the kinetics of nucleation and growth (Di Renzo 1998) (Lethbridge et al. 2005) (Jhung, Lee, and Chang 2008). In the case of synthesizing zeolites, the growth rate is lower than the nucleation rate thus low concentrated solution medium results in larger particle size (Lethbridge et al. 2005). This was proven in a study where the size of zeolite A increased with water content in the synthesizing solution (Brar, France, and Smirniotis 2001). Nevertheless, MOFs have an opposite trend where the size of particles incline with reactant concentration in solvent (Khan et al. 2011) (Gascon, Aguado, and Kapteijn 2008) (Ramos-Fernandez et al. 2011).

Pérez-Pellitero et.al studied the adsorption rate of ZIF-8 for N_2, CH_4, and CO_2 with different pressures by experimental measurements and molecular simulation. An agreement between the experimental and simulation parts was found where the highest rate was recorded for CO_2 and the lowest one was for N_2 as can be shown in Figure 21 (Pérez-Pellitero et al. 2010). These results prove that ZIF-8 has the potential to be used in separation applications specifically for separating CO_2 from N_2 which is the main purpose of this study.
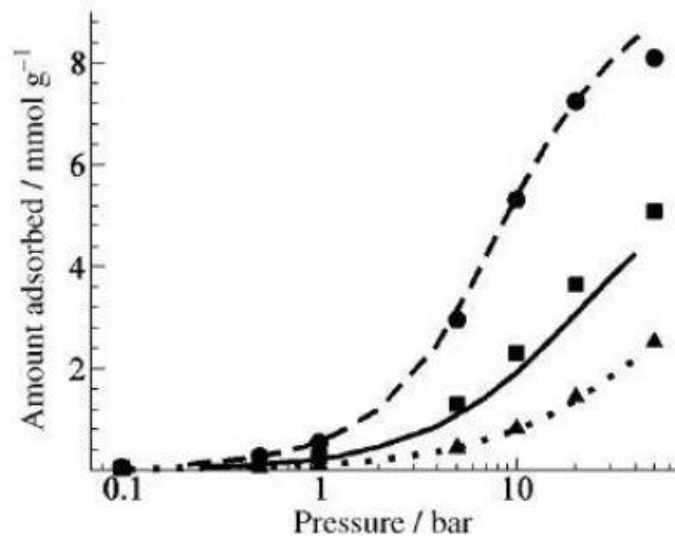
Figure 21. The experimental (**.......** N_2, **_____** CH_4, **-------** CO_2) and simulated (◄N_2, ■ CH_4, ●CO_2) isotherms of N_2, CH_4, CO_2 and in ZIF-8 results (Pérez-Pellitero et al. 2010).

2.8 Ohm's Law for Multi-layer Membranes

As Maxwell equations are considered to be fundamental basics that describe the classical electromagnetic phenomena. In a parallel electrical circuit, the voltage is constant whereas the current varies due to the resistance. For example, the total resistance in the circuit in Figure 22 can be calculated using Equation [10]
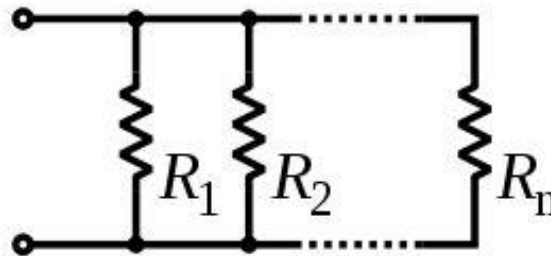
Figure 22. Parallel electrical circuit

$$\frac{1}{R_{total}} = \frac{1}{R_1} + \frac{1}{R_2} + \cdots + \frac{1}{R_n} \quad (10)$$

In membrane technology, the concept of the electrical circuit can be used wherein gas separation resistance can be calculated using Equation [11]

$$R_{total} = \frac{\Delta p_A * L}{J_A * P_{total}} \quad (11)$$

The above equation describes the total resistance within the membrane matrix. Partial pressure and species flux within the matrix are assumed to be constant. Thus, by applying the electrical circuit concept, the latter two parameters represent the voltage in this case where the current is the species permeability over the thickness of each layer. Substituting Equation [11] into Equation [10] gives the following Equation.

$$\frac{\Delta p_A * L}{J_A * P_{total}} = \frac{\Delta p_A * L_1}{J_A * P_1} + \frac{\Delta p_A * L_2}{J_A * P_2} + \cdots + \frac{\Delta p_A * L_n}{J_A * P_n} \quad (12)$$

Which can be simplified more as follows:

$$\frac{1}{P_{total}} = \frac{x_1}{P_1} + \frac{x_2}{P_2} + \cdots + \frac{x_n}{P_n} \quad (13)$$

$$\frac{1}{P_{total}} = \sum_{i=1}^{n} \frac{x_i}{P_i} \quad (14)$$

For this reason, the total permeability of a multi-layer membrane depends mainly on the permeability of each layer and its thickness. This model was used to predict the CO_2 and N_2 permeability of double-layer PEBAX 1657/PDMS membranes. Figure 23 compared the experimental and model results for CO_2 permeability for different thickness ratios (PDMS/PEBAX) (Selyanchyn, Ariyoshi, and Fujikawa 2018). Even with considering the error resulted due to thickness measurements shown with pink shadow, it can be observed that experimental data did not overlap with modeled data. As a result, it can be inferred

that other factors such as mechanical or morphology change within the membrane matrix due to casting a second layer might contribute to making this deviation.
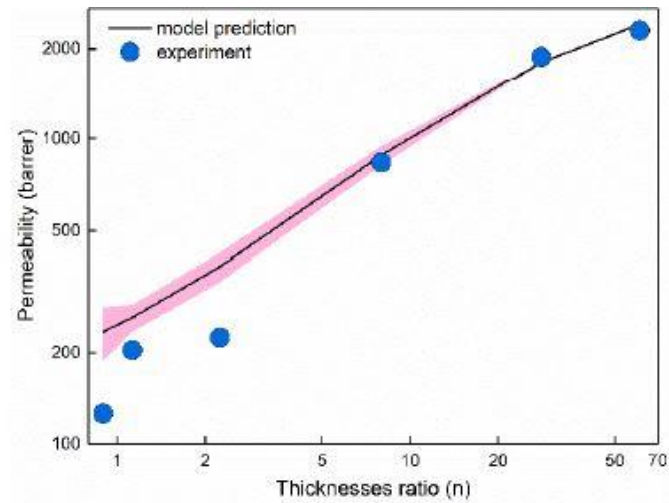
Figure 23. The variation of permeability results (by experiment and simulation) with a thickness ratio of (PDMS/PEBAX 1657) (Selyanchyn et al. 2018)

CHAPTER 3

EXPERIMENTAL METHODS

3.1 Pure PEBAX Synthesis

3.1.1 Materials

PEBAX 1657 granule (code: 10244) was purchased from ARKEMA. Ethanol-water mixture was utilized to dissolve these polymer granules. Absolute ethanol was purchased from J. T. Baker. Deionized water was mixed with ethanol to form the desired solvent for dissolving PEBAX 1657 granules.

3.1.2 Preparation of Membranes

The phase inversion technique was selected to synthesize pure PEBAX 1657 membranes. A 50 grams of ethanol-water mixture (70/30 wt %) was used to dissolve 2 grams of PEBAX 1657 to obtain 4 wt % PEBAX 1657 at 70 ºC. These granules were dried for more than one week in an oven at 80 °C. The water bath was heated to 70 °C and then the mixture was placed in it to be mixed at 300 rpm for 2 hours. This mixing time and power ensured forming a homogenous solution. The mixture was cooled down to room temperature for one hour at ambient conditions while continuing the mixing process. For phase inversion to be accomplished, the solution was poured onto a Teflon dish and placed in the casting system for one day which is going to be explained in Section 3.1.3 in detail.

At this time most of the solvent is expected to be evaporated. To guarantee complete evaporation and to enhance the mechanical and thermal stability of the membrane it was located for one day in an oven at 60 °C and atmospheric pressure. Finally, the oven was vacuumed (0.2 bar) for another day at the same temperature. Table 9 summarizes the selected parameters to synthesize pure PEBAX 1657 membranes.

Table 9. *Selected parameters to synthesize pure PEBAX 1657 membrane*

Parameter	Value	Time
Dissolving Mixing Power	300 rpm	2 hours
Dissolving Mixing Temperature	70 °C	2 hours
Solution Cooling Temperature	Room Temperature	1 hour
Casting Temperature/ Airflow Rate	35 °C/ 7.5 L/s	One Day
Evaporation Temperature	60 °C	One Day
Vacuumed Evaporation (0.2 bar)	60 °C	One Day

3.1.3 Casting System

Regulating the casting temperature was the aim of the casting system since the room temperature cannot be constant due to weather conditions. Moreover, the casting system provides a convection mass transfer at liquid-gas interface to improve the evaporation of the solvent and ensure a phase inversion process. The casting system consists of two parts. The first part is the heating box, which is divided into two areas. The box has a rectangular

window with a 1 cm width that allows air to flow into the first section where the air is heated by two heaters. For improving the heating efficiency, a separator wall with a small roof is located between the two areas to enhance air mixing in that zone. The hot air that flows into the other side is sucked and sent by three computer fans with adjustable inlet air velocity between (0.0-4.0) m/s, then sent to the second part of the casting system which is the tunnel. This tunnel has a length of 50 cm, a width of 15 cm, and a height of 10 cm where 3-4 Teflon dishes can be located there comfortably. A temperature controller was used as well as a fan power controller as shown in Figure 24. The system was operating two hours before casting the membranes to reach stable air temperature at 35 °C. Air temperature was observed to be stable over all the casting period with minimal fluctuating of ±1 °C.
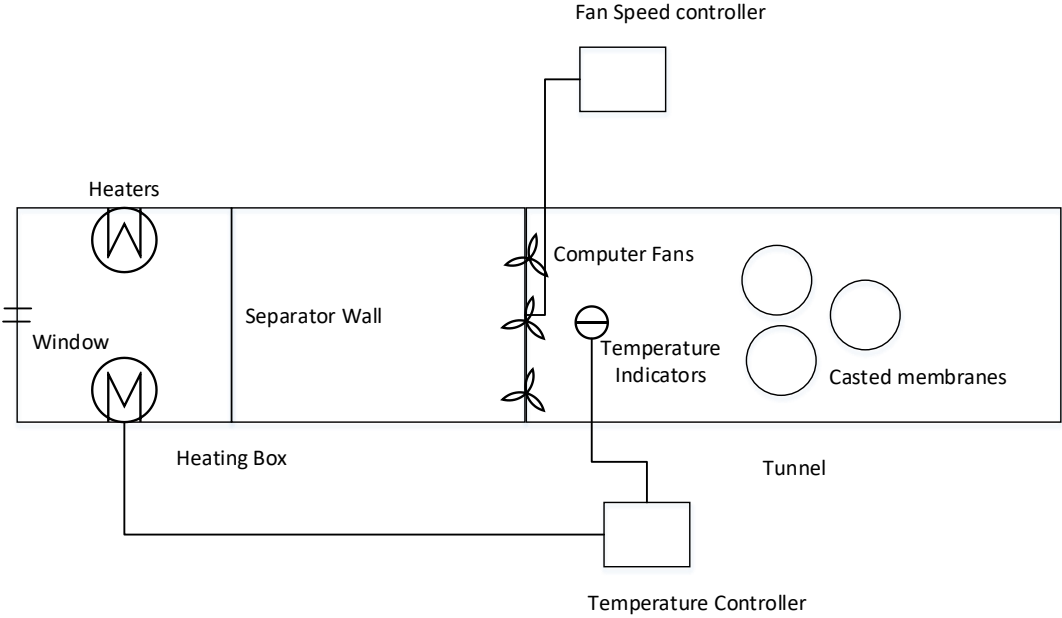
Figure 24. Casting system in 2D

3.2 Synthesizing ZIF-8

3.2.1 Materials and Reaction

Zinc nitrate hexahydrate [ZnNO$_3$6H$_2$O, 98% purity], 2-methylimidazole [C$_4$H$_6$N$_2$, 99% purity] (Hmim) and methanol [MeOH, 98% purity]. These materials were purchased SIGMA ALDRICH, A ALDRICH, and EMSURE, respectively.

The following reaction occurs

$$6Zn(NO_3)_2 * 6H_2O + 12C_4H_6N_2 + CH_3OH$$
$$\rightarrow Zn_6N_{24}C_{48}H_{60} + CH_3OH + 12HNO_3 + 36H_2O$$
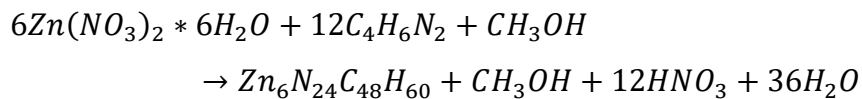
3.2.2 Preparation Method

As shown in Figure 25, two separate solutions should be prepared with methanol medium. The first one contains Hmim whereas the other one contains zinc nitrate hexahydrate. Both solutions are separately mixed at room temperature with a stirring velocity of 450 rpm for only five minutes. Then the obtained Hmim solution is added to the zinc solution and mixed for one hour at the same conditions. The reaction can be observed by color-changing that turns to white from colorless. Later on, ZIF-8 particles can be collected using a centrifuge.
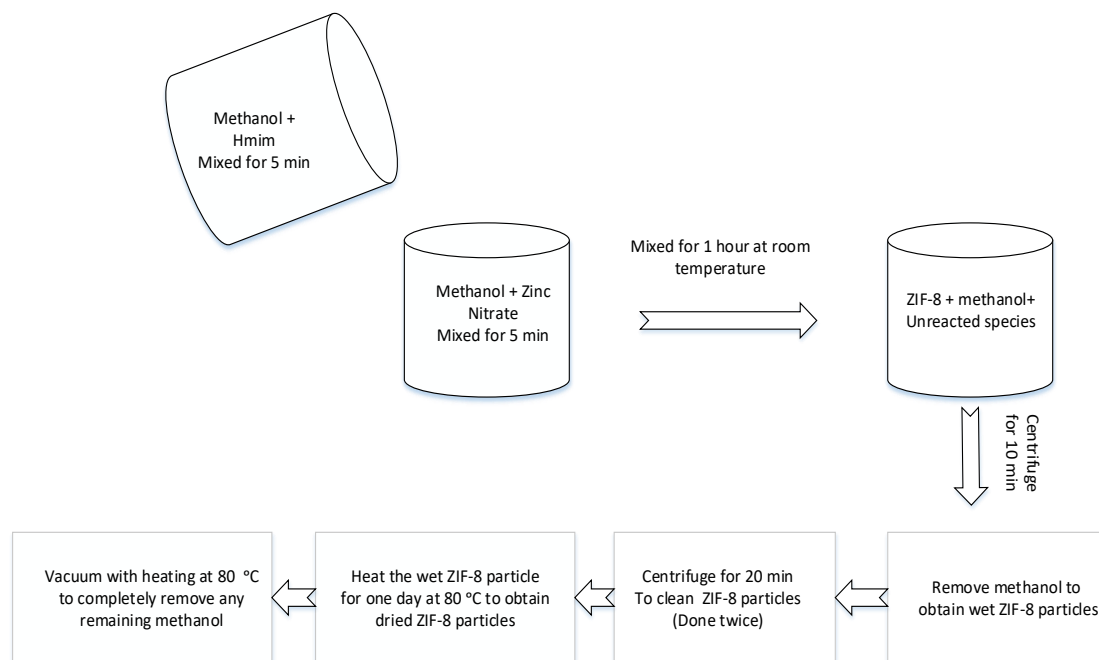
Figure 25. Synthesis procedure of ZIF-8

3.2.3   Controlling the Size of ZIF-8 Particles

In this study, two different sizes of ZIF-8 particles were produced. As mentioned in the literature review, nucleation and crystal growth in ZIFs has a direct relation with the reactant concentration at the initial point. For this reason, as the methanol ratio to the reactant increases, the size of the obtained particles reduces. This was proven in a previous study as can be shown in Table 10 (Keser Demir et al. 2014). The two sizes (67 and 323 nm) have the following ratios as can be seen in Table 11

Table 10. *The effect of methanol/Zn+ ratio on the size of ZIF-8 particles (Keser Demir et al. 2014)*

MeOH/Zn$^+$ ratio	Average particle size by SEM (nm)
1043	60 ± 10
605	80 ± 20
528	120 ± 80
348	190 ± 10
174	360 ± 40
87	600 ± 100

Table 11. *Reactants amounts used in preparing ZIF-8 particles*

ZIF-8 Size (nm)	Methanol mass (g)	Zinc Nitrate mass (g)	Hmim mass (g)	Mass ratio MeOH/Zn$^+$/Hmim	Molar ratio MeOH/Zn$^+$/ Hmim
67	130.18	1.73	3.77	75.25:1:2.18	699:1:7.9
323	135	7.2	15.7	18.75:1:2.18	174.1:1:7.9

3.2.4 Cleaning and Washing Process

After the batch reaction completed, the obtained ZIF-8 particles are collected in plastic cylindrical containers and placed in a centrifuge for ten minutes at 8000 rpm. The collected particles were washed by methanol and gently shaken for 2 minutes before locating them

in the centrifuge for 20 minutes at 8000 rpm to remove the unreacted species. This process was repeated twice to ensure that most of the unreacted species were removed. Furthermore, to get rid of all methanol, particles were placed in the oven at 80 °C for one day. Then, they were vacuumed at 0.2 bar for another day at the same temperature. Removing methanol completely reduces the possibility of blocking the pores in the ZIF-8 structure which is required to enhance the transportation of gas molecules through the particles.

3.3 Mixed Matrix Membranes

3.3.1 Materials

The same materials that were included in synthesizing pure PEBAX 1657 and ZIF-8 were used. Moreover, Triton x100 which was provided by FLUK was used to help in reducing the particle agglomeration

3.3.2 Synthesizing Procedure

In the literature, three methods were proposed to synthesize MMMs as shown in Figure 26 (Lin et al. 2018)
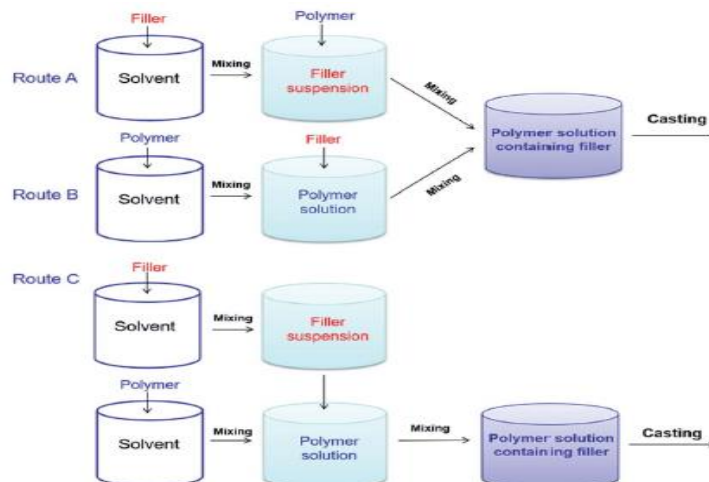
Figure 26. Possible methods to synthesize MMMs (Lin et al. 2018)

49

In this work, the third method was used with making some modifications to improve the homogeneity of ZIF-8 particles distribution within the matrix. The concentration of ZIF-8 particles in all MMMs prepared in this study was 5 wt % of PEBAX 1657. This amount of ZIF-8 was added to 30 wt % of the ethanol-water solvent used in the casting solution to prepare the ZIF-8 solution. An Ultrasonic device was used for 2 min to disperse the ZIF-8 particles then stirred at 400 rpm for one day to form a completely homogenous solution. PEBAX 1657 solution was prepared in the next day by stirring the polymer granules with the solvent for 2.5 hours at 70 °C. Later on, the ZIF-8 solution is added to PEBAX 1657 solution using a plastic pipette to ensure that the few unmixed particles to not be transferred to the final solution. However, this remaining amount is negligible that does not affect the weight of ZIF-8 in the solution. In this step, two drops of Triton x100 were added to reduce the possibility of agglomeration and the whole solution was placed in the ultrasonic device for 2 min and then stirred at 300 rpm for 3 hours at room temperature. After that, before casting, the solution was degassed using the ultrasonic device for 3 minutes to reduce the possibility of any defects in the final structure of the membranes. Finally, casting and annealing process is exactly similar to the synthesis of pure PEBAX 1657 membrane explained in Section 3.1.2. Figure 27 describes the MMM preparation procedure. Moreover, Appendix C shows all the amount of material used to prepare each membrane in this work.

```
┌─────────────────┐
│ Use ultrasonic  │
│ for 2 min to    │
│ dissolve the    │
│ dried ZIF-8     │
│ particles in    │
│ Ethanol-water   │
│ mixture         │
└────────┬────────┘
         │
         ▼
┌─────────────────┐        ┌─────────────────┐
│ Stir the        │        │ Dissolve the    │
│ mixture at      │        │ PEBAX 1657      │
│ 400 rpm for     │        │ granules in the │
│ one day         │        │ ethanol-water   │
│                 │        │ mixture for 2.5 │
│                 │        │ hours at 70 °C  │
└─────────────────┘        └─────────────────┘
```

Add triton x100

```
┌─────────────────┐
│ Put the mixture │
│ in the          │
│ ultrasonic for  │
│ 2 min           │
└────────┬────────┘
         │
         ▼
┌─────────────────┐
│ Stir the        │
│ mixture for 3   │
│ hours at room   │
│ temperature     │
└────────┬────────┘
         │
         ▼
┌─────────────────┐
│ Degas the       │
│ mixture for 3   │
│ min             │
└────────┬────────┘
         │
         ▼
┌─────────────┐      ┌─────────────────┐      ┌─────────────────┐
│ Cast the    │      │ Put the         │      │ Put the         │
│ solution at │ ───▶ │ membrane in     │ ───▶ │ membrane in     │
│ 35 °C for   │      │ oven for 1 day  │      │ vacuumed oven   │
│ one day     │      │ at 60 °C        │      │ for 1 day at    │
│             │      │                 │      │ 60 °C           │
└─────────────┘      └─────────────────┘      └─────────────────┘
```

Figure 27. PEBAX 1657 + ZIF-8 MMM synthesis procedure

3.4 Modification of Membrane Surface by Solvent Penetration and Preparation of Double-layer Membranes

In this section, membranes with two PEBAX-1657 layers were prepared. The bottom layer was prepared in the same procedure that was used for pure and mixed matrix membranes. After one day of casting and solvent evaporation, a 10 mL of 1-4 % PEBAX 1657 solution in ethanol-water (70%-30% w) mixture was poured on the top of the bottom layer. Then the casted membranes were kept in casting system for one day under the flow of hot air (35 °C, 7.5 L/s). Later, these membranes were annealed at 60 °C in air at atmospheric pressure for one day and 60 °C in vacuum (0.2 bar) for one day more. To ensure the reproducibility, each type was prepared three times. Table 12 summarizes all the types of membranes that were synthesized in this work. Appendix C was prepared for further details on the amount of all materials used in the synthesizing these membranes.

In addition, the surface of single layer membranes was modified by using ethanol-water (70%-30% w) mixture. After one day of casting, an amount of ethanol-water mixture (3 or 12.5 mL) was poured on the top of the bottom layer. Then, Teflon dishes were covered completely for two hours to reduce the evaporation of ethanol-water mixture and improve the solvent penetration into the membranes. Later, the same procedure used for preparation double-layer membranes was followed.

Table 12. *Synthesized membranes in this study (cast at 35 °C and airflow of 7.5 L/s, annealed at 60 °C in the atmosphere for one day and 0.2 bar for another day)*

Membrane code	Membrane description	Reason of synthesizing
M1.a	Single-layer 4 wt % pure PEBAX 1657	Reference membrane
M1.b	Single-layer 4 wt % pure PEBAX 1657 casted at different airflow (40 m^3/s)	The effect of air flow rate in the casting step
M1.c	Single-layer 4 wt % pure PEBAX 1657 that was cast only and not annealed	The effect of annealing steps on eliminating the solvent from the membrane matrix
M1.d	Single-layer 4 wt % pure PEBAX 1657 casted with stagnant air	The effect of air flow rate in the casting step
M2	Single-layer 4 wt % pure PEBAX 1657 was cast for one day then 3 mL solvent poured on its surface	The effect of the solvent penetration
M3	Single-layer 4 wt % pure PEBAX 1657 was cast for one day then 12.5 mL solvent poured on its surface	

Table 12. *(cont'd) Synthesized membranes in this study (cast at 35 °C and airflow of 7.5 L/s, annealed at 60 °C in the atmosphere for one day and 0.2 bar for another day)*

Membrane code	Membrane description	Reason of synthesizing
M4	The bottom layer of 4 wt % pure PEBAX 1657 was cast for one day then 4 wt % pure PEBAX 1657 solution was cast on its surface as the second layer	The effect of casting a second layer on the top of the first one
M5	The bottom layer of 4 wt % pure PEBAX 1657 was cast for one day then 2% pure PEBAX 1657 solution was cast on its surface as the second layer	The effect of PEBAX 1657 ratio in the top layer
M6	The bottom layer of 4 wt % pure PEBAX 1657 was cast for one day then 1% pure PEBAX 1657 solution was cast on its surface as the second layer	
M7	Single-layer 4 wt % pure PEBAX 1657 (4 wt %) loaded with 5 wt % ZIF-8 (67 nm)	Mixed matrix membranes with different sizes of ZIF-8 particles

Table 12. *(cont'd) Synthesized membranes in this study (cast at 35 °C and airflow of 7.5 L/s, annealed at 60 °C in the atmosphere for one day and 0.2 bar for another day)*

Membrane code	Membrane description	Reason of synthesizing
M8	Single-layer 4 wt % pure PEBAX 1657 loaded with 5 wt % ZIF-8 (323 nm)	Mixed matrix membranes with different sizes of ZIF-8 particles
M9	Bottom layer 4 wt % pure PEBAX 1657 loaded with 5 wt % ZIF-8 (67 nm) was cast for one day then 4 wt % pure PEBAX 1657 loaded with 5 wt % ZIF-8 (67 nm) was cast as the top layer	Effect of the double-layer method on MMMs
M10	Bottom layer 4 wt % pure PEBAX 1657 loaded with 5 wt % ZIF-8 (323 nm) was cast for one day then 4 wt % pure PEBAX 1657 loaded with 5 wt % ZIF-8 (323 nm) was cast as the top layer	

3.5   Single-gas Permeability Test

The objective of this work is to improve the carbon dioxide permeability relative to the pure PEBAX 1657 membrane. Nitrogen permeability was also measured to calculate the ideal selectivity of these modified membranes. Single-gas system was used to accomplish this target. Both gases are sent to a three-way valve from cylindrical storages. The gases are sent to feed pressure transducer, feed valve for membrane module, and purge valve. The permeated gases are measured by another pressure transducer which is in vacuum initially. The system as shown in Figure 28 is designed such that all parts can be vacuumed. Moreover, the purge routes were located in the feed storage and the testing system for safety purposes. The variation of the permeate pressure with time is recorded by software on the computer. The membrane thickness is measured by taking the average of the thickness of ten different locations in the membrane by Vernier Caliper. Later on, a calculation which is shown in detail in Appendix D is done to find the permeability of both gases. Consequently, the ideal selectivity of the membrane can be found. Figure 29 shows the algorithm that was used in testing the synthesized membranes. The repeatability was verified by testing the carbon dioxide permeability since it takes a shorter time compared to nitrogen which took more than 12 hours. Furthermore, the reproducibility was checked by measuring three different membranes that were synthesized in three different batches. The results were taken as long as the three membranes give the same outputs with a tolerated error of 10 % from their average. The system was checked regularly by applying a vacuum for one day and observing the pressure change in the feed and permeate sides. As long as no significant change in pressure occurs, this proves that the system works properly with no leaks. This process eliminated any experimental error that the system might produce. Table 13 summarizes the parameters of the single-gas permeating test

Table 13. *Parameters of single-gas permeability test*

Parameter	Value
Feed pressure	4 Bar
Permeate pressure	0.09 Bar
Final pressure to stop the testing process	0.7 Bar
Permeation temperature	35 °C
Permeate chamber volume	27.3 cm^3
Active membrane area	9.6 cm^2
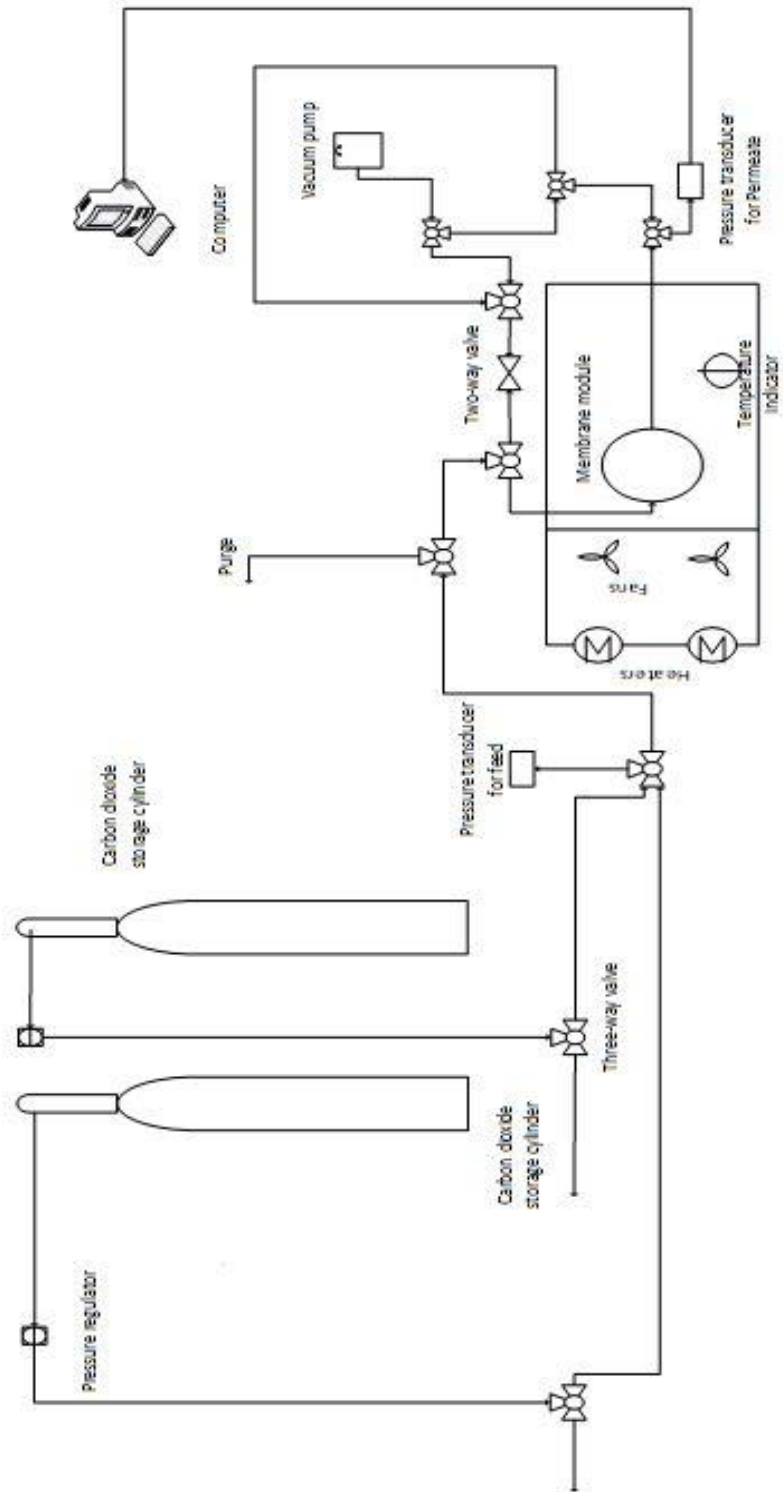
Figure 28. Single-gas system used for testing the synthesized membranes
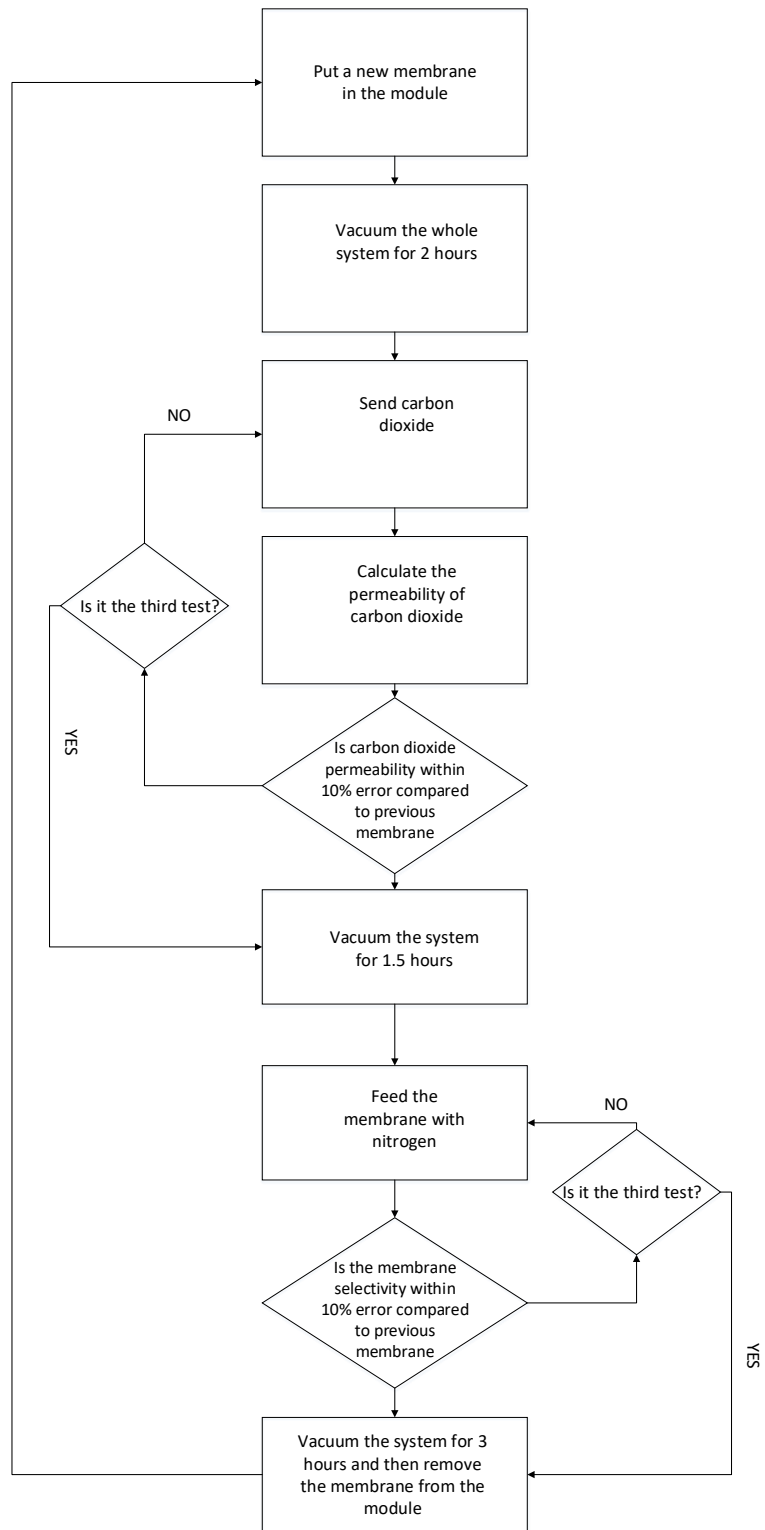
Figure 29. Algorithm of testing membranes in single-gas system

3.6 Characterization Methods

In this study, five types of techniques were used to characterize the synthesized materials. Characterization played a crucial role to understand and prove the fundamental theories of this work. A brief description and usage are given in this section for each characterization method.

3.6.1 X-Ray Diffraction (XRD)

This technique aims to measure the crystallinity of powder materials. X-rays produced in the cathode tube is sent to the sample which is reflected due to elastic diffraction and received in the detector. Bragg equation (15) describes the principle mathematically where θ is the half-angle between the incident and scattered beams, d is the distance between the atoms and λ is the wavelength. At different angles, the intensity is calculated and peaks are formed and compared to the material reference to identify the material and its crystallinity.

$$n\lambda = 2dsin\theta \qquad (15)$$

In this work, ZIF-8 crystallinity was measured by Philips model PW1840 (1729) X-ray diffractometer utilizing Ni filtered Cu-Ka radiation at a scan rate of 0.05 °/s. Furthermore, the voltage and current were 30 kV and 24 mA, respectively.

3.6.2 Scanning Electron Microscope (SEM)

SEM was used in this study to analyze the structure of the ZIF-8 and cross-sectional area of synthesized membranes. Electrons beams are sent and narrowed down to the sample by using anode and magnetic lenses. Then, more than one detector is used to detect all possible types of electrons that resulted from the contact of electron beams with samples which can be later presented as clear images. The electron beam requires an extremely high vacuum to protect the filament. In addition, electrons must be able to adequately interact with the sample. Polymers are typically long chains of repeating units composed primarily of "lighters" (low atomic number) elements such as carbon, hydrogen, nitrogen, and oxygen. These lighter elements have fewer interactions with the electron beam which

yields poor contrast, so often a stain or coating is required to view polymer samples. SEM imaging requires a conductive surface, so a large majority of polymer samples are sputter-coated with metals, such as gold.

ZIF-8 was diluted with ethanol and two drops were taken to the top of the flat sheet of tin which was covering a metal surface. Besides, liquid nitrogen was used to cut the polymers which were coated later by gold or platinum. The magnification varied from one sample to another as required.

3.6.3   Energy Dispersive X-ray (EDX)

This method was used in this work to investigate solvent penetration through the polymer matrix. After one day casting, an amount of solvent was poured on the top of the dried pure PEBAX 1657 membrane. This solvent contained sodium sulfate (Na_2SO_4). This experiment aimed to track sodium through the membrane matrix. As a result, the penetration depth of the solvent can be estimated. This analysis was also done for the pure PEBAX 1657 membrane that has no additional factor to figure out the difference.

3.6.4   Optical Microscope

The optical microscope was used to understand the behavior of the solvent that dissolves through the membrane matrix. Since colors can be differentiated and seen in the optical microscope a pink dye was mixed with a solvent. A 50-ppm dye solution was prepared where the medium was ethanol. Only 4 wt % of this solution was added in each type of the membranes synthesized for characterization.   For analysis by optical microscopy, another set of membranes with the same conditions given in Table 4. Since the colored membranes cannot be used in gas permeation, a new set was prepared. The code numbers and preparation conditions for this new set of membranes was summarized in Table 14 and Appendix C contains all the compositions of these membranes.

Table 14. *Synthesized membranes for Optical Microscope (cast at 35 °C and airflow of 7.5 L/s, annealed at 60 °C in the atmosphere for one day and 0.2 bar for another day)*

Membrane code	Membrane Description	Parameter to investigate
OPM1	Single-layer 4 wt % pure PEBAX 1657	Reference
OPM2	4 wt % pure PEBAX 1657 cast for one day, then 10 mL ethanol-water solvent with pink dye was poured on the top	To observe the penetration of the solvent into the membrane matrix
OPM3	4 wt % pure PEBAX 1657 cast for one day, then 4 wt % PEBAX 1657 solution with pink dye was poured on the top	To observe how the solvent penetrates in the double layer from the top and bottom
OPM4	4 wt % PEBAX 1657 solution with dye was cast for one day, then pure PEBAX 1657 solution was poured on the top	
OPM5	4 wt % pure PEBAX 1657 cast for one day, then ethanol-water solvent with pink dye was poured on the top and removed after 5 min	The time required for the solvent to penetrate
OPM6	4 wt % pure PEBAX 1657 cast for one day, then ethanol-water solvent with pink dye was poured on the top and removed after 30 min	

Table 14. *(cont'd) Synthesized membranes for Optical Microscope (cast at 35 °C and airflow of 7.5 L/s, annealed at 60 °C in the atmosphere for one day and 0.2 bar for another day)*

Membrane code	Membrane Description	Parameter to investigate
OPM7	4 wt % pure PEBAX 1657 cast for one day, then ethanol-water solvent with pink dye was poured on the top and removed after 1 hour	The time required for the solvent to penetrate
OPM8	4 wt % pure PEBAX 1657 cast for one day, then ethanol-water solvent with pink dye was poured on the top and removed after 2 hours	
OPM9	4 wt % pure PEBAX 1657 cast for one day, then 0.5 mL ethanol-water solvent with pink dye was poured on the top	The effect of the solvent amount
OPM10	4 wt % pure PEBAX 1657 cast for one day, then 1 mL ethanol-water solvent with pink dye was poured on the top	
OPM11	4 wt % pure PEBAX 1657 cast for one day, then 3 mL ethanol-water solvent with pink dye was poured on the top	
OPM12	4 wt % pure PEBAX 1657 cast for one day, then 12 mL ethanol-water solvent with pink dye was poured on the top	

3.6.5 Thermogravimetric Analysis (TGA)

The thermal behavior of the membrane samples was determined by the variation of the temperature. Physical and chemical phenomena such as thermal decomposition or evaporation can be understood by using TGA. This analysis aims to figure out the effect of the remaining amount of the residue solvent. Moreover, TGA can provide a solid comparison between the single- to double-layer membranes. Three types of membranes were tested by TGA. These membranes are, single-layer pure PEBAX 1657 cast for one day only, single-, and double-layer pure PEBAX 1657 membranes. The conditions used for TGA are summarized in Table 15

Table 15. *The parameters that were used in TGA analysis*

Detector Type	DTG-60H
Atmosphere	Air
Flow Rate	60 [mL/min]
Heating Rate	20 [°C/min]
Hold Temperature	500 °C
Sampling Time	1 sec

CHAPTER 4

RESULTS AND DISCUSSION

4.1   Effect of Casting Process on the Synthesized Single-Layer Membranes

4.1.1   Structure of Single-Layers Membranes Observed by Naked-Eye

One of the main goals of this study is to synthesize neat membranes using the phase inversion technique without any bending, shrinkages, and wrinkles. After dissolving PEBAX 1657 in ethanol-water (70/30 wt %) mixture, the solution was cast on a Teflon dish at room conditions for one day. However, the naked-eye structure of membranes was not reproducible due to the change of the room conditions such as temperature. Figure 30 shows 4 wt % pure PEBAX 1657 membrane that was cast at winter in the room temperature where bindings and shrinkages were observed.
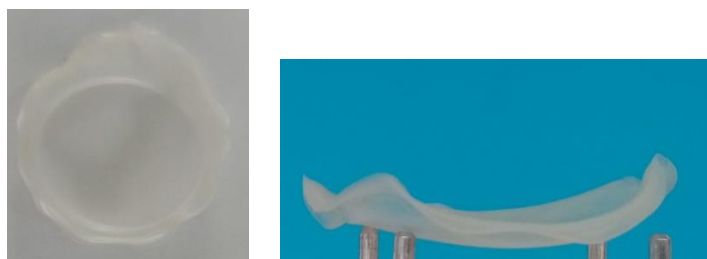
Figure 30. 4 wt % pure PEBAX membrane cast at room conditions in the winter

For this reason, membranes were cast in the system explained in Section 3.1.3, where an adjusted preheated airflow sweeps the evaporated ethanol-water mixture and controls the temperature. The representative concentration profiles in the casting step are demonstrated in Figure 31, where molecular diffusion occurs within the Teflon dish that has almost 2mm depth. On the other side, convective mass transfer due to the airflow can be considered as a boundary condition at the gas-liquid interface.
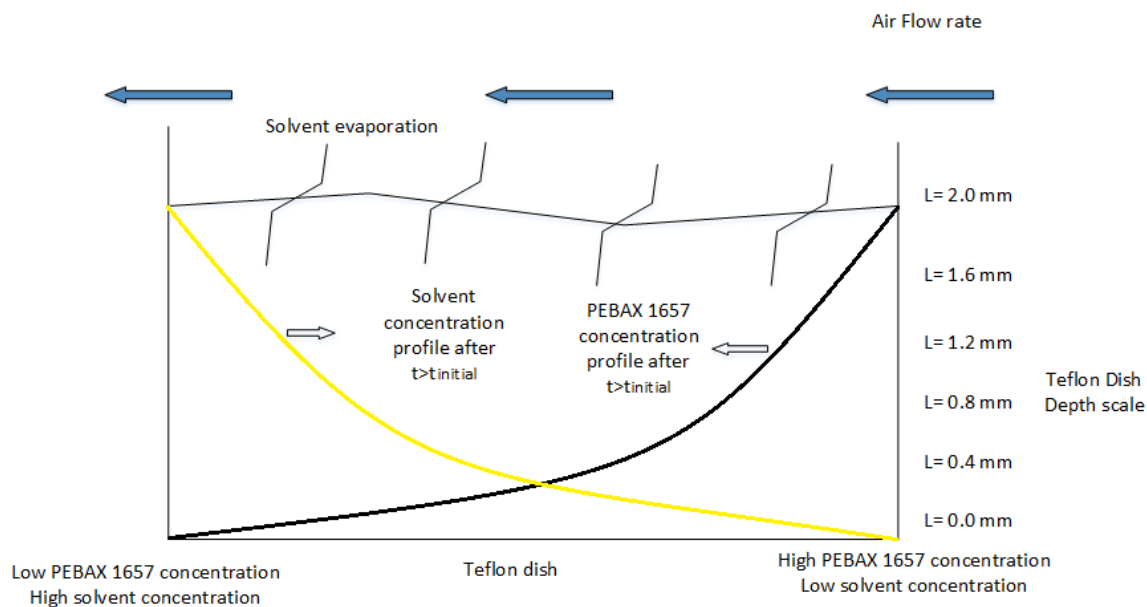
Figure 31. Simple schematic for evaporation of the casting solvent

This type of casting mechanism played a role in the polymer concentration as demonstrated hypothetically in Figure 31 where PEBAX 1657 wt % is expected to be highest at the gas-liquid interface and lower at the bottom of the Teflon dish. Moreover, the variation of the concentration is expected to be higher as it reaches the gas-liquid interface where mass transfers by convection, due to the flow of air, enhancing the solvent evaporation and sweeping the solvent vapor to keep the driving force for evaporation.

Two airflow rates (40 and 7.5 L/s) were used to investigate their impacts on the final structure of single-layer membranes. M1.b membrane was cast in a system that has an

airflow rate of 40 L/s at 35 °C and the obtained final structure was wrinkled and ruptured as shown in Figure 32. Whereas at an airflow rate of 7.5 L/s Figure 33 and Figure 34 show that the membranes are flat with no bending, shrinkages, nor wrinkles.

a   b

Figure 32. Top (a) and side (b) view of M1.b that was cast at an airflow rate of 40 L/s at 35 °C

a   b   c
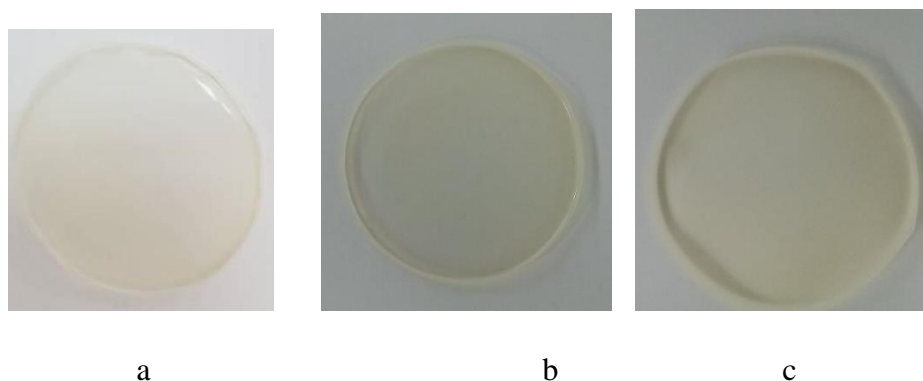
Figure 33. Top view of the final structure of membranes: a) M1.a b) M7 c) M8 was cast at an airflow rate of 7.5 L/s at 35 °C

a   b   c
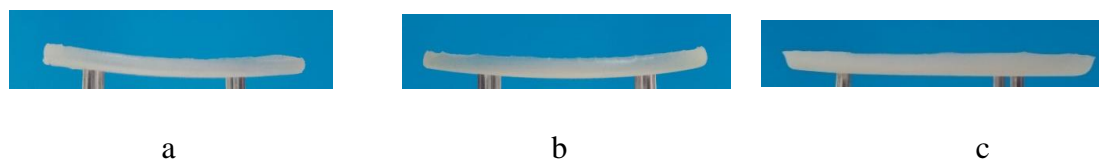
Figure 34. Side view of the final structure of membranes: a) M1.a b) M7 c) M8 was cast at an airflow rate of 7.5 L/s at 35 °C

At an airflow rate of 40 L/s, a significant variation of polymer concentration within the casting solution was created. In other words, there was a variation of density and viscosity within the matrix that created uneven forces. Furthermore, a temperature gradient might occur due to the solvent evaporation. Thus, these variations built up some stress within the membrane matrix that resulted in producing ruptured and wrinkled membranes. It was reported that at slow evaporation and condensation, these variations can be neglected if the thermodynamic factors such as temperature, pressure, and chemical potential are considered to be constant in the two phases (Bedeaux et al. 1992). For this reason, in our case, the best selection was to reduce the airflow.

Casting at room temperature which is the most economical method gives a disturbing error since the weather is changing over the year thus temperature cannot be controlled. It was reported that the casting conditions affect the membrane morphology thus separation performance (Borisov et al. 2019). For this reason, the casted system which is shown in Figure 24 was designed to guarantee a constant temperature and sweep the evaporated solvent through all the casting period. The airflow rate was set to be 7.5 L/s that has a Reynolds number of approximately 3840. Furthermore, Biot number was roughly estimated to be 45.6 which means that mass transfer convection had a great impact on the evaporation process at the liquid -gas interface.

An experimental analysis was performed to compare casting with the designed system at the two different flow rates (7.5 and 40 L/s) and room conditions. The change of weight with time, caused by solvent evaporation was recorded and showed in Figure 35. In all cases, an exponential decrease was observed where it was clearly higher at the airflow rate of 40 L/s.

For the other two cases, a slight difference in the evaporation rate appeared after five hours as the solvent amount decreased. However, over a long time, all cases are expected to evaporate almost the same amount of solvent. In general, this result proves that the effect of casting in the design system at 7.5 L/s was not significantly higher than casting in room temperature on the evaporation rate.
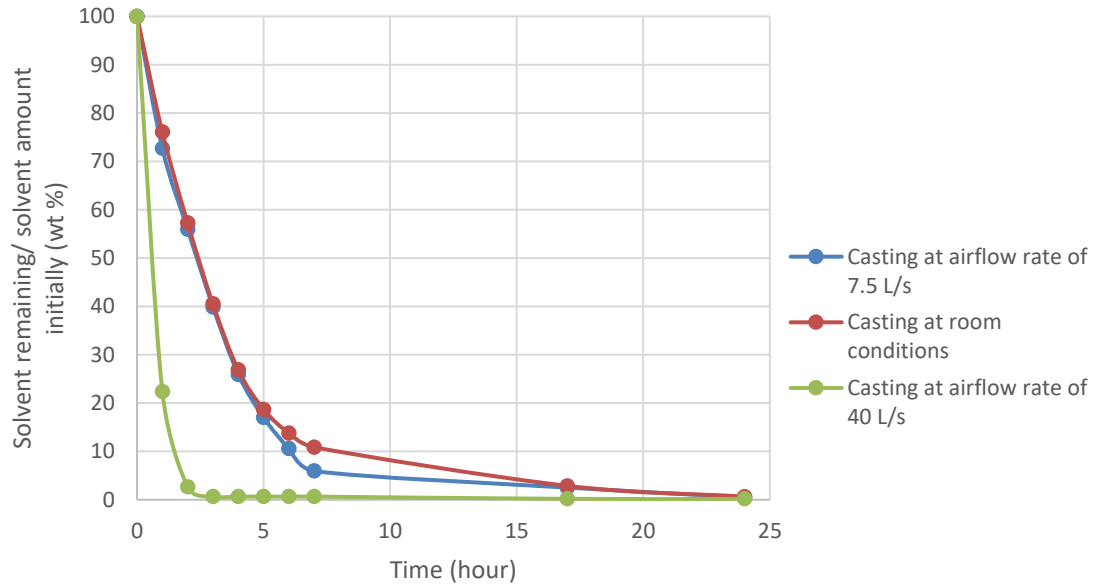
Figure 35. Evaporation rate of solvent in the casting step

Moreover, the variation of average PEBAX 1657 concentration within the film with time in Figure 36 was estimated by assuming that the evaporated amount did not contain PEBAX 1657. From the wight of the casted solution, the initial amount of PEBAX 1657 which is 4 wt % and ethanol-water mixture (96 wt %) could be estimated. Moreover, by weighing the casted solution at different times the evaporated amounts of ethanol-water mixture could be estimated. Consequently, the average PEBAX 1657 concentration within the film could be calculated.

At the airflow rate of 40 L/s, PEBAX 1657 concentration increased exponentially within the first four hours, with the succeeding hours displaying only a slight incline to peak at 96 wt % after one day of casting.

In the other two cases, the concentration of the polymer increased linearly and reached a maximum at around 90 wt %. The polymer concentration in both cases was similar in the first 5 hours. In that period, phase inversion from liquid to solid was approximately achieved, and the impact of uneven forces, caused by viscosity and density variation, became minimal. Consequently, this minimal impact did not affect the final structure of the membrane as can be seen in Figure 33 and Figure 34.

69
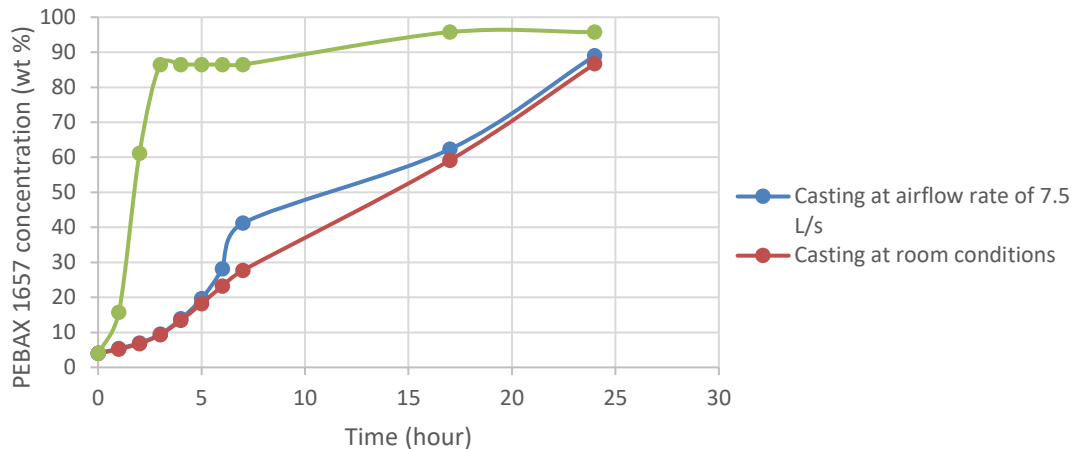
Figure 36. Variation of PEBAX 1657 concentration in the casting step in M1 membrane

4.1.2 TGA Analysis

4.1.2.1 Comparison of Thermal Behavior of Cast and Annealed membranes

All membranes after the casting step undergo two final steps to approximately eliminate all the solvent in the membrane matrix. Membranes were placed in the oven at 60 °C for one day then vacuum was applied (0.2 bar) at the same temperature for another day. TGA analysis given in Figure 37 shows that the weight of the M1.a that exposed to the whole drying process had no significant drop around a temperature of 350 °C. Thus, it can be argued that M1.a membrane is thermally stable within this range.

On the other side, the M1.c membrane that was cast only for one day showed a drop in the mass % within a temperature range of 30 – 80 °C. The main reason for this drop is the solvent remained in the membrane matrix after one day of casting which evaporated in this temperature range in TGA analysis. Similar results were reported with PES membranes where annealing process played a significant role in their thermal stability. It

70

was claimed that annealing contributed to removing the residue solvent which improved the thermal stability of the synthesized membranes (Oral, Yilmaz, and Kalipcilar 2014)
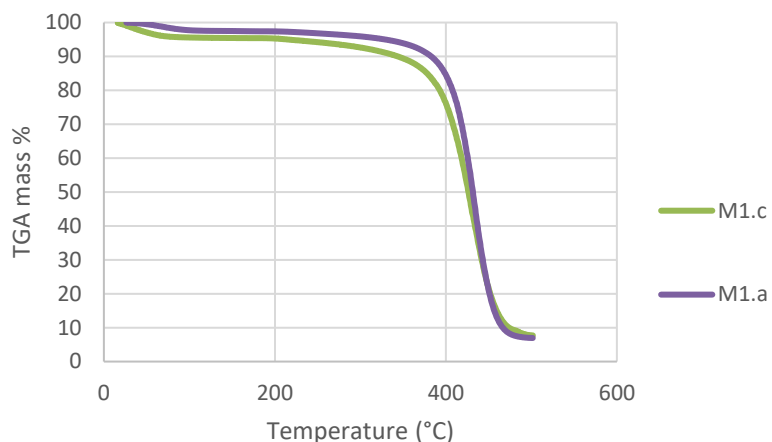
Figure 37. TGA results to compare the amount of remained solvent in M1.c cast for one day with the one prepared with the whole drying process (M1.a)

4.1.2.2 TGA Analysis to Compare 4 wt % Pure PEBAX 1657 Single- (M1) and Double-(M4) Membranes

Besides, TGA analysis was performed to compare the 4 wt % pure PEBAX 1657 single-(M1.a) and double-(M4) layer membranes as shown in Figure 38. It can be noticed that both types of membranes can be considered to be thermally stable until 350 °C, and significant weight loss occurred after that temperature. Moreover, the double-layer membrane lost weight slightly less than the single-layer membrane within the stable region.
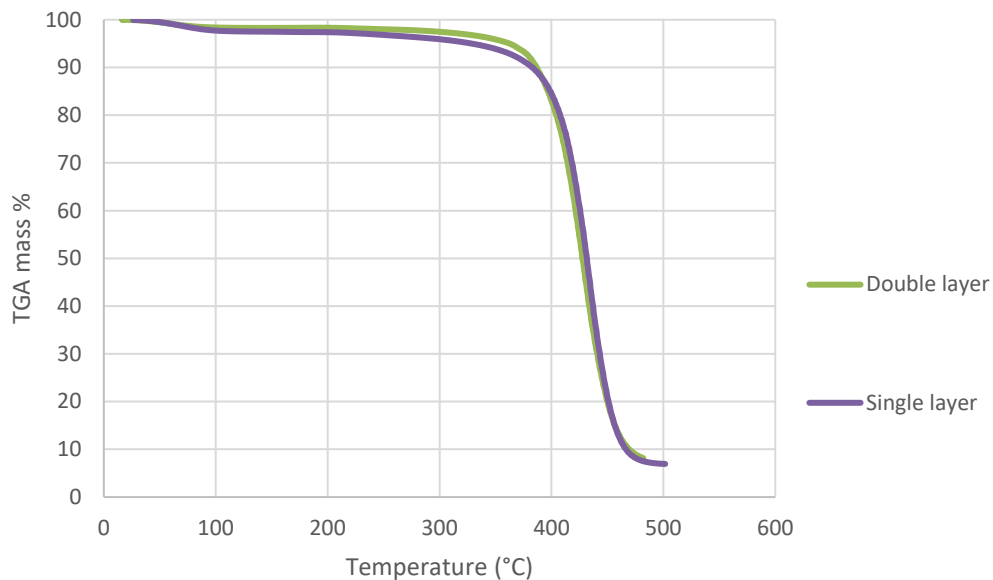
Figure 38. TGA for (M1.a) single- and (M4) double-layer 4 wt % pure PEBAX 1657.
M1 and M4 respectively

4.2 Characterization of Pure PEBAX 1657 Membranes Modified by Solvent Penetration

In this section, the characterization of the 4 wt% pure PEBAX 1657 membranes that were modified by pouring 3 mL and 12.5 mL (M2 and M3) is to be investigated. Figure 39 shows hypothetically the expected modification that may occur within the matrix of the membranes. Three methods (SEM, Optical Microscope, and EDX) were utilized to observe the real modifications through the matrix of these membranes.
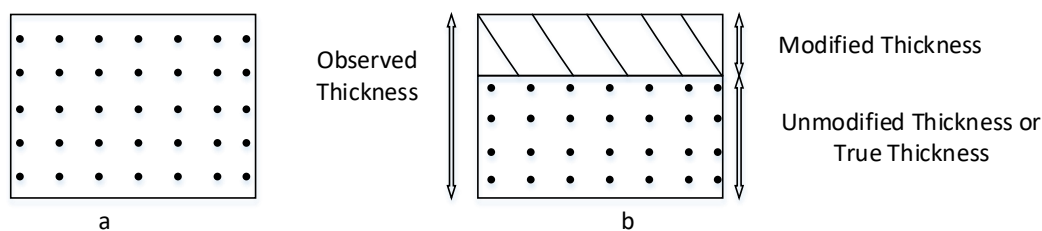
Figure 39. Hypothetical representation for membrane matrix a) unmodified b) modified, by 4 wt % PEBAX 1657 membranes

4.2.1 Microscopic Analysis to Investigate the Modification Occurred for 4 wt% Pure PEBAX 1657 Treated with Additional Solvent

Two different membranes were prepared (OPM1 and OPM 2) to investigate the behavior of modifying 4 wt% pure PEBAX 1657 membrane by treating the membrane surface with additional solvent. Later, each membrane was analyzed by an optical microscope to check the color change within its matrix. Figure 40.a shows an OPM 1 membrane that went through all the synthesizing process without adding any solvent after one day of casting. The color of this membrane is gray which is going to be taken as reference in this section.

Moreover, to investigate the penetration of the solvent into a polymer film, a pink dye was mixed with the solvent and the variation of the color within the membrane matrix was observed by using an optical microscope. Thus, an OPM2 membrane was prepared with pouring 10 mL of ethanol-water solvent that was mixed with a pink dye solution (4 wt%) on the surface after casting for one day. For this purpose, a stock solution of pink dye with 50 ppm was used. Figure 40.b shows the whole matrix turned to pink color which suggests that solvent re-mixed and the membrane partially re-dissolved in the additional solvent. Some of this solvent penetrated through the undissolved part of the membrane.

Moreover, at the top part of the matrix of OPM2 a wrinkled line was observed. It can be claimed that this line determines the interface between the modified and unmodified parts of the membrane matrix. In other words, from the color change it can be inferred that the

73

solvent went through all the membrane matrix but it modified only 10-20% of the membrane matrix. Furthermore, from the scale in the two figures which is 20 µm, the membrane thickness of the two membranes is almost the same (60 µm). As known, concentration of the polymer plays a crucial role in membrane thickness. Consequently, if it is assumed that solvent significantly changed the PEBAX 1657 concentration in the matrix, lower thickness was going to be observed. Thus, it can be argued that sorbate solvent had no significant effect on the total thickness of the membrane. It is expected that the modification by the solvent is going to affect the final separation performance of the membrane which is going to be investigated later.

a   b
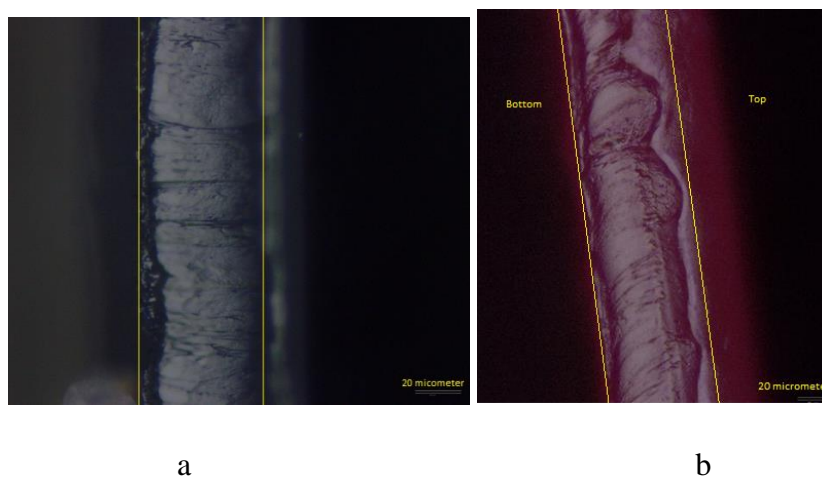
Figure 40. The cross-sectional view of (a) OPM1 and (b) OPM2 membranes

4.2.2 Change of Penetration Depth of Ethanol-Water Solvent Penetration into 4 wt % Pure PEBAX 1657 Membrane Matrix with Time and Solvent Amount

In this section, the aim is to find out the time required for the solvent to penetrate the M1.c membrane matrix by observing the change of color. To observe that, 10 mL of the solvent which was mentioned in Section 1.1.3.1 was poured on the top of the M1.c membrane and kept there for different periods before removing it, after that the membrane went through the whole drying process. The obtained results are shown in Figure 41.a Figure 41.b

Figure 41.c, Figure 41.d Figure 41.e, and Figure 41.f for periods of 30 sec, 1 min, 5 min, 30 min, one hour and two hours, respectively. Comparing these results, it can be inferred that after 30 min there was distinguishable difference in the color of these three membranes compared to the one with 30 sec only.

Thus, the solvent penetration depends mainly on the time where it required 5 min to start observing a slight change in the color of the membrane matrix. As time increases, the amount of penetrated solvent increases thus clear change in the color was noticed. A possible reason for that is the hydrophilicity of the PEBAX 1657 that helps in enhancing the sorption process (Hamouda et al. 2011). Moreover, the thin thickness of the one-day casted membrane played a role in this fast sorption. The amount of solvent used which is exactly the same amount used for the top-layer solution in the double-layer method seems to be large enough according to the matrix thickness to star penetrating within a few minutes.

a

b

c

d
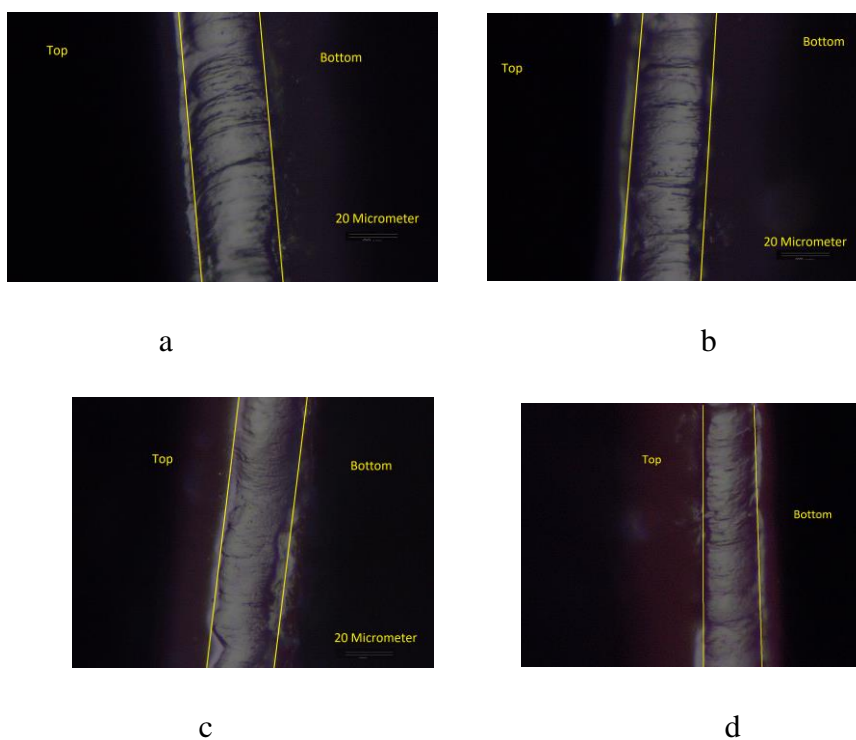
Figure 41. Keeping the solvent that mixed with pink dye on one-day cast membrane (M1.c) for a) 30 sec, b) 1 min, c) 5 min, d) 30 min e) 1-hour f) 2 hours

75
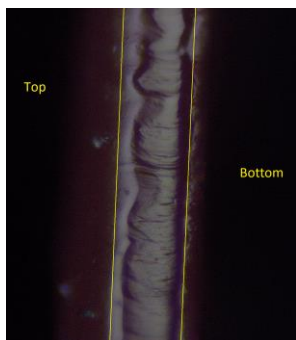
e   f

Figure 41. (cont'd) Keeping the solvent that mixed with pink dye on one-day cast membrane (M1.c) for a) 30 sec, b) 1 min, c) 5 min, d) 30 min e) 1-hour f) 2 hours

Besides, the amount of the solvent is expected to play a main role in the solvent penetration mechanism. For that reason, different amounts of solvent were used and time was fixed to be one day which is the normal casting period. Figure 42 shows that color did not change with solvent amounts of 0.5 and 1 mL, respectively. It can be claimed that these amounts are low thus the solvent may evaporate before it had the chance to penetrate. For amount of 3 mL and above, minimal difference in color was observed. It can be argued that, the sorption capacity was reached by using these three amounts thus a significant variation in color could not be observed.
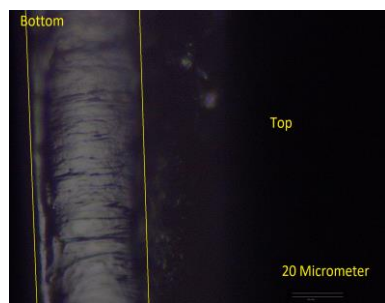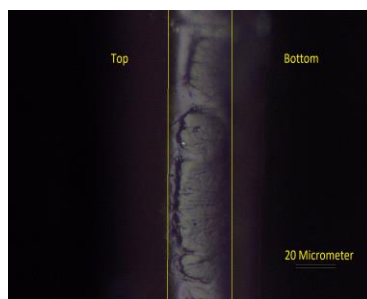
a   b

Figure 42. Keeping different amounts of solvent (a. 0.5 mL, b.1 mL, c. 3 mL, d. 10 mL, and e.12.5 mL) that mixed with pink dye on one-day cast membrane for one day

76

c   d   e
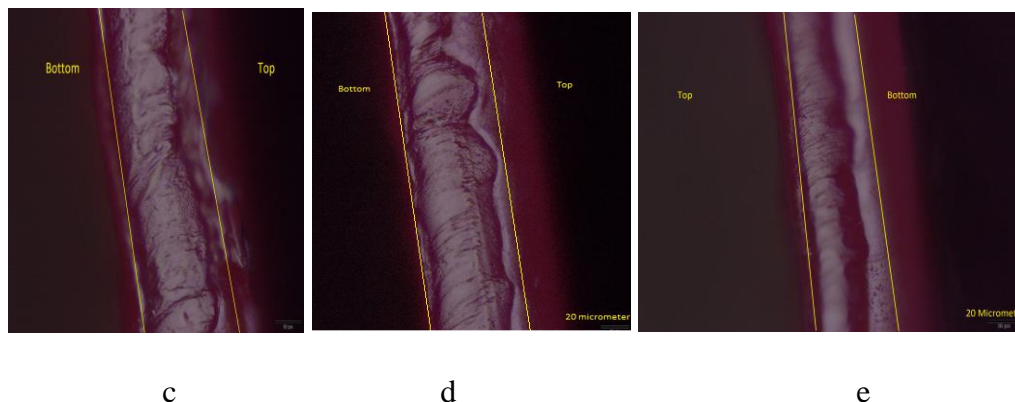
Figure 42. (cont'd) Keeping different amounts of solvent (a. 0.5 mL, b.1 mL, c. 3 mL, d. 10 mL, and e.12.5 mL) that mixed with pink dye on one-day cast membrane for one day

4.2.3 SEM Analysis to Investigate the Modification Occurred for 4 wt% Pure PEBAX 1657 Treated with Additional Solvent

SEM analysis was performed for M2 (Figure 43.b) and M3 (Figure 43.c) alongside with M1.a (Figure 43.a) to investigate the effect of modifying 4 wt % pure PEBAX 1657 membrane using an additional solvent. An arrow was drawn to indicate the y-axis direction of the membrane matrix. The tail indicates the bottom whereas the head points to the top surface. In both membranes, in the rectangular areas, there was a clear change in the cross-sectional morphology due to the solvent modification. The impact of the solvent was demonstrated with wrinkled lines whereas the rest of the membrane matrix was similar to the M1.a membrane in (Figure 43) which has an agreement with morphology reported in the literature (Hosseinzadeh Beiragh et al. 2016). In both cases, the solvent penetration impact reached approximately 30-35 % of the membrane thickness from the top. This observation shows a good agreement with the analysis performed by the optical microscope in Section 4.2.1. Both analysis methods give a hint on the behavior of the solvent penetration rate within the matrix. If the penetration rate of the solvent was linear, the modification on the morphology would be observed through the whole matrix. Nevertheless, the presence of the pink dye in Figure 40.b in the bottom indicates that rate

of penetration did not stop in the modified part, despite not having an effect on the morphology in this bottom part. Consequently, the penetration rate may have an exponential decay behavior within the membrane matrix.

Besides, the re-dissolving of the polymer may be a reason behind this modification. Even though the process was not observed by the naked-eye in the casting step, the possibility of re-dissolving PEBAX 1657 into the additional solvent cannot be neglected. This means that the solvent created a variation in PEBAX 1657 concentration through the matrix, thus the density. Consequently, after re-casting the membrane for one-day, the two parts with different densities may have different morphologies.

From the above discussion on this section it can be concluded that the observed modification may be a result of different factors. More precisely, this modification could be a combination of solvent penetration and the partial re-dissolving of the polymer.
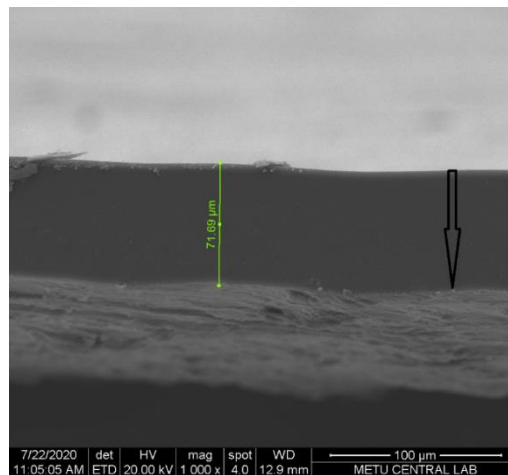
a

Figure 43. SEM analysis for synthesized membranes a) M1.a, b) M2, c) M3, d) M2 (modified part is magnified), and e) M3 (modified part is magnified)
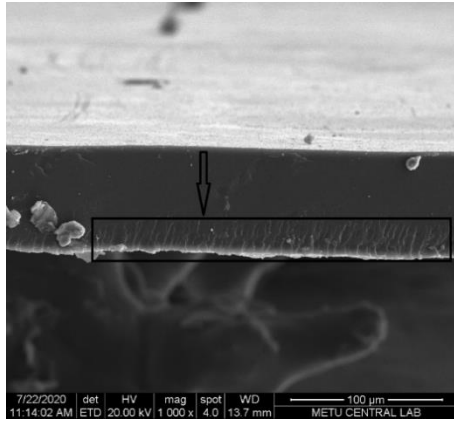
b   c

d

e

Figure 43. (cont'd) SEM analysis for synthesized membranes a) M1.a, b) M2, c) M3, d) M2 (modified part is magnified), and e) M3 (modified part is magnified)

According to the results obtained from SEM analysis, the modified thickness fraction of the matrix was estimated as Figure 44. shows. It was found that both amounts of the solvent impacted almost the same fraction of the total matrix. It can be inferred from this graph that higher amount of additional solvent does not guarantee a higher modification impact. This can be related to the sorption capacity of the membrane.
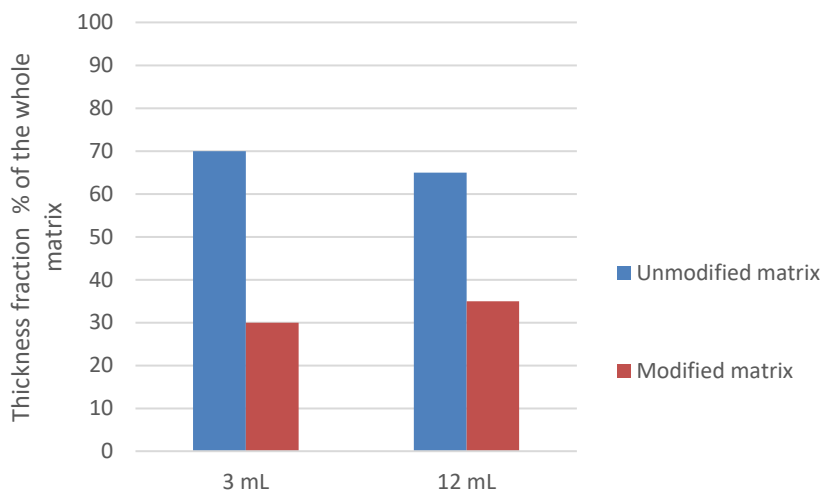
Figure 44. Estimation of the unmodified/modified thickness caused by solvent treatment according to SEM analysis

4.2.4 EDX Analysis to Investigate the Modification Occurred for 4 wt% Pure PEBAX 1657 Treated with Additional Solvent

To investigate further the behavior of modifying 4 wt % of pure PEBAX membrane by additional solvent treatment, EDX analysis was performed. The 10 mL of the solvent was mixed with 0.003 g of Na_2SO_4. Selected points (199 points) in the matrix of the membrane was analyzed to track the atomic % of Na^+. Later, the obtained results were compared to EDX analysis for M1.a where no modification interfered as shown in Figure 45. Surprisingly, according to these results, Na^+ was migrated only 10 % from the top of the membrane matrix. It was expected to observe two distinguishable profiles for Na^+ in these membranes since the results obtained from the optical microscope proved that solvent could migrate through the whole matrix. This may result due to the difference in the penetration rate of the solvent, comparably higher than that of Na^+. If Na^+ particles did not penetrate, they would accumulate on the surface of the membrane after the evaporation occurs and would not appear in the membrane matrix. Thus, EDX analysis confirm the results found in optical microscope and SEM analysis considering the difference sodium ions penetration rate.

80
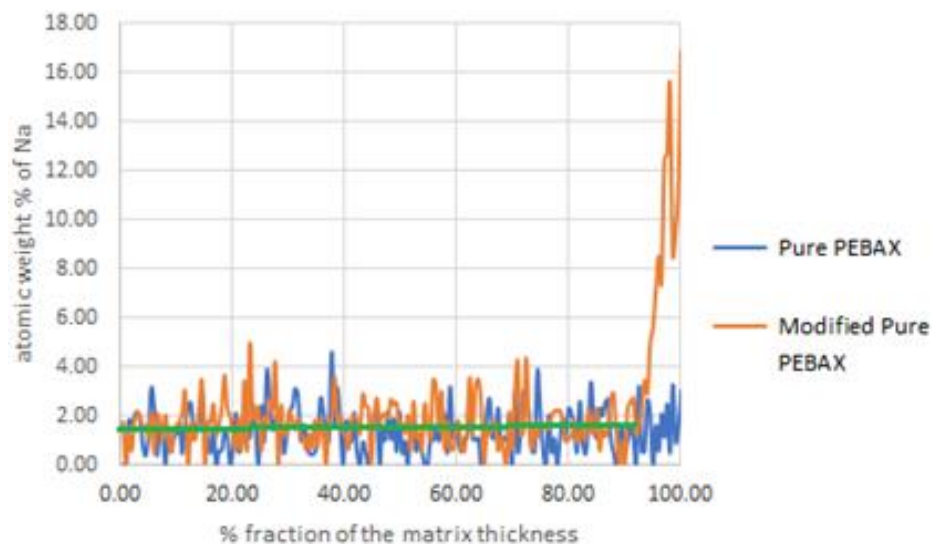
Figure 45. The atomic weight profile of Na$^+$ through the matrix of M1.a and M2 obtained by EDX analysis

4.3   Characterization of Double-layer Pure PEBAX 1657 Membranes

The results obtained from treating pure PEBAX 1657 with additional solvent were motivation to investigate casting a solution that includes PEBAX 1657. Alongside with solvent effect, an interface layer is expected to be formed that may enhance the permeability further as shown hypothetically in Figure 46. To characterize this proposal, both the optical microscope and SEM analysis were used.
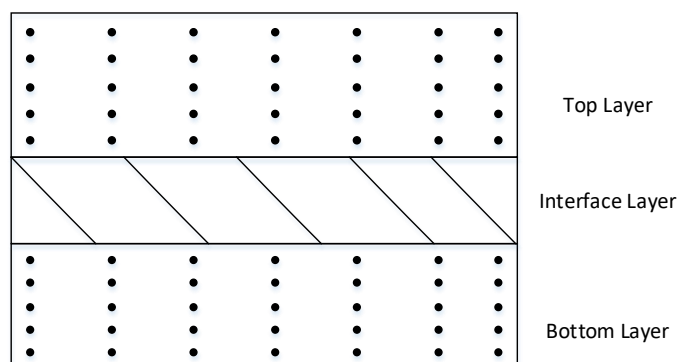
Figure 46. Hypothetical representation for double-layer membranes

4.3.1.1 Microscopic Analysis Using a Pink Dye to Investigate Casting a Second Layer on the Top of the One-day Casted Layer

In this study, to enhance the permeability, double-layer membranes were prepared. In these types of membranes, a bottom-layer was cast for one day then a top-layer that was prepared in the exact way of the bottom-layer was cast on its surface. As explained in Section 1.3.1. a pink dye with the same concentration was used to investigate the color change in the microscopic level within these membranes. Similar to the mechanism of pouring solvent that has no PEBAX 1657, a liquid-solid interface was formed at the moment of casting the top layer. However, since the presence of PEBAX 1657 made the solution to be more viscous, the penetration of the solvent into the matrix is expected to be less effective. Figure 47.a shows that there are two separate layers, visibly from the color, the dye concentration is higher in the top layer. Besides, the distance ratio between the two layers is approximately the same which is expected since the amount used for each layer was almost the same.

Furthermore, to investigate the re-dissolving of the polymer in the bottom layer into the top solution another membrane was prepared (OPM4). The pink dye was mixed with the casting solution of the bottom layer. Then, after one day casting, a top layer solution without the pink dye was cast over the bottom layer. The obtained results are shown in

Figure 47.b. Similar results obtained in Figure 47.a were observed but with reversed locations. Thus, these two cases showed that a portion of the solvent penetrated to membrane matrix, and some of the PEBAX 1657 in the bottom-layer re-dissolved since the color of the dye appeared in the top-layer as Figure 47.b shows. Further, these results support the discussion in Section 4.2.1 where the effect of partial re-dissolving of PEBAX 1657 into solvent was assumed to be a reason for this modification alongside with the solvent penetration. The two-layer segregation was more obvious in the double-layer membranes which indicates that the effect of these two factors was less. As mentioned previously, this decreased effect may happen due to the presence of PEBAX 1657 in the additional solvent that might reduce the effect of both factors.

a   b
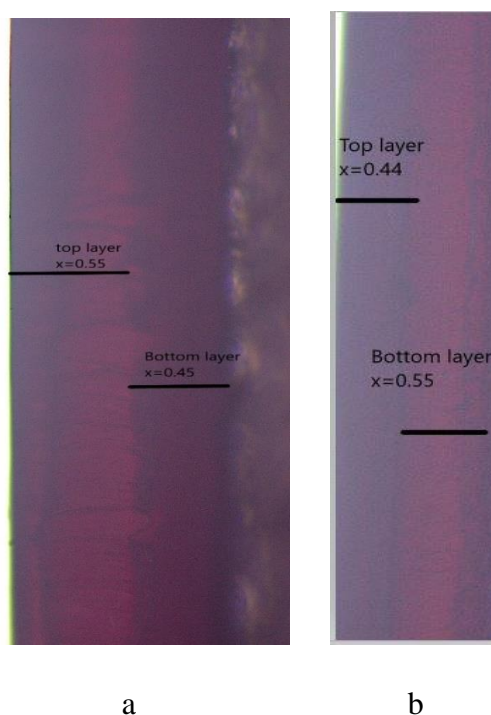
Figure 47. The cross-sectional view of two double-layer pure PEBAX 1657 a) PPM 3 and b) OPM4. Dye was mixed with the top and bottom layer; respectively

Besides, the thicknesses of the membranes in Figure 47.a and Figure 47.b were measured and compared to the thickness of a single membrane that has the same amount of casting solution used for bottom layers. The thickness of the single-layer membrane is 67.33 nm

which has acceptable errors of 7.8 and 5.8 % from the bottom layer of membranes in Figure 47.a and Figure 47.b, respectively. This agreement helped in confirming that two distinguishable layers were formed.

4.3.2 SEM Analysis for Pure Double-Layer PEBAX 1657 Membranes

Pure PEBAX 1657 Double-layer membranes M4, M5, and M6, where PEBAX 1657 concentration in the bottom is 4 wt % and in the top varies as 4 wt %, 2 wt %, and 1wt % were analyzed by SEM, respectively. Almost all membranes of this kind showed two separate layers with distinguishable morphologies as shown in Figure 48. but the segregation was less clear in M6. The top-layer thickness increased with PEBAX 1657 concentration, even though that was not clear with M5 and M6. That may result because of a small difference in PEBAX 1657 wt% in both membranes. Furthermore, with the same analogy, the total thickness of these three membranes had a direct relationship with the PEBAX 1657 concentration in the top-layer which was expected since with the same casted solution the membrane with higher PEBAX 1657 concentration should be thicker.

a   b
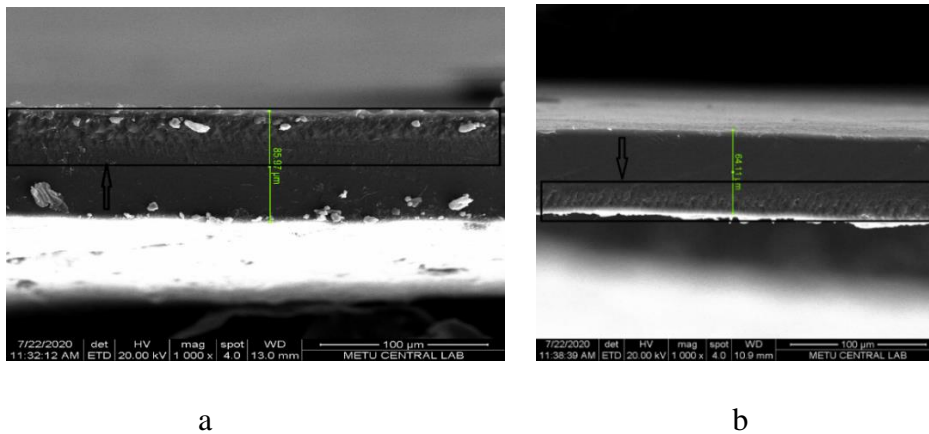
Figure 48. SEM analysis for synthesized membranes a) M4, b) M5, and c) M6, d) M4 (modified part is magnified), e) M5 (modified part is magnified), and h) M6 (modified part is magnified)
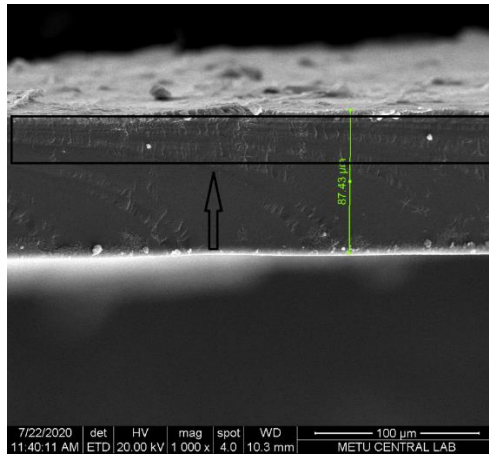
c
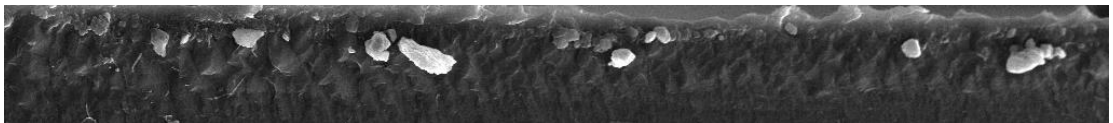
d)
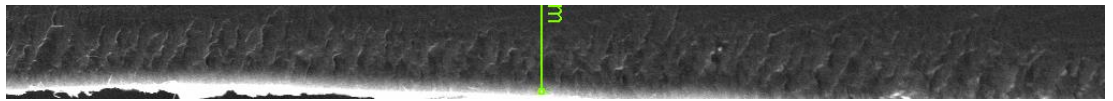
e)
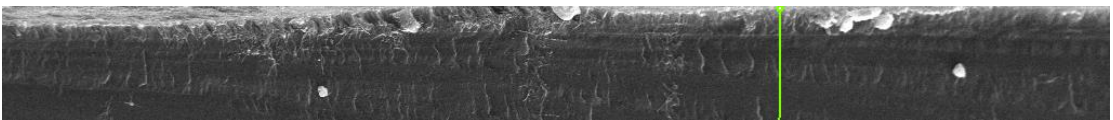
h)

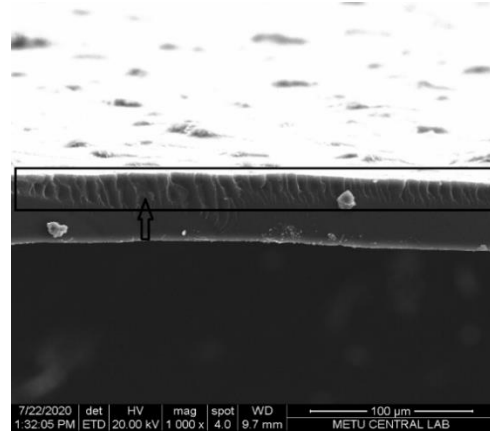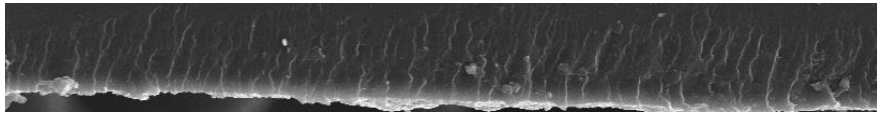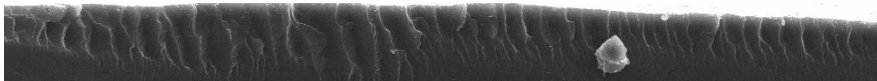Figure 48. (cont'd) SEM analysis for synthesized membranes a) M4, b) M5, and c) M6, d) M4 (modified part is magnified), e) M5 (modified part is magnified), and h) M6 (modified part is magnified)

4.4 Characterization of ZIF-8

ZIF-8 particles were synthesized in this study to prepare mixed matrix membranes with PEBAX 1657. Two sizes of ZIF-8 particles were synthesized to investigate the effect of filler size in the structure of the matrix of the membranes and separation performance.

4.4.1 XRD Analysis for ZIF-8 Particles

The produced ZIF-8 particles were analyzed by XRD as shown in Figure 49. The results were compared with reference XRD pattern for ZIF-8 and showed an acceptable agreement. Few deviations were recorded due to the impurities in the given samples for XRD analysis such as the small peak around 2-theta angle of 15. As was expected, sharp peaks were obtained which indicates that the particles are crystalline. In general, the identification and crystallinity of synthesized particles to be ZIF-8 was proved from the obtained results.
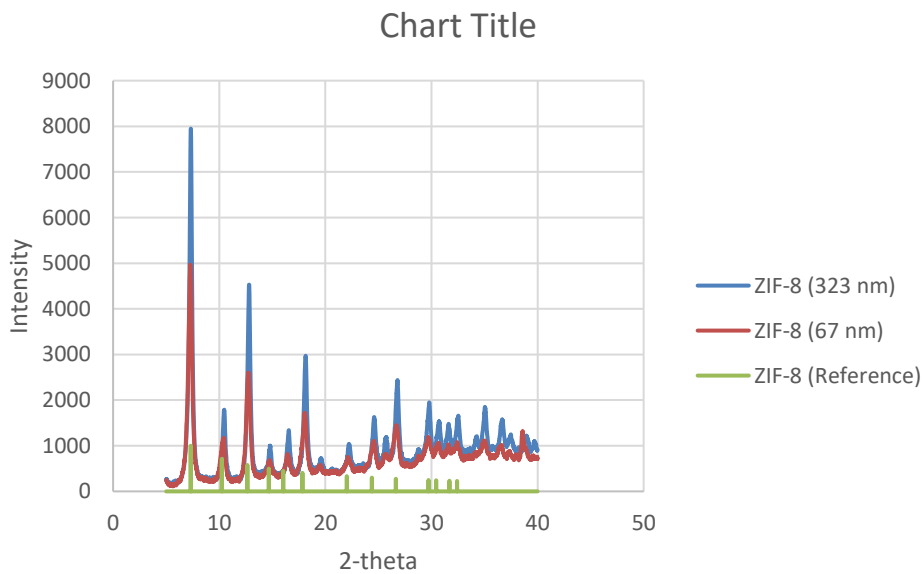
Figure 49. XRD analysis for two different sizes of ZIF-8

4.4.2 SEM Analysis for ZIF-8 Particles

In addition to XRD analysis, SEM analysis was required to determine the morphology of the synthesized particles. As shown in Figure 50, ZIF-8 with two different particle sizes were synthesized. The crystals shown in Figure 50.a have an average size of 67 ± 8.0 nm whereas the ones in Figure 50.b have an average size of 323 ± 15.0 nm (average estimation is explained in detail in Appendix B). These results have a great agreement with the study that was mentioned in the experimental methods (Keser Demir et al. 2014). Moreover, the shape of particles (hexagonal) is similar to the one obtained in the same study.
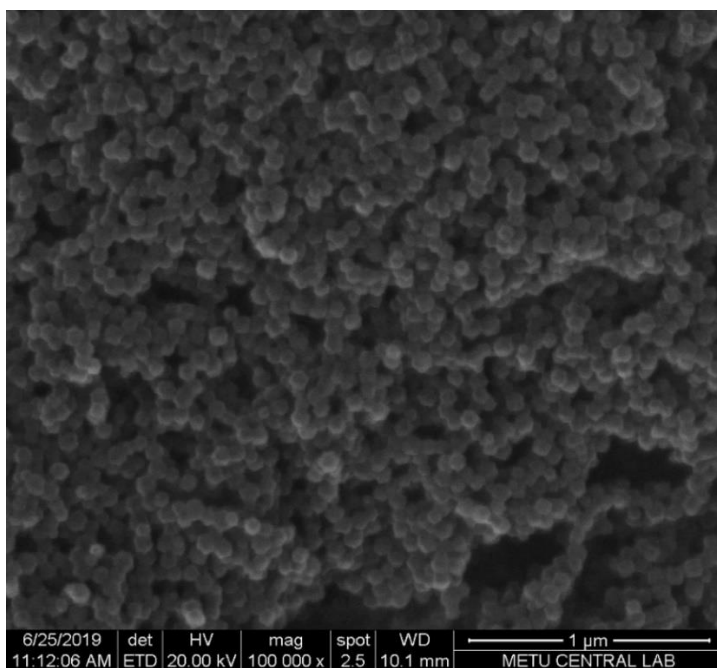
a

Figure 50. SEM analysis for ZIF-8 particles (a) 67 nm and (b) 323 nm
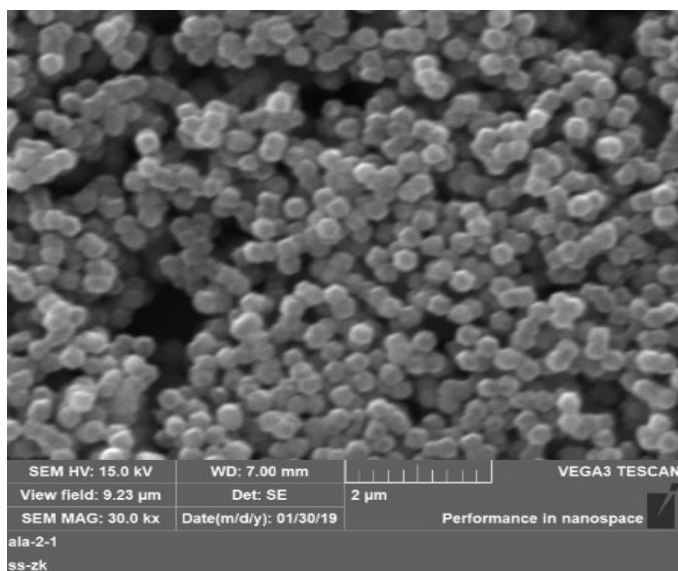
b

Figure 50. (cont'd) SEM analysis for ZIF-8 particles (a) 67 nm and (b) 323 nm

4.5   Characterization of ZIF-8/PEBAX 1657 Membranes

SEM analysis was used to investigate further the cross-sectional morphology of the ZIF-8/PEBAX mixed matrix membranes (MMMs) with high magnification images. Single-layer (M7 and M8) and double-layer ZIF-8/PEBAX (M9 and M10) were synthesized and analyzed by SEM. The distribution of ZIF-8 particles within the membrane matrix which was demonstrated in M7 (Figure 51.c) and M8 (Figure 51.d) with circles, as was reported (Song et al. 2012b), had good contact with the polymer matrix.

In addition, ZIF-8 particles were well distributed within the matrix which means that using Triton x100 had a positive impact on reducing the agglomeration as shown in M7 (Figure 51.a). Only two drops in the mixing step of this material could improve their distribution within the matrix. White spots in ZIF-8/PEBAX 1657 membranes that were prepared without adding Triton x100 were observed by naked-eye that indicated a presence of particles agglomeration.

ZIF-8 particles in M7 (Figure 51.a) have an average size of 93 ± 15 nm. This value is noticeably larger than the ones obtained from Figure 50.a. This deviation might result from experimental error in synthesizing ZIF-8 particles. However, this can be tolerated since the particle size is relatively smaller than the ZIF-8 (323 nm) particles. For large particles, it was difficult to observe them within the matrix for two reasons. First, the number of particles is supposed to be approximately 5 times less than small particles since the mass added and density are approximately same in both sizes. This made it difficult to be observed easily in the cross-sectional view. Besides, since the particles are large the volume occupied by single one to the total volume of the matrix is again 5 times higher compared to the small particles. Thus, the homogeneity of the matrix decreased as shown in M8 Figure 51.b and M10 Figure 51.f compared to other synthesized membranes such as M7 in Figure 51.a. In double-layer membranes, two segregated layers appeared distinctly in M9 where each layer has almost the same thickness. This observation was less in case of M10, possibly, due to the homogeneity issue that ZIF-8 (323) created within the matrix of the membrane.

a   b
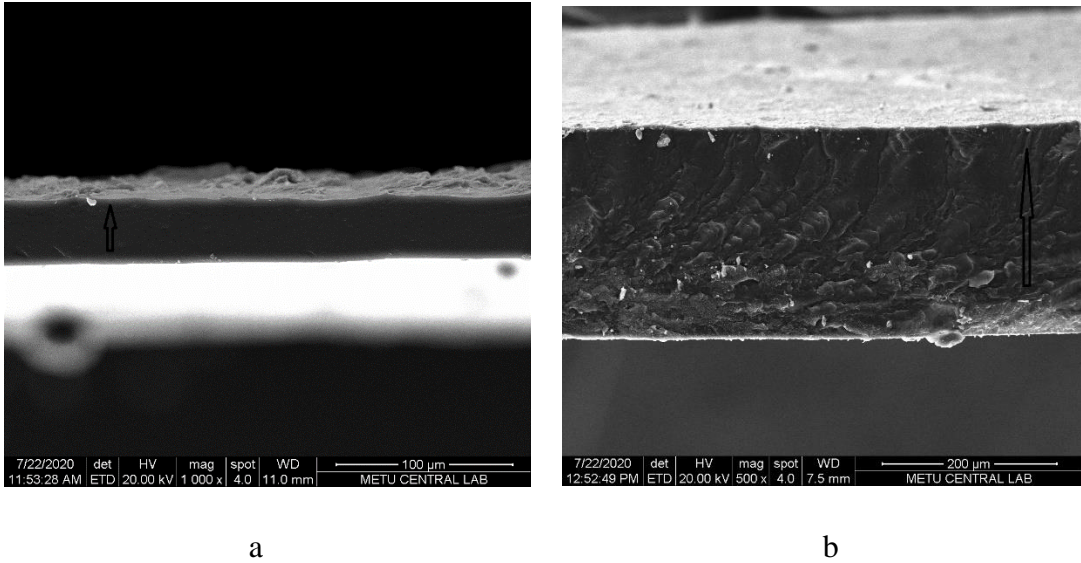
Figure 51. SEM analysis for synthesized membranes a) M7, b) M8, c) M7 (magnified), d) M8 (magnified), e) M9 f) M10
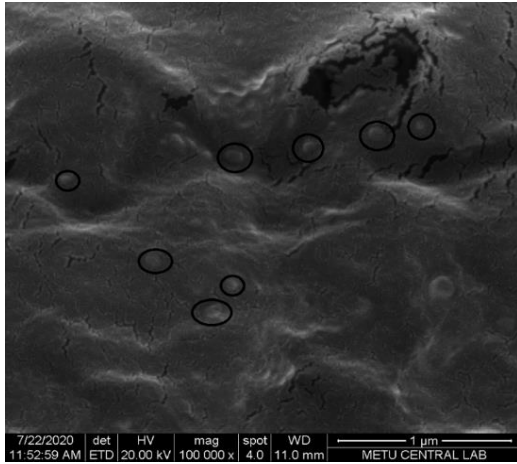
c
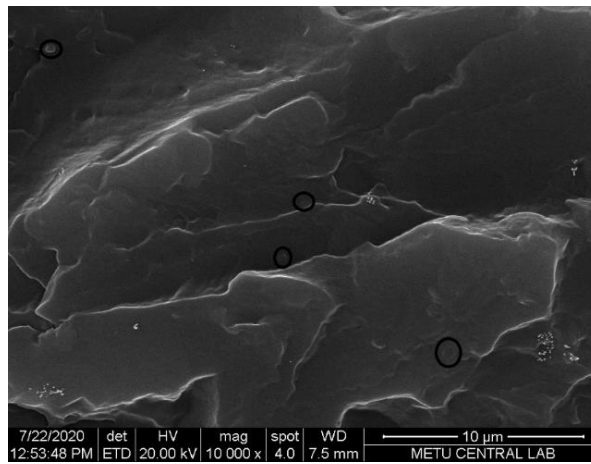
d
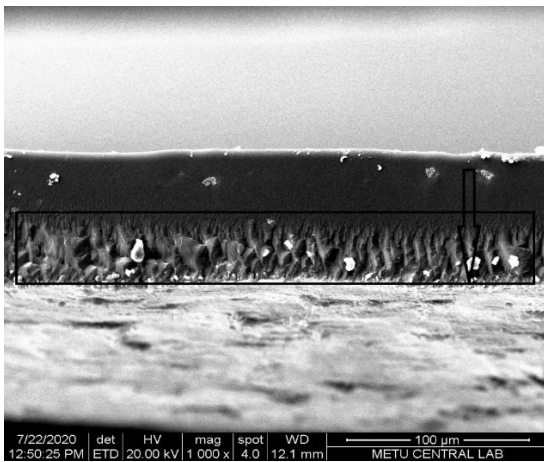
e
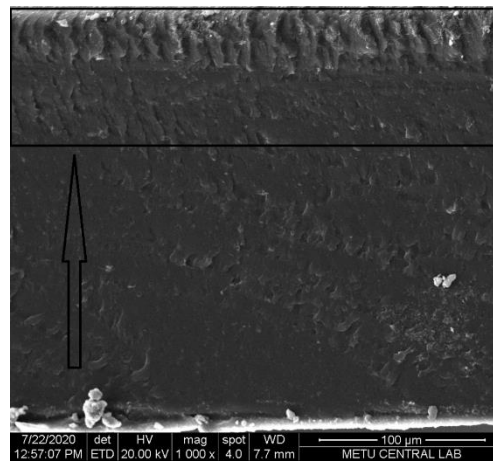
f

Figure 51. (cont'd) SEM analysis for synthesized membranes a) M7, b) M8, c) M7 (magnified), d) M8 (magnified), e) M9 f) M10

4.6 Gas Permeability Results

4.6.1 Method of Ethanol-Water Solvent Penetration

Table 16 and Figure 52 show how the permeability and selectivity of CO_2/N_2 were improved due to adding the ethanol-water mixture on the casted membrane for one day. Two amounts of solvent were used to observe their effects on the membrane separation performance. Firstly, 3 mL of ethanol-water solvent was poured on the top of single-layer 4 wt % pure PEBAX 1657 after one-day casting. This simple modification enhanced the permeability of carbon dioxide by a factor of 1.21 and the selectivity slightly by a factor of 1.05 compared to the M1.a membrane.

A larger amount (12.5 mL) was used in the same exact procedure to prepare M3 membrane. No change in CO_2 permeability whereas a minimal increase by a factor of 1.07 in the selectivity was recorded in the performances of this membrane compared to M2. This implies that the amount of the solvent has no major effect on the separation performance. It was expected that the one with 12.5 mL should have different CO_2 permeability since the penetrated solvent into the membrane matrix is larger. This can be related to the sorption capacity of the bottom layer. The sorption capacity, in this case, is defined as the amount of sorbate (ethanol-water solvent) taken up by the sorbent (single-layer 4 wt % pure PEBAX 1657) per unit mass (or volume) of the sorbent (Mokhatab, Poe, and Mak 2019). According to the single gas permeability test which was done three times, by neglecting the slight difference in the selectivity, the sorption capacity of the adsorbent should be less than 3 mL which means that further increase in the solvent amount does not contribute in the sorption process. In other words, a certain amount of solvent was sorbate and the rest evaporated.

Table 16. *The effects of two amounts of solvent that penetrated, on the separation performance of 4 wt % pure PEBAX 1657*

Membrane Code	Membrane Description	CO_2 Permeability (Barrer)	N_2 Permeability (Barrer)	Ideal Selectivity	Thickness (μm)
M1.a	Single-layer 4 wt % pure PEBAX 1657	155.2 ± 9.00	4.25 ± 0.18	36.5 ± 0.83	121
M2	Single-layer 4 wt % pure PEBAX 1657 was modified by 3 mL solvent	188.0 ± 6.90	4.9 ± 0.35	38.4 ± 1.48	83
M3	Single-layer 4 wt % pure PEBAX 1657 was modified by 12.5 mL solvent	188.6 ± 1.60	4.6 ± 0.21	41.4 ± 1.54	99
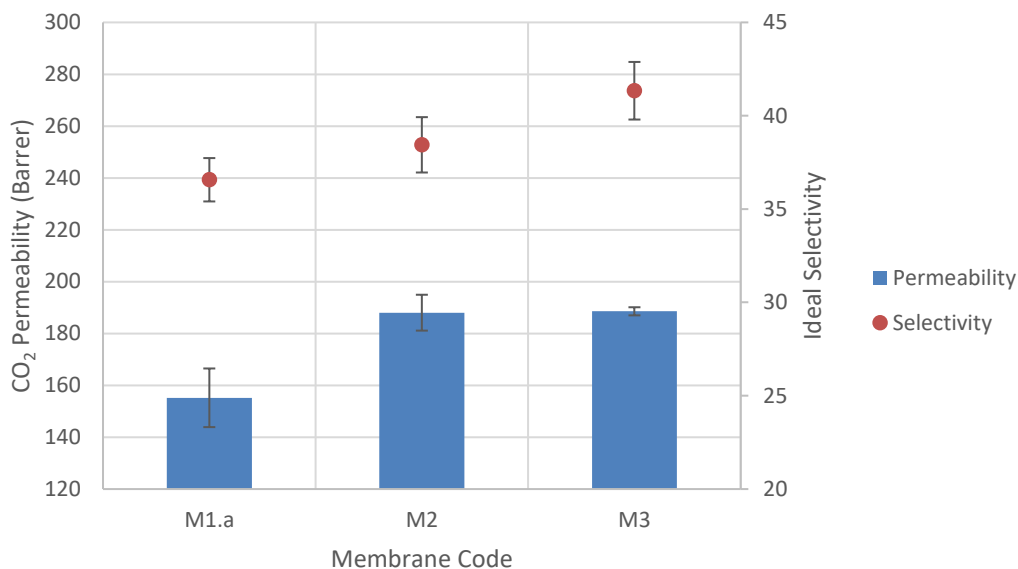
Figure 52. The effects of two amounts of solvent that penetrated on the separation performance of 4 wt % pure PEBAX 1657

The first reason that may explain this enhancement is the contribution of the modified part thickness. In other words, this part could be considered as highly permeable section (no resistance) whereas the unmodified part represents the effective thickness. To investigate this proposal the permeance of M2 that has thickness of 83 nm was calculated to be 2.27 GPU. Then, using the results represented in Figure 44 the permeability of unmodified part, estimated to be 70 % of the total thickness (58nm), can be calculated to be 132 Barrer. Obviously, this is less than the permeability of 4 wt % pure PEBAX membrane (M1.a) at 155.2 Barrer, meaning that additional solvent made some changes within the membrane film. Possible changes could be in the chain packaging of the membrane or the voids within the membrane matrix.

Besides, for the PEBAX membrane, the literature showed as shown in Table 17 that the synthesis process has a significant impact on the separation performance. Since permeability is a material property, it is expected to have similar results regardless of the method of preparation. Nevertheless, it seems that the morphologies of these membranes are affected by the synthesizing process.

Table 17. *Recorded pure PEBAX 1657 Carbon dioxide permeability in literature*

CO₂ Permeability (Barrer)	Testing Temperature (°C)	Wt % of PEBAX 1657	Dissolving Solvent	Reference
155.2	35	4	Ethanol-water (70/30 wt %)	This Study
190.87	35	4	Ethanol-water (70/30 wt %)	(ÖZDEMİR N. K. 2017)
130	-	4	Ethanol-water (70/30 wt %)	(Jomekian et al. 2016)
55.85	30	4	Ethanol-water (70/30 wt %)	(Surya Murali et al. 2010b)
82	25	4	Ethanol-water (70/30 wt %)	(Wu et al. 2014b)
78.9	20	3	Ethanol-water (70/30 wt %)	(Zheng et al. 2019)
73	30	3	Ethanol-water (70/30 wt %)	(Rahman et al. 2013)
66.5	25	3	Ethanol-water (70/30 wt %)	(Bernardo and Clarizia 2020)
123.46	25	2.5	DMF	(Farashi et al. 2019)

In general, the free volume has a major impact on the separation performance of the polymeric membranes. It can be analyzed from two aspects, their distribution and fraction.

According to Fujita's theory, permeability has a direct relation with fraction free volume (FFV) as shown in Equation [17] (Recio et al. 2008)

$$P = A_D \exp\left(-\frac{B}{FFV}\right) S \qquad (17)$$

Where A_D and B are constants for a given gas and polymer. The former represents the size and kinetic velocity of the penetrant whereas the latter represents the free volume of voids needed for penetrant diffusion. Thus, a possible explanation is that the membrane was swollen by the solvent that may result in increasing the free volume within the matrix thus carbon dioxide permeability enhanced. Similarly, the poured solvent might have caused a plasticization to the membrane that improved CO_2 diffusion within the membrane film. Another possible scenario is that the solvent at a certain time in the casting period acted as an anti-plasticizer which may explain the insignificant enhancement in the selectivity. Moreover, solvent modification might have created porous media in the modified part which made it highly permeable compared to unmodified part

Polymeric membranes, in general, have the disadvantage of the trade-off between permeability and selectivity as was estimated by Equation [18] (Alentiev and Yampolskii 2000). The constants a and b are correlated from the tested membranes, α_{12} is the selectivity and P_1 is the permeability of gas 1.

$$log\alpha_{12} = -a - (b-1)logP_1 \qquad (18)$$

 As a result, it was expected to have a drop in selectivity. This leads us to further investigate the contribution of the distribution of the free volume (DFV). It was found that for some polymers the diffusivity has an inverse relation with free volume which was attributed to differences in the DFV (Recio et al. 2008). In this study, the permeability of carbon dioxide and nitrogen was increased, but the solvent slightly has more impact on the permeability of carbon dioxide. Thus, it can be concluded that adding solvent on the top of a casted membrane has a major effect on FFV more than DFV. Moreover, it can be assumed that DFV was constant in both cases, which explains the minimal effect on the selectivity.

One of the reasons that may explain further this improvement is the residue solvent in the membrane before annealing. Residue solvent is a small amount of ethanol-water mixture that was remained within the matrix after one-day casting which is assumed to contribute in the solvent modification process. This explanation was done experimentally where three pure PEBAX 1657 (4 wt%) membranes were prepared and annealed. After that, these membranes were modified by 3 mL additional solvent. In other words, the small residue solvent was removed by annealing before pouring the solvent on the top of the membrane surface. These membranes were tested and it was found that the permeability of carbon dioxide is 165 ± 4 Barrer which is a value between the CO_2 permeability through M1.a and, M2 and M3. Thus, it can be argued that the presence of residue solvent helped in solvent modification process.

4.6.2 Pure PEBAX 1657 Double-Layer Membranes

4.6.2.1 4 wt % PEBAX 1657 in each Layer

Another proposal to increase the CO_2 permeability through the PEBAX 1657 membrane was to use a double-layer technique. The promising results obtained in section 4.2.1 supported the feasibility of this proposal. Evaporation of the solvent, in this case, was controlled by the PEBAX 1657 concentration alongside with temperature and airflow rate. Table 18 and Figure 53 compare the separation performance of the single-layer (M1.a) and double-layer (M4) of 4 wt % PEBAX 1657 membranes. The permeability was increased by a factor of 1.13 only whereas selectivity decreased slightly by 6.6 %. It can initially be inferred that the double-layer method has a trade-off between permeability and selectivity. Nevertheless, its negative impact on selectivity is minimal and can be tolerated.

Table 18. *Comparing the separation performance between the (M1.a) single- and (M4)*
double-layer 4 wt % pure PEBAX 1657 membranes

Membrane Code	Membrane Description	CO_2 Permeability (Barrer)	N_2 Permeability (Barrer)	Ideal selectivity	Thickness (μm)
M1	Single-layer 4 wt % pure PEBAX 1657	155.2 ± 9.02	4.25 ± 0.18	36.5 ± 0.83	121
M4	Double-layer 4 (top)/4 (Bottom) wt % pure PEBAX 1657	175 ± 8.45	5.13 ± 0.06	34.1 ± 1.64	152
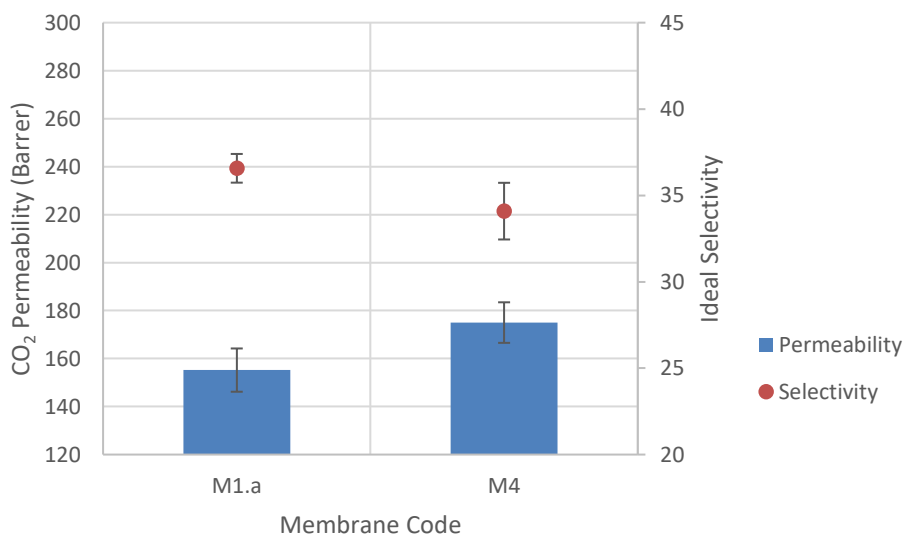
Figure 53. Comparing the separation performance between the (M1.a) single- and (M4)
double-layer 4 wt % pure PEBAX 1657 membranes

Furthermore, the CO_2 permeability of M4 has a value between the permeability of M1 and membranes where the solvent was poured on their surfaces after one day casting (M2 and M3). Thus, the presence of PEBAX 1657 in the poured solution increased its viscosity resulted in reducing the effect of solvent penetration within the matrix. However, these results are interesting since in overall both the single- and double-layers membranes have the same weight ratio of PEBAX 1657 to the ethanol-water mixture in the casted solution which is 4 wt % but they have different CO_2 permeability values. Thus, a modification in membrane structure occurred that caused this improvement in the CO_2 permeability. As was discussed in Section 4.3 This modification can be noticed in Figure 48.a where wrinkled lines appeared in the top part of the membrane matrix.

4.6.2.2 Double-layer Membranes with Different PEBAX 1657 Concentrations in the Top Layer

It was found that permeability increases with reducing the PEBAX 1657 concentration (Wang et al. 2014). For this reason, the concentration of PEBAX 1657 was reduced in the top layer to enhance the permeability of CO_2 by considering the impact on the selectivity. The gas permeability results were reported in Table 19 and Figure 54. As it was expected, the permeability had an inverse relation with PEBAX 1657 concentration in the top layer. Nevertheless, selectivity was highest at 37.8 with 2 wt % PEBAX 1657 concentration in the top layer.

Table 19. *The separation performance of M4, M5, and M6 (pure PEBAX 1657 double-layer membranes with different PEBAX 1657 wt % ratios in the top layer)*

Membrane Code	Membrane Description	CO_2 Permeability (Barrer)	N_2 Permeability (Barrer)	Ideal Selectivity	Thickness (µm)
M4	Double-layer 4 (top)/4 (Bottom) wt % pure PEBAX 1657	175.0 ± 8.45	5.1 ± 0.06	34.1 ± 1.64	152
M5	Double-layer 2 (top)/4 (Bottom) wt % pure PEBAX 1657	188.6 ± 3.02	5.0 ± 0.17	37.8 ± 1.59	91
M6	Double-layer 1 (top)/4 (Bottom) wt % pure PEBAX 1657	206.5 ± 6.78	5.6 ± 0.32	36.7 ± 0.96	96
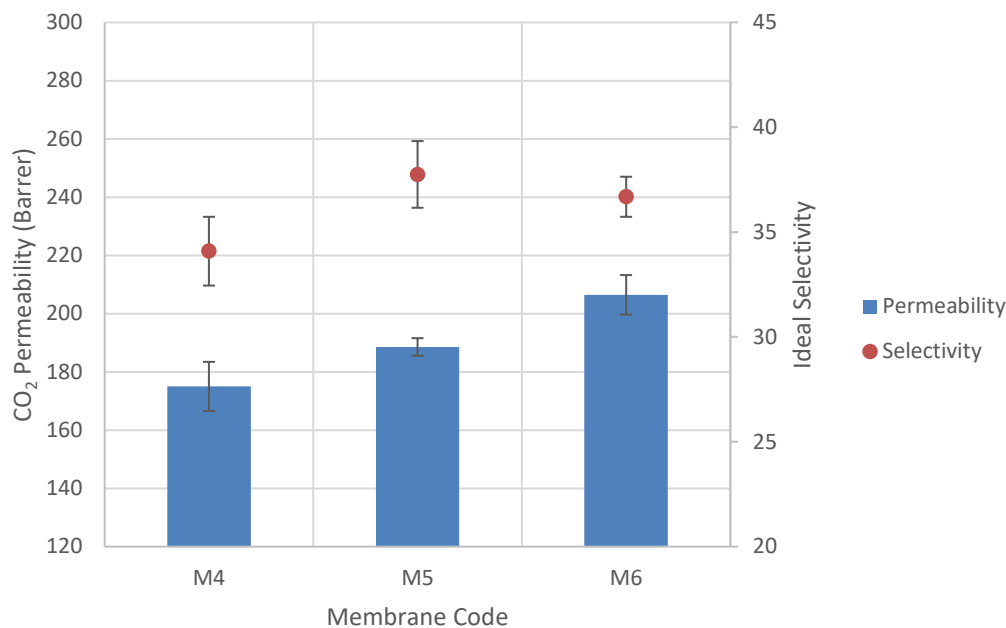
Figure 54. The separation performance of M4, M5, and M6 (pure PEBAX 1657 double-layer membranes with different PEBAX 1657 wt % ratios in the top layer)

4.6.3 ZIF-8/PEBAX 1657 Single-Layer Membranes

The main aim of this work is to improve the permeability and ideal selectivity of CO_2/N_2. As it was explained in the literature review section, ZIF-8 particles were proved to enhance the permeability and selectivity of the PEBAX 1657 membranes. In this study, two different sizes of particles were used to figure out their impact on separation performance. The theoretical explanation for this improvement is that the link between the organic units and MOFs creates interfacial voids having well-defined shapes and sizes that have a three-dimensional structure. As a result, the free volume elements of a matrix are enhanced that leads to an increase in gas permeability (Esposito et al. 2020). Furthermore, the preferential pathway for a specific gas is formed that improves the separation selectivity (Esposito et al. 2020).

The gas permeability of these membranes was compared to the M1.a as can be shown in Table 20 and Figure 55. These results proved that ZIF-8 particles could improve the separation performance of 4 wt % pure PEBAX 1657 single-layer membrane in terms of both the permeability and selectivity. Besides, ZIF-8 (323 nm) had a better positive impact compared to ones with a size of 67nm.

The particles with larger volume are assumed to have higher impact on the free volume of the matrix compared to small ones, thus the permeability was enhanced relatively. A study (Zheng et al. 2019) on the effect of the ZIF-8 particle size on PEBAX 1657 showed similar results where permeability enhanced with the particle size. For selectivity, in the same study a clear trend was not observed with the particle size. Although, it was expected that selectivity has an inverse relation with particle size due to the specific surface area that may cause a chain rigidification within the matrix. It was reported that this change creates more active sites for carbon dioxide and enhances the mass transfer resistance for nitrogen which has higher kinetic diameter compared to CO_2 (Zheng et al. 2019). Furthermore, ZIF-8 particles (67) may create more non-selective voids compared to the ZIF-8 (323) since their number is approximately five times higher. Besides, the selectivity of PEBAX 1657 membranes loaded with ZIF-8 particles is slightly higher than the pure PEBAX 1657. It can be argued that the selective nature of ZIF-8 particles could compensate the negative impact on selectivity due to the increasing of the free volume within the membrane matrix.

Table 20. *Single-layer MMMs (M7 and M8) separation performances compared to single-layer 4 wt % pure PEBAX 1657 membrane (M1.a)*

Membrane Code	Membrane Description	CO_2 Permeability (Barrer)	N_2 Permeability (Barrer)	Ideal selectivity	Thickness (μm)
M1	Single-layer 4 wt % pure PEBAX 1657	155.2 ± 9.02	4.3 ± 0.18	36.5 ± 0.83	121
M7	Single-layer 4 wt % pure PEBAX 1657 loaded with 5 wt % ZIF-8 (67 nm)	183.8 ± 3.82	4.8 ± 0.21	38.6 ± 1.16	106
M8	Single-layer 4 wt % pure PEBAX 1657 loaded with 5 wt % ZIF-8 (323 nm)	195.2 ± 0.48	5.0 ± 0.32	38.9 ± 2.32	110
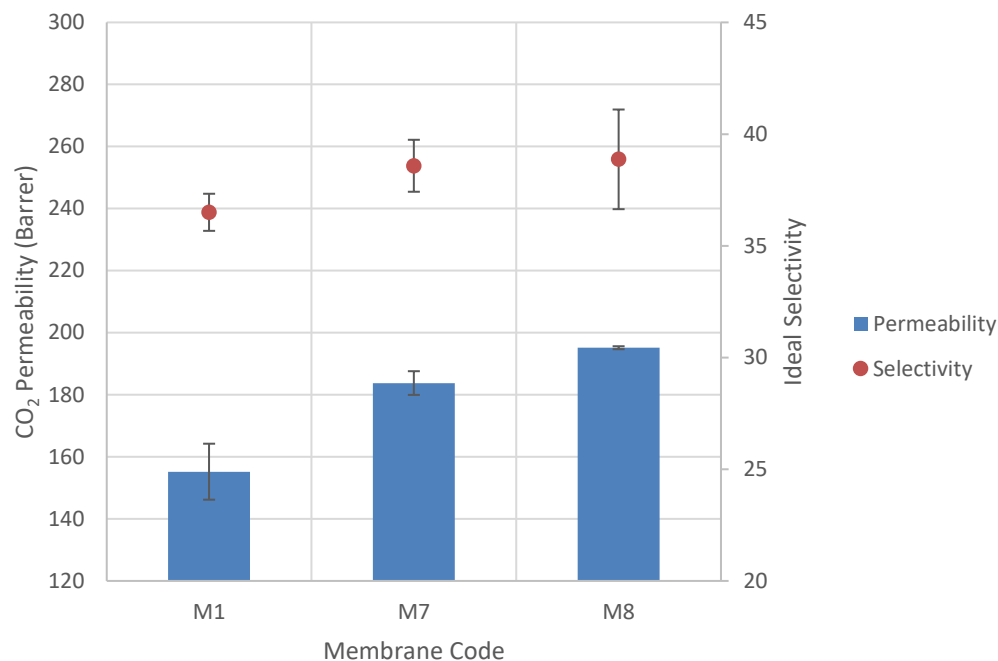
Figure 55. Single-layer MMMs (M7 and M8) separation performances compared to single-layer 4 wt % pure PEBAX 1657 membrane (M1.a)

4.6.4 ZIF-8/PEBAX 1657 Double-Layer Membranes

The permeability of M7 and M8 showed an increase compared to the M1a membrane. Moreover, previous results showed that a double layer is much better than a single layer in terms of CO_2 permeability. Thus, the influence of the combination of these two factors in one membrane was reason enough to be tested. Table 21 and Figure 56 showed that this combination deserved to be made due to the significant improvement in the permeability. It can be proved by these results that double-layer membranes have higher permeability and slightly lower selectivity compared to the single-layer membranes with the same type. On the other hand, membranes that were loaded with 323 nm of ZIF-8 showed an improvement in CO_2 permeability by factors of 1.3, 1.46, and 1.63 compared to M7, M4, and M1.a, respectively. Thus, the double-layer technique was more effective with ZIF-8 particles (323 nm), which is reasonable since the solvent diffusion into the membrane

matrix is higher with these particles due to larger interfacial voids that were created within the matrix. As aforementioned, the presence of ZIF-8 (323 nm) created larger free volumes.

Table 21. *The effect of the double-layer method on MMMs (4 wt % PEBAX 1657 loaded with different ZIF-8 particles sizes)*

Membrane Code	Membrane description	CO_2 Permeability (Barrer)	N_2 Permeability (Barrer)	deal selectivity	Thickness (µm)
M7	Single-layer 4 wt % pure PEBAX 1657 loaded with 5 wt % ZIF-8 (67 nm)	183.8 ± 3.82	4.8 ± 0.21	38.6 ± 1.16	106
M8	Single-layer 4 wt % pure PEBAX 1657 loaded with 5 wt % ZIF-8 (323 nm)	195.2 ± 0.48	5.0 ± 0.32	38.9 ± 2.32	110

Table 21. (cont'd) *The effect of the double-layer method on MMMs (4 wt % PEBAX 1657 loaded with different ZIF-8 particles sizes)*

Membrane Code	Membrane description	CO$_2$ Permeability (Barrer)	N$_2$ Permeability (Barrer)	deal selectivity	Thickness (µm)
M9	Double-layer 4 wt % pure PEBAX 1657 loaded with 5 wt % ZIF-8 (67 nm)	209.3 ± 11.9	5.9 ± 0.4	35.3 ± 0.38	170
M10	Double-layer 4 wt % pure PEBAX 1657 loaded with 5 wt % ZIF-8 (323 nm)	253.7 ± 11.42	6.8 ± 0.25	37.14 ± 1.36	169
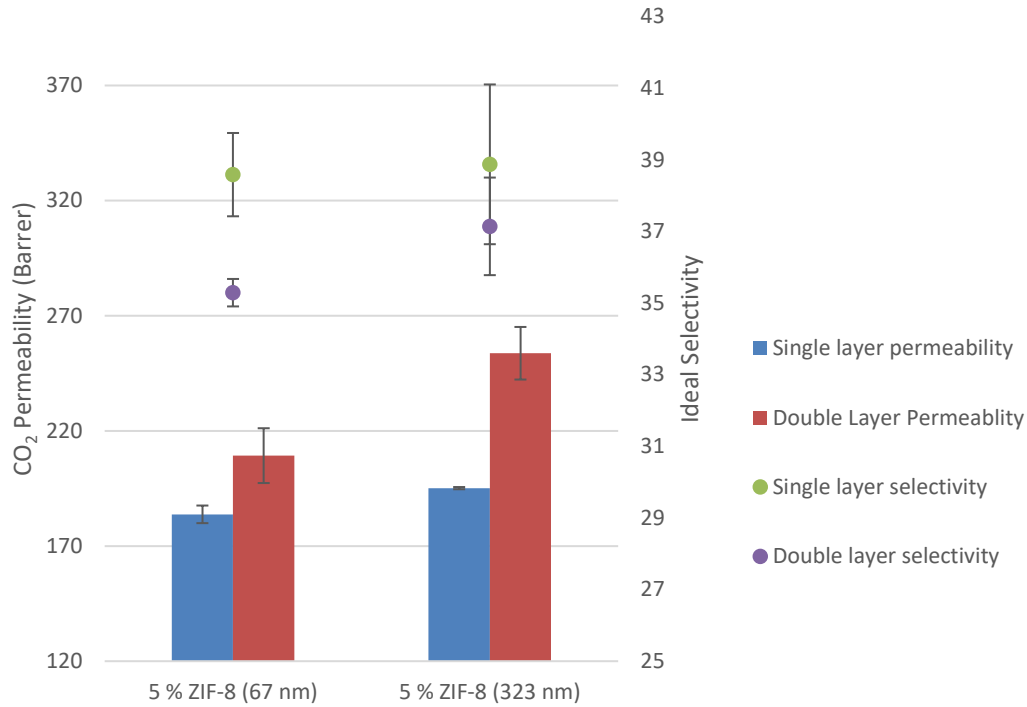
Figure 56. The effect of the double-layer method on MMMs (4 wt % PEBAX 1657 loaded with different ZIF-8 particles sizes)

4.7 Proposed Models to Explain the Enhancement of the Carbon Dioxide Permeability in Double-Layer Membranes Compared to Single-Layer Membranes

In the previous sections, the impact of the double-layer method was proved experimentally. For example, carbon dioxide permeability was increased in all types of double-layer membranes (M4, M9, and M10) compared to single-layers membranes (M1.a, M7, and M8), respectively. In this section, different assumptions are given to explain this theory mathematically.

4.7.1 Effective Thickness Model

The first assumption can be stated as that double-layer membranes have an effective thickness in their matrix whereas the other part (the modified part) is a very highly permeable section that has approximately no resistance as Figure 57 shows.
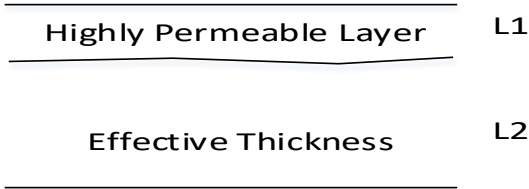
Figure 57. Simple schematic for effective thickness model

To calculate this effective thickness, the permeance for the double-layer membranes was calculated using the experimental results of permeability and thickness measurements as Equation [19] shows

$$Permeance_{double-layer} = \frac{Permeability_{double-layer}}{thikcness_{double-layer}} \tag{19}$$

In case that morphologies of both double-layer and single-layer membranes are the same, permeability should be the same in both membrane types since it is a material property. Thus, effective thickness according to this proposal can be calculated using the permeance of the double-layer membranes as Equation [20] shows. The calculated effective thicknesses of the double-layer membranes are listed in

$$Effective\ thickness = \frac{Permeability_{single-layer}}{permeance_{double-layer}} \tag{20}$$

Table 22. *Estimation of the effective thickness of the double-layer membranes using permeance of single-layer membranes*

Membrane Type	CO_2 Permeability (Barrer) of double-layer	True thickness (μm) of double-layer	Permeance (GPT) of double-layer	CO_2 Permeability (Barrer) of single-layer	Effective thickness (μm)
Pure PEBAX 1657	174.3	147.6	1.18	155.2	131.4
MMM (67 nm ZIF-8)	209.3	169.6	1.24	183.8	148.7
MMM (323) nm ZIF-8)	253.7	152.2	1.67	195.2	117.1

The effective thickness is less than the true thickness in all types. According to this model, 11%, %, 12.2%, and 23.1% of the total thickness of these membranes, respectively, were highly permeable sections with no resistance. However, SEM analysis showed that the modified matrix is, almost all cases, more than 30 %. Moreover, optical microscopic results in Figure 47 showed that both layers have almost the same fraction. Thus, from the point of view of the two characterization methods these values are small to represent the modified matrix. Nevertheless, since effective thickness is not even a quarter of the matrix, this modified portion may belong to the interface layer between the two layers.

4.7.2 Interface Model

Ohms' law was the tool in this study to demonstrate the effect of the interface mathematically. As it was explained in the literature review section, Ohm's Equation for membranes mainly depends on the idea of parallel resistances as Equation [21] shows:

$$\frac{L}{P} = \sum \frac{1}{R_i} \quad (21)$$

Since all the double-layer membranes were synthesized by casting the top layer on the solid form of the bottom one, an interface layer formation was expected. Furthermore, this interface was expected to have a high-volume void fraction compared to the other two membranes thus it has a lower resistance. This proposal has the following form of Ohm's Equation:

$$\frac{1}{P} = \frac{x_{top}}{P_{top}} + \frac{x_{int}}{P_{int}} + \frac{x_{bot}}{P_{bot}} \quad (22)$$

P is the total permeability where x is the thickness fraction of each layer. The above equation can be simplified more to Equation [23] by assuming that the resistances of the top and bottom layers are the same and equal to their resistances in the single-layer condition.

$$\frac{1}{P_{double}} = \frac{1 - x_{int}}{P_{single}} + \frac{x_{int}}{P_{int}} \quad (23)$$

Rearrange Equation [23] to calculate the interface layer permeability forms Equation [24]

$$P_{int} = x_{int} * (\frac{1}{P_{double}} - \frac{1 - x_{int}}{P_{single}})^{-1} \quad (24)$$

Table 23. *Interface thickness values for three different double-layer membranes according to Ohm's Equation*

Interface layer thickness	Interface Permeability (Barrer)		
	4 wt % pure PEBAX 1657	Pure PEBAX 1657 (4 wt %) loaded with 5 wt % ZIF-8 (67 nm)	Pure PEBAX 1657 (4 wt %) loaded with 5 wt % ZIF-8 (323 nm)
0.00	0.00	0.00	0.00
0.10	-	-	-
0.20	342.32	-	-
0.30	244.19	-	-
0.40	213.57	-	-
0.50	198.63	-	-
0.60	189.78	1410.94	-
0.70	183.93	462.48	807.57
0.80	179.77	307.47	422.91
0.90	176.66	243.89	308.59
1.00	174.25	209.27	253.72

According to Table 23, the interface thickness should be at least 0.7 to prove the validity of the interface proposal since at lower thicknesses negative values were calculated and presented as dash lines. However, due to the characterization analysis interface thickness for any type of these membranes does not have this value. These results prove mathematically that the morphologies of microscopic membranes were modified according to Ohm's Equation.

CHAPTER 5

CONCLUSION

Capturing carbon dioxide grabbed a lot of attention recently due to its positive impact on the environment. Membrane technology was one of the promising methods to achieve the target of reducing the amount of carbon dioxide. However, gas-separation by polymeric membranes faces some challenges such as the trade-off between permeability and selectivity which was presented by Robeson-line. For this reason, research has been focusing on surpassing these drawbacks to improve the efficiency of the separation process and get optimal outcomes. Besides, the economy and environment play a crucial rule alongside the membrane separation performance. Thus, surpassing Robeson-line should not be the only criterion since that might be economically and environmentally infeasible.

In this study, preheated air at 35 °C with a flow rate of 7.5 L/s was used to sweep the evaporated solvent from the casted membranes. As a result, naked-eye observation showed that produced membranes in this system are flat with neither wrinkles nor shrinkages.

Furthermore, it was observed by the optical microscope that solvent could travel though the membrane matrix by tracing the pink color. Moreover, it was observed by the optical microscope that solvent penetration depends mainly on the time and solvent amount.

Finally, this analysis showed that two separate layers were formed in the double-layer method. This was also proven by SEM analysis where segregated layers were seen in most of the double-layer membranes (M4, M5, M6, M9 and M10).

Modifying pure PEBAX 1657 membranes by additional solvent enhanced the permeability of CO_2 by 1.21 compared to M1.a. Moreover, there was a slight increase in the selectivity of M2 and M3 by 1.05 and 1.07. Thus, the two membranes showed a better separation performance in terms of permeability and selectivity.

Alongside the solvent modification, the double-layer membranes (M4, M5 and M6) in which the PEBAX 1657 wt % was varied (4, 2 and 1, respectively) had higher permeability of carbon dioxide compared to M1.a by 1.13, 1.23, and 1.33; respectively. This improvement combined with a minimal drop in selectivity. Furthermore, as it was expected, CO_2 permeability of these membranes had an inverse relation with the wt % of PEBAX 1657 in the top layer.

Besides, the CO_2 permeability of single-layer MMMs (M7 and M8) were higher by 1.18 and 1.26 respectively, compared to M1.a, with insignificant enhancement in the selectivity (increased by 1.06 only). On the other side, double-layer MMMs (M9 and M10) increased the carbon dioxide permeability by 1.14 and 1.3 compared to M7 and M8, respectively. In addition, selectivity dropped in both cases slightly, which proves that the double-layer membranes have higher CO_2 permeability with minimal loss in the selectivity compared to single-layers membranes. Finally, M10 has the highest CO_2 permeability that is higher by 1.63 compared to M1.a membrane which is the reference membrane in this study. The two membranes were located in Robeson graph with green circles as Figure 58 shows
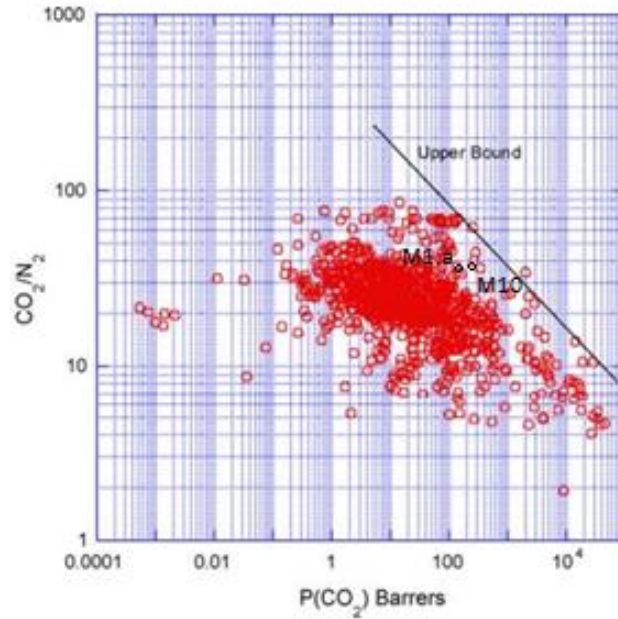
Figure 58: Locating M1.a and M10 in Robeson graph

In this work, two cheap methods were used to enhance carbon dioxide permeability. These modified membranes could not surpass Robeson-line; however, they can be economically more feasible than the ones above this line. Therefore, this study opens a new discussion to re-define what is "good membrane" for gas separation. Consequently, the economic aspects of the synthesizing process should be considered alongside with membrane efficiency in the gas separation process.

REFERENCES

Adams, Ryan, Cantwell Carson, Jason Ward, Rina Tannenbaum, and William Koros. 2010. "Metal Organic Framework Mixed Matrix Membranes for Gas Separations." *Microporous and Mesoporous Materials* 131(1–3):13–20.

Alentiev, A. Yu, and Yu P. Yampolskii. 2000. "Free Volume Model and Tradeoff Relations of Gas Permeability and Selectivity in Glassy Polymers." *Journal of Membrane Science* 165(2):201–16.

Anon. 2009. "Energy and Climate Change: Climate Energy and Change World Energy Outlook Special Report." *INTERNATIONAL ENERGY AGENCY*.

Anon. 2019. "Turkey - CO2 Emissions per Capita." *Knoema*. Retrieved (https://knoema.com/atlas/Turkey/CO2-emissions-per-capita).

Anon. n.d. *Edited by Membranes in Clean Technologies Nonporous Inorganic Membranes Materials Science of Membranes for Gas and Vapor Separation Membranen Ceramic Membranes for Separation and Reaction*.

Azizi, Navid, Mehran Arzani, Hamid Reza Mahdavi, and Toraj Mohammadi. 2017. "Synthesis and Characterization of Poly(Ether-Block-Amide) Copolymers/Multi-Walled Carbon Nanotube Nanocomposite Membranes for CO2/CH4 Separation." *Korean Journal of Chemical Engineering* 34(9):2459–70.

Baena-Moreno, Francisco M., Mónica Rodríguez-Galán, Fernando Vega, Bernabé Alonso-Fariñas, Luis F. Vilches Arenas, and Benito Navarrete. 2019. "Carbon Capture and Utilization Technologies: A Literature Review and Recent Advances." *Energy Sources, Part A: Recovery, Utilization and Environmental Effects* 41(12):1403–33.

Baker, Richard W. 2012. *Membrane Technology and Applications*. 2nd ed. Menlo Park, California: Jhon Wiley & Sons, Ltd.

Basile, Angelo, A. Gugliuzza, A. Iulianelli, and P. Morrone. 2011. "Membrane Technology for Carbon Dioxide (CO2) Capture in Power Plants." *Advanced Membrane Science and Technology for Sustainable Energy and Environmental Applications* (2008):113–59.

Bedeaux, D., J. A. M. Smit, L. J. F. Hermans, and T. Ytrehus. 1992. "Slow Evaporation and Condensation." *Physica A: Statistical Mechanics and Its Applications* 182(3):388–418.

Bernardo, Paola, and Gabriele Clarizia. 2020. "Enhancing Gas Permeation Properties of Pebax® 1657 Membranes via Polysorbate Nonionic Surfactants Doping." *Polymers* 12(2).

Berthod, A., M. J. Ruiz-Ángel, and S. Carda-Broch. 2008. "Ionic Liquids in Separation Techniques." *Journal of Chromatography A* 1184(1–2):6–18.

Bhole, Y. S., U. K. Kharul, S. P. Somani, and S. C. Kumbharkar. 2005. "Benzoylation of Polyphenylene Oxide: Characterization and Gas Permeability Investigations." *European Polymer Journal* 41(10):2461–71.

Bi, J., G. P. Simon, A. Yamasaki, C. L. Wang, Y. Kobayashi, and H. J. Griesser. 2000. "Effects of Solvent in the Casting of Poly(1-Trimethylsilyl-1-Propyne) Membranes." *Radiation Physics and Chemistry* 58(5–6):563–66.

Borisov, Ilya, Vladimir Vasilevsky, Dmitry Matveev, Anna Ovcharova, Alexey Volkov, and Vladimir Volkov. 2019. "Effect of Temperature Exposition of Casting Solution on Properties of Polysulfone Hollow Fiber Membranes." *Fibers* 7(12):1–16.

Bos, A., I. G. M. Pünt, M. Wessling, and H. Strathmann. 1999. "CO2-Induced Plasticization Phenomena in Glassy Polymers." *Journal of Membrane Science* 155(1):67–78.

Brar, Tejinder, Paul France, and Panagiotis G. Smirniotis. 2001. "Control of Crystal Size and Distribution of Zeolite A." *Industrial and Engineering Chemistry Research* 40(4):1133–39.

Bungay, P. M. 1987. "Transport Principles-Porous Membranes." Pp. 109–53 in *Synthetic Membranes: Science, Engineering and Applications*. Vol. 223. Springer.

Cao, Chun, Tai Shung Chung, Ye Liu, Rong Wang, and K. P. Pramoda. 2003. "Chemical Cross-Linking Modification of 6FDA-2,6-DAT Hollow Fiber Membranes for Natural Gas Separation." *Journal of Membrane Science* 216(1–2):257–68.

Car, Anja, Chrtomir Stropnik, and Klaus Viktor Peinemann. 2006. "Hybrid Membrane Materials with Different Metal-Organic Frameworks (MOFs) for Gas Separation." *Desalination* 200(1–3):424–26.

Car, Anja, Chrtomir Stropnik, Wilfredo Yave, and Klaus V. Peinemann. 2008. "PEG Modified Poly(Amide-b-Ethylene Oxide) Membranes for CO2 Separation." *Journal of Membrane Science* 307(1):88–95.

Cebrucean, Dumitru, Viorica Cebrucean, and Ioana Ionel. 2014. "CO2 Capture and Storage from Fossil Fuel Power Plants." *Energy Procedia* 63(ii):18–26.

Chun-hong, HE, LIU Jia-qi, and ZHANG Jian-ping. 2006. "Effects of Heating Treatment of the Membrane Abstrate on the Separation Performance of Composite Hollow Fiber Membrane." *Natural Gas Chemical Industry* 39(2):29–33.

Cong, Hailin, Xudong Hu, Maciej Radosz, and Youqing Shen. 2007. "Brominated Poly(2,6-Diphenyl-1,4-Phenylene Oxide) and Its Silica Nanocomposite Membranes for Gas Separation." *Industrial and Engineering Chemistry Research* 46(8):2567–75.

Cong, Hailin, Bing Yu, Jianguo Tang, and Xiu Song Zhao. 2012. "Ionic Liquid Modified Poly(2, 6-Dimethyl-1, 4-Phenylene Oxide) for CO 2 Separation." *Journal of Polymer Research* 19(2):4–9.

Cravillon, Janosch, Simon Münzer, Sven Jare Lohmeier, Armin Feldhoff, Klaus Huber, and Michael Wiebcke. 2009. "Rapid Room-Temperature Synthesis and Characterization of Nanocrystals of a Prototypical Zeolitic Imidazolate Framework." *Chemistry of Materials* 21(8):1410–12.

Cserjési, Petra, Nándor Nemestóthy, and Katalin Bélafi-Bakó. 2010. "Gas Separation Properties of Supported Liquid Membranes Prepared with Unconventional Ionic Liquids." *Journal of Membrane Science* 349(1–2):6–11.

Deolalkar, S. P. 2016. *Designing Green Cement Plants*. Elsevier.

Dollimore, D. 1982. "Physical Aging in Amorphous Polymers and Other Materials." *Thermochimica Acta* 54(1–2):242–43.

Dong, Guangxi, Hongyu Li, and Vicki Chen. 2013. "Challenges and Opportunities for Mixed-Matrix Membranes for Gas Separation." *Journal of Materials Chemistry A* 1(15):4610–30.

Drews, Timothy O., and Michael Tsapatsis. 2005. "Progress in Manipulating Zeolite Morphology and Related Applications." *Current Opinion in Colloid and Interface Science* 10(5–6):233–38.

Esposito, Elisa, Rosaria Bruno, Marcello Monteleone, Alessio Fuoco, Jesús Ferrando Soria, Emilio Pardo, Donatella Armentano, and Johannes Carolus Jansen. 2020. "Glassy PEEK-WC vs. Rubbery Pebax®1657 Polymers: Effect on the Gas Transport in CuNi-MOF Based Mixed Matrix Membranes." *Applied Sciences (Switzerland)* 10(4).

Farashi, Zahra, Saba Azizi, Masood Rezaei-Dasht Arzhandi, Zahra Noroozi, and Navid Azizi. 2019. "Improving CO2/CH4 Separation Efficiency of Pebax-1657 Membrane by Adding Al2O3 Nanoparticles in Its Matrix." *Journal of Natural Gas Science and Engineering* 72(July):103019.

Flesher, Joseph R. 1986. "PEBAX® POLYETHER BLOCK AMIDE - A NEW FAMILY OF ENGINEERING THERMOPLASTIC ELASTOMERS JOSEPH R. FLESHER, JR. Atochem Inc., Polymers Division, 1112 Lincoln Road, Birdsboro, PA."

Freger, Viatcheslav, Jack Gilron, and Sofia Belfer. 2002. "TFC Polyamide Membranes Modified by Grafting of Hydrophilic Polymers: An FT-IR/AFM/TEM Study." *Journal of Membrane Science* 209(1):283–92.

Gary T. Rochelle. 2012. "Carbon Capture and Sequestration: Amine Scrubbing for CO2 Capture." *SCIENCE* 325(September 2009):1652–54.

Gascon, Jorge, Sonia Aguado, and Freek Kapteijn. 2008. "Manufacture of Dense Coatings of Cu3(BTC)2 (HKUST-1) on α-Alumina." *Microporous and Mesoporous Materials* 113(1–3):132–38.

George, Soney C., and Sabu Thomas. 2001. "Transport Phenomena through Polymeric Systems." *Progress in Polymer Science (Oxford)* 26(6):985–1017.

Goyena, Rodrigo, and A. .. Fallis. 2019. *Polymeric Gas Separation Membranes*. Vol. 53.

Grün, F. 1947. "Diffusionsmessungen an Kautschuk." *Experientia* 3(12):490–92.

Hamad, F., K. C. Khulbe, and T. Matsuura. 2002. "Characterization of Gas Separation Membranes Prepared from Brominated Poly (Phenylene Oxide) by Infrared Spectroscopy." *Desalination* 148(1–3):369–75.

Hamad, F., and T. Matsuura. 2005. "Performance of Gas Separation Membranes Made from Sulfonated Brominated High Molecular Weight Poly(2,4-Dimethyl-l,6-PhenyIene Oxide)." *Journal of Membrane Science* 253(1–2):183–89.

Hamid, Mohamad Rezi Abdul, and Hae Kwon Jeong. 2018. "Recent Advances on Mixed-Matrix Membranes for Gas Separation: Opportunities and Engineering Challenges." *Korean Journal of Chemical Engineering* 35(8):1577–1600.

Hamouda, Sofiane Ben, Ali Boubakri, Quang Trong Nguyen, and Mohamed Ben Amor. 2011. "PEBAX Membranes for Water Desalination by Pervaporation Process." *High Performance Polymers* 23(2):170–73.

Hawthorne, C., M. Trossmann, P. Galindo Cifre, A. Schuster, and G. Scheffknecht. 2009. "Simulation of the Carbonate Looping Power Cycle." *Energy Procedia* 1(1):1387–94.

Hillock, Alexis M. W., Stephen J. Miller, and William J. Koros. 2008. "Crosslinked Mixed Matrix Membranes for the Purification of Natural Gas: Effects of Sieve Surface Modification." *Journal of Membrane Science* 314(1–2):193–99.

Ho, Bum Park, Ki Kim Choon, and Moo Lee Young. 2002. "Gas Separation Properties of Polysiloxane/Polyether Mixed Soft Segment Urethane Urea Membranes." *Journal of Membrane Science* 204(1–2):257–69.

Ho, Minh T., Guy W. Allinson, and Dianne E. Wiley. 2008. "Reducing the Cost of CO2 Capture from Flue Gases Using Membrane Technology." *Industrial and Engineering Chemistry Research* 47(5):1562–68.

Hoenig, Volker, Helmut Hoppe, and Bernhard Emberger. 2007. "Carbon Capture Technology-Options and Potentials for the Cement Industry." *PCA R&D Serial No. 3022* (3022):98.

Hosseinzadeh Beiragh, Hosna, Mohammadreza Omidkhah, Reza Abedini, Tayebeh Khosravi, and Saeed Pakseresht. 2016. "Synthesis and Characterization of Poly (Ether-Block-Amide) Mixed Matrix Membranes Incorporated by Nanoporous ZSM-5 Particles for CO2/CH4 Separation." *Asia-Pacific Journal of Chemical Engineering* 11(4):522–32.

Huang, Xiao Chun, Yan Yong Lin, Jie Peng Zhang, and Xiao Ming Chen. 2006. "Ligand-Directed Strategy for Zeolite-Type Metal-Organic Frameworks: Zinc(II) Imidazolates with Unusual Zeolitic Topologies." *Angewandte Chemie - International Edition* 45(10):1557–59.

Husken, Debby, Tymen Visser, Matthias Wessling, and Reinoud J. Gaymans. 2010. "CO2 Permeation Properties of Poly(Ethylene Oxide)-Based Segmented Block Copolymers." *Journal of Membrane Science* 346(1):194–201.

Isanejad, Mojgan, Navid Azizi, and Toraj Mohammadi. 2017. "Pebax Membrane for CO2/CH4 Separation: Effects of Various Solvents on Morphology and Performance." *Journal of Applied Polymer Science* 134(9):1–9.

Ismail, Ahmad Fauzi, Kailash Chandra Khulbe, and Takeshi Matsuura. 2015. *Gas Separation Membranes: Polymeric and Inorganic*.

Jhung, Sung Hwa, Ji Hye Lee, and Jong San Chang. 2008. "Crystal Size Control of Transition Metal Ion-Incorporated Aluminophosphate Molecular Sieves: Effect of

Ramping Rate in the Syntheses." *Microporous and Mesoporous Materials* 112(1–3):178–86.

Jiang, Hai Long, Bo Liu, Tomoki Akita, Masatake Haruta, Hiroaki Sakurai, and Qiang Xu. 2009. "Au@ZIF-8: CO Oxidation over Gold Nanoparticles Deposited to Metal-Organic Framework." *Journal of the American Chemical Society* 131(32):11302–3.

Jomekian, Abolfazl, Reza Mosayebi Behbahani, Toraj Mohammadi, and Ali Kargari. 2016. "CO2/CH4 Separation by High Performance Co-Casted ZIF-8/Pebax 1657/PES Mixed Matrix Membrane." *Journal of Natural Gas Science and Engineering* 31:562–74.

Kasman, Adnan, and Yavuz Selman Duman. 2015. "CO2 Emissions, Economic Growth, Energy Consumption, Trade and Urbanization in New EU Member and Candidate Countries: A Panel Data Analysis." *Economic Modelling* 44:97–103.

Kenarsari, Saeed Danaei, Dali Yang, Guodong Jiang, Suojiang Zhang, Jianji Wang, Armistead G. Russell, Qiang Wei, and Maohong Fan. 2013. "Review of Recent Advances in Carbon Dioxide Separation and Capture." *RSC Advances* 3(45):22739–73.

Keser Demir, Nilay, Berna Topuz, Levent Yilmaz, and Halil Kalipcilar. 2014. "Synthesis of ZIF-8 from Recycled Mother Liquors." *Microporous and Mesoporous Materials* 198:291–300.

Keser, Nilay. 2012. "PRODUCTION AND PERFORMANCE EVALUATION OF ZIF-8 BASED BINARY AND TERNARY MIXED MATRIX GAS SEPARATION MEMBRANES." Middle East Technical University.

Khan, Nazmul Abedin, In Joong Kang, Hwi Young Seok, and Sung Hwa Jhung. 2011. "Facile Synthesis of Nano-Sized Metal-Organic Frameworks, Chromium-Benzenedicarboxylate, MIL-101." *Chemical Engineering Journal* 166(3):1152–57.

Kita, Hidetoshi, Kazuhiro Tanaka, and Tomoko Koga. 2008. *Gas Separation Membranes*. Vol. 57. Ottawa: Springer.

Krishna, S. V., and G. Pugazhenthi. 2011. "Influence of Processing Conditions on the Properties of Polystyrene (PS)/Organomontmorillonite (OMMT) Nanocomposites Prepared via Solvent Blending Method." *International Journal of Polymeric Materials and Polymeric Biomaterials* 60(2):144–62.

Lethbridge, Zoe A. D., Jennifer J. Williams, Richard I. Walton, Kenneth E. Evans, and Christopher W. Smith. 2005. "Methods for the Synthesis of Large Crystals of Silicate Zeolites." *Microporous and Mesoporous Materials* 79(1–3):339–52.

Li, Chia Ling, Da Ming Wang, André Deratani, Damien Quémener, Denis Bouyer, and Juin Yih Lai. 2010. "Insight into the Preparation of Poly(Vinylidene Fluoride) Membranes by Vapor-Induced Phase Separation." *Journal of Membrane Science* 361(1–2):154–66.

Li, Wenjuan, Xiao Ye, Zhan Wang, Jing Zhang, and Jingdi Chao. 2011. "The Preparation and Performance Characteristics of Polyvinyl Chloride-Co-Vinyl Acetate Modified Membranes." *Energy Procedia* 5:1158–62.

Li, Yi, Huai Min Guan, Tai Shung Chung, and Santi Kulprathipanja. 2006. "Effects of Novel Silane Modification of Zeolite Surface on Polymer Chain Rigidification and Partial Pore Blockage in Polyethersulfone (PES)-Zeolite A Mixed Matrix Membranes." *Journal of Membrane Science* 275(1–2):17–28.

Liang, Lizhe, Quan Gan, and Paul Nancarrow. 2014. "Composite Ionic Liquid and Polymer Membranes for Gas Separation at Elevated Temperatures." *Journal of Membrane Science* 450:407–17.

Lin, Rijia, Byron Villacorta Hernandez, Lei Ge, and Zhonghua Zhu. 2018. "Metal Organic Framework Based Mixed Matrix Membranes: An Overview on Filler/Polymer Interfaces." *Journal of Materials Chemistry A* 6(2):293–312.

Liu, Li, Amit Chakma, and Xianshe Feng. 2006. "Propylene Separation from Nitrogen by Poly(Ether Block Amide) Composite Membranes." *Journal of Membrane Science* 279(1–2):645–54.

Lloyd, Douglas R. 1990. "MICROPOROUS MEMBRANE FORMATION VIA

THERMALLY INDUCED PHASE SEPARATION. I. SOLID-LIQUID PHASE SEPARATION." *Journal of Membrane Science* 52:239–61.

Mahajan, Rajiv, and William J. Koros. 2000. "Factors Controlling Successful Formation of Mixed-Matrix Gas Separation Materials." *Industrial and Engineering Chemistry Research* 39(8):2692–96.

Mahajan, Rajiv, and William J. Koros. 2002. "Mixed Matrix Membrane Materials with Glassy Polymers. Part 1." *Polymer Engineering and Science* 42(7):1420–31.

Marek, Miroslav, Eduard Brynda, Milan Houska, Jan Schauer, Vladimír Hynek, and Milan Šípek. 1996. "Crosslinked ULTRA-THIN Ultra-Thin Polyimide Film as a Gas-Separation Layer for Composite Membranes." *Polymer* 37(12):2577–79.

Mccabe, Warren L., Julian C. Smith, and Peter Harriott. 2012. "Unit Operations of Chemical Engineering." *McGraw-Hill*.

McCaig, M. S., and D. R. Paul. 1999. "Effect of UV Crosslinking and Physical Aging on the Gas Permeability of Thin Glassy Polyarylate Films." *Polymer* 40(26):7209–25.

Mokhatab, Saeid, William A. Poe, and John Y. Mak. 2019. *Natural Gas Dehydration and Mercaptans Removal*.

Moore, Theodore T., and William J. Koros. 2005. "Non-Ideal Effects in Organic-Inorganic Materials for Gas Separation Membranes." *Journal of Molecular Structure* 739(1–3):87–98.

Mulder, Marcel. 1991. *Basic Principles of Membrane Technology*.

Oral, Edibe Eda, Levent Yilmaz, and Halil Kalipcilar. 2014. "Effect of Gas Permeation Temperature and Annealing Procedure on the Performance of Binary and Ternary Mixed Matrix Membranes of Polyethersulfone, SAPO-34, and 2-Hydroxy 5-Methyl Aniline." *Journal of Applied Polymer Science* 131(17):8498–8505.

Ordoñez, Ma Josephine C., Kenneth J. Balkus, John P. Ferraris, and Inga H. Musselman. 2010. "Molecular Sieving Realized with ZIF-8/Matrimid® Mixed-Matrix Membranes." *Journal of Membrane Science* 361(1–2):28–37.

ÖZDEMİR N. K. 2017. "POLYIMIDE AND PEBAX FLAT AND HOLLOW FIBER MEMBRANES FOR GAS SEPARATION." *Universitas Nusantara PGRI Kediri* 01(July).

Pan, Yichang, Yunyang Liu, Gaofeng Zeng, Lan Zhao, and Zhiping Lai. 2011. "Rapid Synthesis of Zeolitic Imidazolate Framework-8 (ZIF-8) Nanocrystals in an Aqueous System." *Chemical Communications* 47(7):2071–73.

Panapitiya, Nimanka, Sumudu Wijenayake, Do Nguyen, Chamaal Karunaweera, Yu Huang, Kenneth Balkus, Inga Musselman, and John Ferraris. 2016. "Compatibilized Immiscible Polymer Blends for Gas Separations." *Materials* 9(8).

Paul, D. R., and D. R. Kemp. 1973. "THE DIFFUSION TIME LAG IN POLYMER MEMBRANES CONTAINING ADSORPTIVE FILLERS." *Journal of Polymer Science: Polymer Symposia* 93(41):79–93.

Pérez-Pellitero, Javier, Hedi Amrouche, Flor R. Siperstein, Gerhard Pirngruber, Carlos Nieto-Draghi, Gerald Chaplais, Angélique Simon-Masseron, Delphine Bazer-Bachi, David Peralta, and Nicolas Bats. 2010. "Adsorption of CO2, CH4, and N2 on Zeolitic Imidazolate Frameworks: Experiments and Simulations." *Chemistry - A European Journal* 16(5):1560–71.

Potreck, Jens, Kitty Nijmeijer, Thomas Kosinski, and Matthias Wessling. 2009. "Mixed Water Vapor/Gas Transport through the Rubbery Polymer PEBAX® 1074." *Journal of Membrane Science* 338(1–2):11–16.

R.D. Behling, K. Ohlrogge, K. V. Peinemann and E. Kyburz. 1989. "The Separation of Hydrocarbons from Waste Vapor Streams." *AIChE Symposium Series* 85(272):68.

Radovanovic, Philip, Stephen W. Thiel, and Sun Tak Hwang. 1992. "Formation of Asymmetric Polysulfone Membranes by Immersion Precipitation. Part I. Modelling Mass Transport during Gelation." *Journal of Membrane Science* 65(3):213–29.

Rahman, Md Mushfequr, Volkan Filiz, Sergey Shishatskiy, Clarissa Abetz, Silvio Neumann, Sabrina Bolmer, Muntazim Munir Khan, and Volker Abetz. 2013. "PEBAX® with PEG Functionalized POSS as Nanocomposite Membranes for CO2

Separation." *Journal of Membrane Science* 437:286–97.

Ramos-Fernandez, Enrique V., Mariana Garcia-Domingos, Jana Juan-Alcañiz, Jorge Gascon, and Freek Kapteijn. 2011. "MOFs Meet Monoliths: Hierarchical Structuring Metal Organic Framework Catalysts." *Applied Catalysis A: General* 391(1–2):261–67.

Recio, Roberto, Ángel E. Lozano, Pedro Prádanos, Ángel Marcos, Fernando Tejerina, and Antonio Hernández. 2008. "Effect of Fractional Free Volume and Tg on Gas Separation through Membranes Made with Different Glassy Polymers." *Journal of Applied Polymer Science* 107(2):1039–46.

Di Renzo, Francesco. 1998. "Zeolites as Tailor-Made Catalysts: Control of the Crystal Size." *Catalysis Today* 41(1–3):37–40.

Robeson, L. M. 2012. *Polymer Membranes*. Vol. 8. Elsevier B.V.

Robeson, L. M., B. D. Freeman, D. R. Paul, and B. W. Rowe. 2009. "An Empirical Correlation of Gas Permeability and Permselectivity in Polymers and Its Theoretical Basis." *Journal of Membrane Science* 341(1–2):178–85.

Robeson, Lloyd M. 1991. "Correlation of Separation Factor versus Permeability for Polymeric Membranes." *Journal of Membrane Science* 62(2):165–85.

Robeson, Lloyd M. 2008. "The Upper Bound Revisited." *Journal of Membrane Science* 320(1–2):390–400.

Rowe, B. W., B. D. Freeman, and D. R. Paul. 2011. "Chapter 3. Physical Aging of Membranes for Gas Separations." 1:58–83.

Rowe, Brandon W., Benny D. Freeman, and Donald R. Paul. 2009. "Physical Aging of Ultrathin Glassy Polymer Films Tracked by Gas Permeability." *Polymer* 50(23):5565–75.

Sanders, David F., Zachary P. Smith, Ruilan Guo, Lloyd M. Robeson, James E. McGrath, Donald R. Paul, and Benny D. Freeman. 2013. "Energy-Efficient Polymeric Gas Separation Membranes for a Sustainable Future: A Review." *Polymer* 54(18):4729–

61.

Scholes, Colin, Minh Ho, and Dianne Wiley. 2016. "Membrane-Cryogenic Post-Combustion Carbon Capture of Flue Gases from NGCC." *Technologies* 4(2):14.

Selyanchyn, Roman, Miho Ariyoshi, and Shigenori Fujikawa. 2018. "Thickness Effect on CO 2 /N 2 Separation in Double Layer Pebax-1657®/PDMS Membranes." *Membranes* 8(4).

Şener, Tansel, Emin Okumuş, Türker Gürkan, and Levent Yilmaz. 2010. "The Effect of Different Solvents on the Performance of Zeolite-Filled Composite Pervaporation Membranes." *Desalination* 261(1–2):181–85.

Shahid, Salman. 2015. "Polymer-Metal Organic Frameworks (MOFs) Mixed Matrix Membranes for Gas Separation Applications Salman Shahid." *Uni of Twente*.

Shao, Lu, Tai Shung Chung, Suat Hong Goh, and Kumari Pallathadka Pramoda. 2004. "Transport Properties of Cross-Linked Polyimide Membranes Induced by Different Generations of Diaminobutane (DAB) Dendrimers." *Journal of Membrane Science* 238(1–2):153–63.

Shinbo, Toshio, Tomohiko Yamaguchi, Hiroshi Yanagishita, Keiji Sakaki, Dai Kitamoto, and Masaaki Sugiura. 1993. "Supported Liquid Membranes for Enantioselective Transport of Amino Acid Mediated by Chiral Crown Ether - Effect of Membrane Solvent on Transport Rate and Membrane Stability." *Journal of Membrane Science* 84(3):241–48.

Song, Qilei, S. K. Nataraj, Mina V. Roussenova, Jin Chong Tan, David J. Hughes, Wei Li, Pierre Bourgoin, M. Ashraf Alam, Anthony K. Cheetham, Shaheen A. Al-Muhtaseb, and Easan Sivaniah. 2012a. "Zeolitic Imidazolate Framework (ZIF-8) Based Polymer Nanocomposite Membranes for Gas Separation." *Energy and Environmental Science* 5(8):8359–69.

Song, Qilei, S. K. Nataraj, Mina V. Roussenova, Jin Chong Tan, David J. Hughes, Wei Li, Pierre Bourgoin, M. Ashraf Alam, Anthony K. Cheetham, Shaheen A. Al-Muhtaseb, and Easan Sivaniah. 2012b. "Zeolitic Imidazolate Framework (ZIF-8)

Based Polymer Nanocomposite Membranes for Gas Separation." *Energy and Environmental Science* 5(8):8359–69.

Stanger, Rohan, Terry Wall, Reinhold Spörl, Manoj Paneru, Simon Grathwohl, Max Weidmann, Günter Scheffknecht, Denny McDonald, Kari Myöhänen, Jouni Ritvanen, Sirpa Rahiala, Timo Hyppänen, Jan Mletzko, Alfons Kather, and Stanley Santos. 2015. "Oxyfuel Combustion for CO2 Capture in Power Plants." *International Journal of Greenhouse Gas Control* 40:55–125.

Surya Murali, R., S. Sridhar, T. Sankarshana, and Y. V. L. Ravikumar. 2010a. "Gas Permeation Behavior of Pebax-1657 Nanocomposite Membrane Incorporated with Multiwalled Carbon Nanotubes." *Industrial and Engineering Chemistry Research* 49(14):6530–38.

Surya Murali, R., S. Sridhar, T. Sankarshana, and Y. V. L. Ravikumar. 2010b. "Gas Permeation Behavior of Pebax-1657 Nanocomposite Membrane Incorporated with Multiwalled Carbon Nanotubes." *Industrial and Engineering Chemistry Research* 49(14):6530–38.

Tocci, Elena, Annarosa Gugliuzza, Luana De Lorenzo, Marialuigia Macchione, Giorgio De Luca, and Enrico Drioli. 2008. "Transport Properties of a Co-Poly(Amide-12-b-Ethylene Oxide) Membrane: A Comparative Study between Experimental and Molecular Modelling Results." *Journal of Membrane Science* 323(2):316–27.

Tong, Zi, and W. S. Winsto. Ho. 2017. "Facilitated Transport Membranes for CO2 Separation and Capture." *Separation Science and Technology (Philadelphia)* 52(2):156–67.

Venna, Surendar R., and Moises A. Carreon. 2010. "Highly Permeable Zeolite Imidazolate Framework-8 Membranes for CO 2/CH4 Separation." *Journal of the American Chemical Society* 132(1):76–78.

Wang, Lianjun, Yang Li, Shuguang Li, Pengfei Ji, and Chengzhang Jiang. 2014. "Preparation of Composite Poly(Ether Block Amide) Membrane for CO2 Capture." *Journal of Energy Chemistry* 23(6):717–25.

Wu, Hong, Xueqin Li, Yifan Li, Shaofei Wang, Ruili Guo, Zhongyi Jiang, Chan Wu, Qingping Xin, and Xia Lu. 2014a. "Facilitated Transport Mixed Matrix Membranes Incorporated with Amine Functionalized MCM-41 for Enhanced Gas Separation Properties." *Journal of Membrane Science* 465:78–90.

Wu, Hong, Xueqin Li, Yifan Li, Shaofei Wang, Ruili Guo, Zhongyi Jiang, Chan Wu, Qingping Xin, and Xia Lu. 2014b. "Facilitated Transport Mixed Matrix Membranes Incorporated with Amine Functionalized MCM-41 for Enhanced Gas Separation Properties." *Journal of Membrane Science* 465:78–90.

Yang, Zhe, Hongdan Peng, Weizhi Wang, and Tianxi Liu. 2010. "Membranes Prepared by TiO2 Sol–Gel Method and PVDF–TiO2 Composite Hollow Fiber Ultrafiltration Blending Method." *Journal of Applied Polymer Science* 116(5):2658–67.

Yeldan, Erinç. 2017. "The Economics of Climate Change Action in Turkey: A Commentary." *New Perspectives on Turkey* 56(2000):139–45.

Young, Tai Horng, Yao Huei Huang, and Li Yen Chen. 2000. "Effect of Solvent Evaporation on the Formation of Asymmetric and Symmetric Membranes with Crystallizable EVAL Polymer." *Journal of Membrane Science* 164(1–2):111–20.

Yuan, Hua, Bing Yu, Hailin Cong, Qiaohong Peng, Ruixia Yang, Shujing Yang, Zhen Yang, Yongli Luo, Tao Xu, Hongbo Zhang, and Zhun Li. 2016. "Modification Progress of Polymermembranes for Gas Separation." *Reviews on Advanced Materials Science* 44(3):207–20.

Yuan, Shushan. n.d. "Advanced Membrane Synthesis Methods : Exploration of 3D Printed Membranes for Oil / Water Separation and Development of Novel Polymers for Organic Solvent Advanced Membrane Synthesis Methods : Exploration of 3D Printed Membranes for Oil / Water Separation." (December 2018).

Zhang, Chen, Ying Dai, Justin R. Johnson, Oguz Karvan, and William J. Koros. 2012. "High Performance ZIF-8/6FDA-DAM Mixed Matrix Membrane for Propylene/Propane Separations." *Journal of Membrane Science* 389:34–42.

Zhao, Hong Yong, Yi Ming Cao, Xiao Li Ding, Mei Qing Zhou, and Quan Yuan. 2008.

"Poly(N,N-Dimethylaminoethyl Methacrylate)-Poly(Ethylene Oxide) Copolymer Membranes for Selective Separation of CO2." *Journal of Membrane Science* 310(1–2):365–73.

Zhao, Jian, Gaoxing Luo, Jun Wu, and Hesheng Xia. 2013. "Preparation of Microporous Silicone Rubber Membrane with Tunable Pore Size via Solvent Evaporation-Induced Phase Separation." *ACS Applied Materials and Interfaces* 5(6):2040–46.

Zheng, Wenji, Rui Ding, Kai Yang, Yan Dai, Xiaoming Yan, and Gaohong He. 2019. "ZIF-8 Nanoparticles with Tunable Size for Enhanced CO 2 Capture of Pebax Based MMMs." *Separation and Purification Technology* 214(April 2018):111–19.

APPENDICES

APPENDIX A –Calculation used to synthesize different sizes of ZIF-8 particles

Amount used

Zn$^+$= 1.73 g   MeOH= 130.2 g   Hmim= 3.77   Small particles (67 nm)

Zn$^+$= 7.2 g   MeOH= 135 g   Hmim= 15.7   Large particles (323 nm)

Molar mass

Zn$^+$=297.4 g/mol   MeOH=32.04 g/mol   Hmim= 82.11 g/mol

Number of moles

Small Particles (67 nm)   Large particles (323 nm)

$$Zn^+ = \frac{1.73g}{297.4 \ g/mol} = 0.00582 \ mol \qquad Zn^+ = \frac{7.2 \ g}{297.4 \ g/mol} = 0.0242 \ mol$$

$$MeOH = \frac{130.2g}{32.04 \ g/mol} = 4.06 \ mol \qquad MeOH = \frac{135 \ g}{32.04 \ g/mol} = 4.21 \ mol$$

$$Hmim = \frac{3.77g}{82.11g/mol} = 0.0458 \ mol \qquad Hmim = \frac{15.7 \ g}{82.11 \ g/mol} = 0.191 \ mol$$

Molar Ratio

Small Particles (67 nm)

$$\frac{0.00582}{0.00582} : \frac{4.06}{0.00582} : \frac{0.0458}{0.00582} = 1 : 699 : 7.9$$

Large Particles (323 nm)

$$\frac{0.0242}{0.0242} : \frac{4.21}{0.0242} : \frac{0.191}{0.0242} = 1 : 174 : 7.9$$

APPENDIX B – Measuring the sizes of synthesized ZIF-8 particles
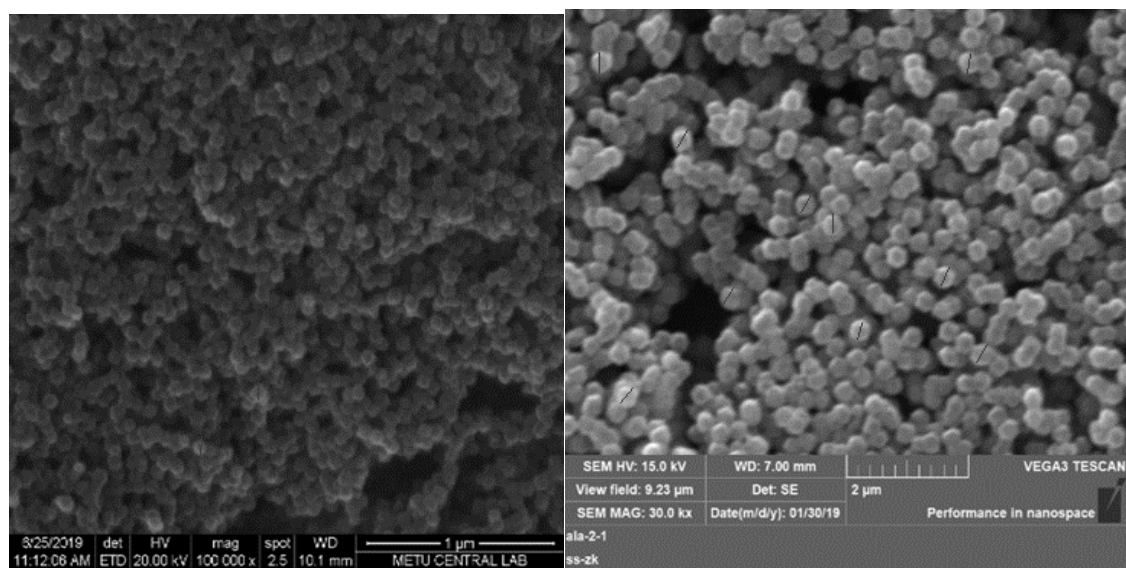
a   b

Figure 59. SEM analysis for ZIF-8 particles a) 67 and b) 323

Ten particles from each type in Figure 59 were measured and the average size of ZIF-8 particles prepared in this work is estimated as Table 24 shows

Table 24. *The average size of the synthesized ZIF-8 particles*

Particle Number	Large Particles (323 nm)	Small Particles (67 nm)
1	320.52	72.98
2	331.286	65.13
3	297.765	60.45
4	321.519	75.67

Table 25. (cont'd) *The average size of the synthesized ZIF-8 particles*

Particle Number	Large Particles (323 nm)	Small Particles (67 nm)
5	323.328	58.45
6	308.028	58.63
7	330.128	63.29
8	351.677	63.78
9	338.355	83.52
10	310.825	66.27
Average	323.34	66.82
Standard Deviation	14.81	7.73

APPENDIX C –The amounts of the materials used to prepare the membranes

Table 25. *The amount of the materials used to prepare the membranes tested in single-gas system*

| Membrane code | Bottom / Top solution | | | | Casting conditions | Annealing at oven 1st day (60 °C, 1 bar) 2nd day (60 °C, vacuum) |
	PEBAX 1657 (g)	Ethanol-water mixture	ZIF-8 (g)	Casted solution per Teflon dish (ml)	Temperature °C/ Airflow rate m³/s	
M1.a	0.6/-	15 g/-	0/-	15/-	35/0.0075	Done
M1.b	0.6/-	15 g/-	0/-	15/-	35/0.04	Done
M1.c	0.6/-	15 g/-	0/-	15/-	35/0.0075	
M2	0.6/0	15/ 3 mL	0/0	15/3	35/0.0075	Done
M3	0.6/0	15/12.5 mL	0/0	15/12.5	35/0.0075	Done

Table 25. (cont'd) *The amount of the materials used to prepare the membranes tested in single-gas system*

Membrane code	Bottom / Top solution			Casting conditions		Annealing at oven 1st day (60 °C, 1 bar) 2nd day (60 °C, vacuum)
	PEBAX 1657 (g)	Ethanol-water mixture	ZIF-8 (g)	Casted solution per Teflon dish (ml)	Temperature °C/ Airflow rate m³/s	
M4	0.6/0.6	15 g/15 g	0/0	10/10	35/0.0075	Done
M5	0.6/0.3	15 g/15 g	0/0	10/10	35/0.0075	Done
M6	0.6/0.15	15 g/15 g	0/0	10/10	35/0.0075	Done
M7	0.6/-	15 g/-	0.0315/-	15/-	35/0.0075	Done
M8	0.6/-	15 g/-	0.0315/-	15/-	35/0.0075	Done
M9	0.6/0.6	15 g/15 g	0.0315/ 0.0315	10/10	35/0.0075	Done
M10	0.6/0.6	15 g/15 g	0.0315/0.0315	10/10	35/0.0075	Done

Table 26. *The amount of the materials used to prepare the membranes analyzed by optical microscope*

Membrane code	Bottom / Top solution			Casting conditions		Casting period of the top solution	Annealing at oven 1st day (60 °C, 1 bar) 2nd day (60 °C, vacuum)
	PEBAX 1657 (g)	Ethanol-water mixture	Pink Dye solution (% wt)	Casted solution per Teflon dish (ml)	Temperature °C/ Airflow rate m^3/s		
OPM1	0.6/-	15 g/-	0/-	15/-	35/0.0075	-	Done
OPM2	0.6/0	15 g/10 mL	0/4 wt %	15/10 mL	35/0.0075	One day	Done
OPM3	0.6/0.6	15 g/15 g	4 wt % /0	10/10	35/0.0075	One day	Done
OPM4	0.6/0.6	15 g/15 g	0 /4 wt %	10/10	35/0.0075	One day	Done
OPM5	0.6/0	15 g/10 mL	0/4 wt %	15/10 mL	35/0.0075	5 min	Done

Table 26. (cont'd) *The amount of the materials used to prepare the membranes analyzed by optical microscope*

| Membrane code | Bottom / Top solution | | | | Casting conditions | Casting period of the top solution | Annealing at oven 1st day (60 °C, 1 bar) 2nd day (60 °C, vacuum) |
	PEBAX 1657 (g)	Ethanol-water mixture	Pink Dye solution (% wt)	Casted solution per Teflon dish (ml)	Temperature °C/ Airflow rate m³/s		
OPM6	0.6/0	15 g/10 mL	0/4 wt %	15/10 mL	35/0.0075	30 min	Done
OPM7	0.6/0	15 g/10 mL	0/4 wt %	15/10 mL	35/0.0075	1 hour	Done
OPM8	0.6/0	15 g/10 mL	0/4 wt %	15/10 mL	35/0.0075	2 hours	Done
OPM9	0.6/0	15 g/0.5 mL	0/4 wt %	15/10 mL	35/0.0075	One day	Done

139

Table 26. (cont'd) *The amount of the materials used to prepare the membranes analyzed by optical microscope*

Membrane code	Bottom / Top solution				Casting conditions	Casting period of the top solution	Annealing at oven 1st day (60 °C, 1 bar) 2nd day (60 °C, vacuum)
	PEBAX 1657 (g)	Ethanol-water mixture	Pink Dye solution (% wt)	Casted solution per Teflon dish (ml)	Temperature °C/ Airflow rate m³/s		
OPM10	0.6/0	15 g/1 mL	0/4 wt %	15/10 mL	35/0.0075	One day	Done
OPM11	0.6/0	15 g/3 mL	0/4 wt %	15/10 mL	35/0.0075	One day	Done
OPM12	0.6/0	15 g/12 mL	0/4 wt %	15/10 mL	35/0.0075	One day	Done

APPENDIX D –Sample of Calculation of Carbon Dioxide Permeability

The change of pressure in the permeate side was recorded and line function was fit as shown in Figure 60
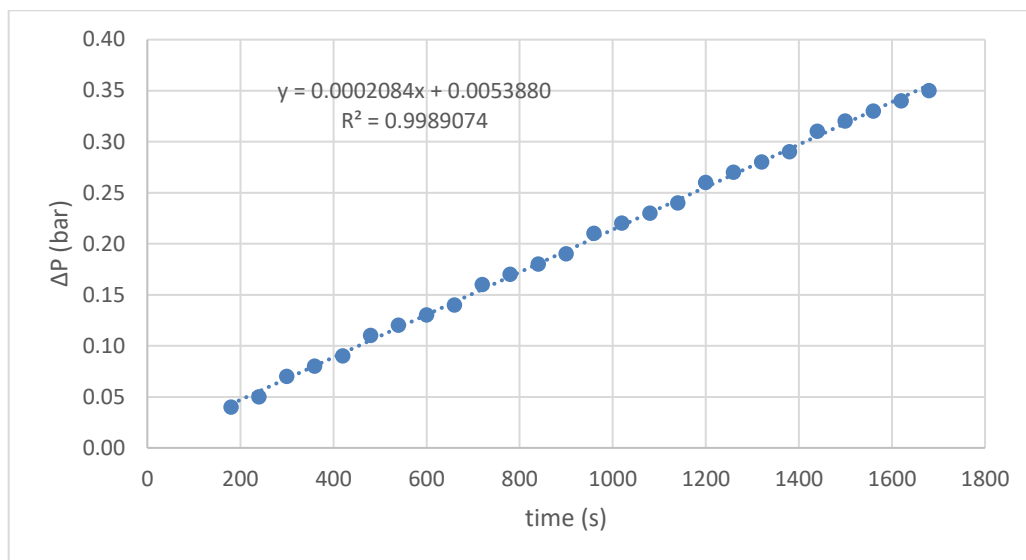
Figure 60. Change of permeate pressure with time in single-gas system

Feed Pressure, $P_F = 4$ bar

Permeated Pressure, $P_P = 0.09$ bar

Permeation Temperature, $T_p = 308.15$ K

Dead Volume, $V_D = 27.3$ cm^3

Gas-constant, R = 83.144 (cm^3*bar)/(K*mol)

Membrane Area = 9.6 m^2

STP pressure, $P_{stp} = 1$ bar

STP Temperature, $T_{stp} = 273.15$ K

Thickness, l= 105.4 µm

Change of pressure in the permeate side with time, slope = 0.0002084 bar/s

Conversion factor to GPU, Fac = $10^6/75$

$$Permeance, \pi = \frac{slop * V_D * T_{STP} * Fac}{T * P_{stp} * (P_F - P_P) * A} = 1.79 \; GPU$$

$$Permeability, Per = \pi * l = 188.7 \; Barrer$$

APPENDIX E –Data for membranes that were tested in the single-gas system

Test Number	Membrane code	CO_2 Permeability	Error	N_2 Permeability (Barrer)	Selectivity	Error	Thickness (μM)	Permeance (GPU)
Test 1		160.80	3.61	4.30	37.40	2.44	105.80	1.52
Test 2		160.00	3.09	4.40	36.36	0.38	126.80	1.26
Test 3	M1.a	144.80	6.70	4.05	35.75	2.06	130.00	1.11
Average		155.20		4.25	36.50		120.87	1.30
Standard deviation		9.02		0.18	0.83			
Test 1		193.90	3.12	5.10	38.02	1.10	86.20	2.25
Test 2		180.40	4.06	4.50	40.09	4.29	72.60	2.48
Test 3	M2	189.80	0.94	5.10	37.22	3.19	90.40	2.10
Average		188.03		4.90	38.44		83.07	2.28
Standard deviation		6.92		0.35	1.48			
Test 1		186.90	0.88	4.40	42.48	2.75	93.20	2.01
Test 2		188.80	0.12	4.50	41.96	1.49	115.90	1.63
Test 3	M3	190.00	0.76	4.80	39.58	4.25	87.00	2.18

Average		188.57		4.57	41.34		98.70	1.94
Standard deviation		1.56		0.21	1.54			
Test 1		182.60	4.34	5.10	35.80	5.02	140.50	1.30
Test 2		165.90	5.20	5.10	32.53	4.58	154.60	1.07
Test 3	M4	176.50	0.86	5.20	33.94	0.44	162.30	1.09
Average		175.00		5.13	34.09		152.47	1.15
Standard deviation		8.45		0.06	1.64			
Test 1		186.3	1.20	4.9	38.02	0.72	111.20	1.68
Test 2		192.0	1.82	4.9	39.18	3.80	83.10	2.31
Test 3	M5	187.40	0.62	5.20	36.04	4.53	80.00	2.34
Average		188.57		5.00	37.75		91.43	2.11
Standard deviation		3.02		0.17	1.59			
Test 1		200.10	3.08	5.40	37.06	1.01	93.10	2.15
Test 2		205.70	0.37	5.50	37.40	1.95	95.70	2.15
Test 3	M6	213.60	3.45	6.00	35.60	2.96	97.80	2.18
Average		206.47		5.63	36.69		95.53	2.16

Standard deviation		6.78		0.32	0.96		
Test 1		187.80	2.19	5	37.56	2.65	118.80	1.58
Test 2		180.2	1.94	4.7	38.34	0.63	84.10	2.14
Test 3	M7	183.3	0.25	4.6	39.85	3.28	116.00	1.58
Average		183.77		4.77	38.58		106.30	1.77
Standard deviation		3.82		0.21	1.16			
Test 1		194.94	0.11	4.80	40.61	4.48	112.60	1.73
Test 2		194.81	0.17	4.90	39.76	2.28	117.00	1.67
Test 3	M8	195.70	0.28	5.40	36.24	6.76	101.40	1.93
Average		195.15		5.03	38.87		110.33	1.78
Standard deviation		0.48		0.32	2.32			
Test 1		223.0	6.56	6.4	34.84	1.25	192.60	1.16
Test 2		202.4	3.28	5.7	35.51	0.63	163.30	1.24
Test 3	M9	202.4	3.28	5.7	35.51	0.63	152.20	1.33
Average		209.27		5.93	35.29		169.37	1.24
Standard deviation		11.90		0.40	0.38			

Test 1		253.20	0.21	6.60	38.36	3.30	169.50	1.49
Test 2		242.57	4.39	6.80	35.67	3.95	166.90	1.45
Test 3	M10	265.40	4.60	7.10	37.38	0.65	170.10	1.56
Average		253.72		6.83	37.14		168.83	1.50
Standard deviation		11.42		0.25	1.36			

APPENDIX F –Linearization of Double-Layer Method

Another proposal is that the double-layer method has a linearized effect on the single-layer membrane types (M1.a, M6, M7). Data in Table 22 was used and demonstrated in Figure 61 to find the relation between the double-layer permeability and the single-layer permeability for each type of membranes.
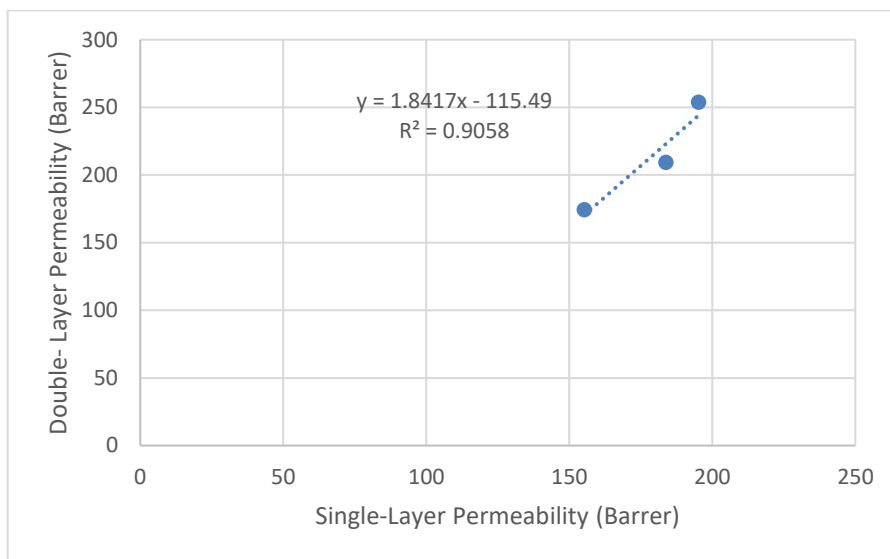

Figure 61. Fitting a linear relation between CO_2 permeability through different single- and double-layers membranes

It can be seen easily that a linear function does not fit thus the double-layer method has a different effect for each membrane type. Table 27 shows the modification factor of CO_2 permeability that occurred for every single-layer of membranes compared to double-layer membranes. It was found that the impact of the double-layer method increases with the permeability of the single-layer membranes.

Table 27. *Modification factors estimation for different membrane types from single- to double-layer condition*

Type of the Membrane	Modification Factor
4 wt % pure PEBAX 1657	1.12
Pure PEBAX 1657 (4 wt %) loaded with 5 wt % ZIF-8 (67 nm)	1.14
Pure PEBAX 1657 (4 wt %) loaded with 5 wt % ZIF-8 (323 nm)	1.30